

Positronium in physics and medicine

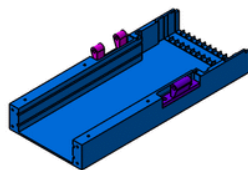
**Seminar at University of Geneva
Geneva, 15 May 2019**

P. Moskal, Jagiellonian University, Poland
<http://koza.if.uj.edu.pl>



Positronium in physics and medicine

18-11



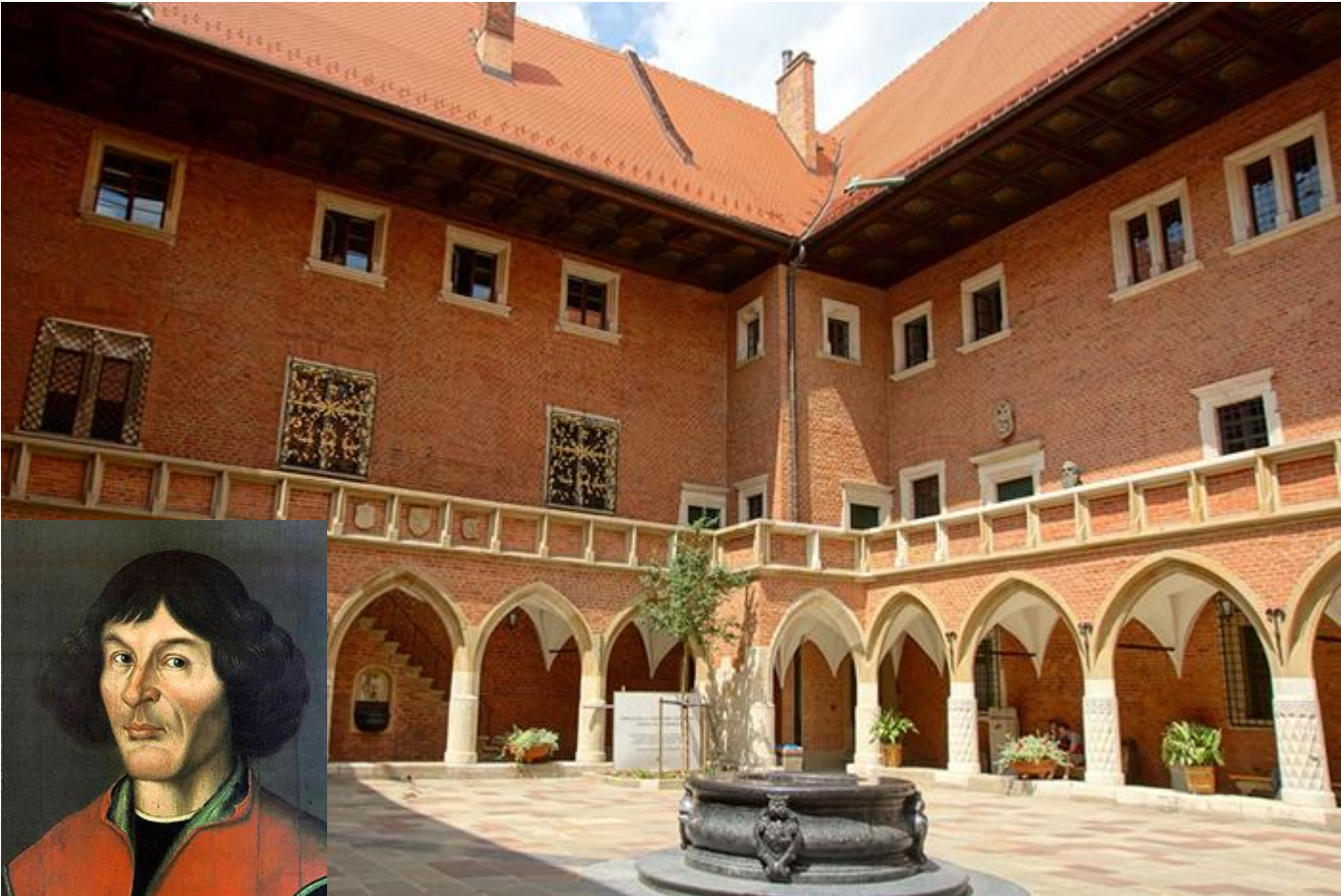
**Seminar at University of Geneva
Geneva, 15 May 2019**

P. Moskal, Jagiellonian University, Poland
<http://koza.if.uj.edu.pl>





Jagiellonian University 1364



Collegium Maius at the University since **1400**



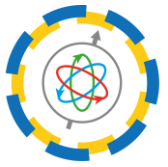
Collegium Maius 2015



J-PET

J-PET: First PET

based on plastic scintillators



J-PET

Jagiellonian-PET Collaboration:

P. Moskal¹, C. Curceanu², E. Czerwiński¹, K. Dulski¹, A. Gajos¹, M. Gorgol³, B. Hiesmayr⁴,

B. Jasińska³, D. Kisielewska¹, G. Korcyl¹, P. Kowalski⁵, T. Kozik¹, W. Krzemień⁵, E. Kubicz¹, N. Krawczyk¹

M. Mohammed¹, M. Pawlik-Niedźwiecka¹, Sz. Niedźwiecki¹, M. Pałka¹, L. Raczyński⁵, J. Raj¹,

N. Sharma¹, S. Sharma¹, Shivani¹, M. Silarski¹, M. Skurzok¹, W. Wiślicki⁵, B. Zgardzińska³

¹Jagiellonian University, Poland; ²LNF INFN, Italy; ³Maria Curie-Skłodowska University, Poland;

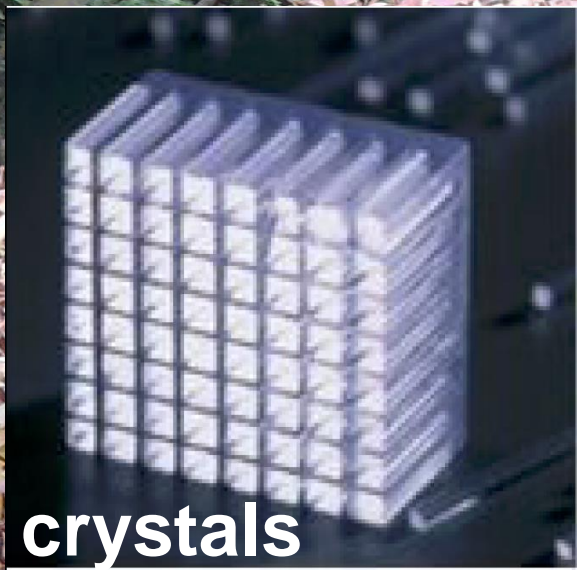
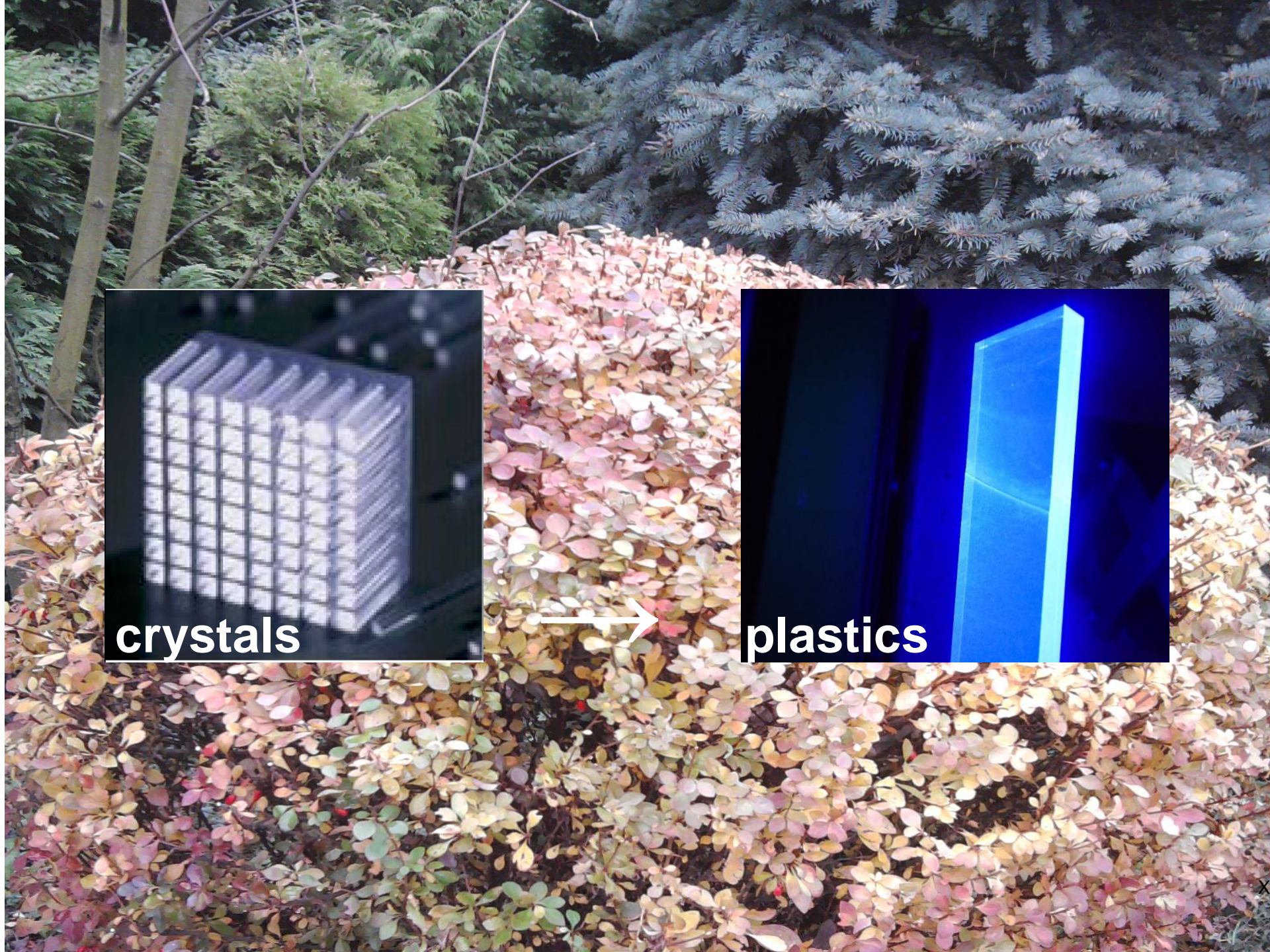
⁴University of Vienna, Austria; ⁵National Centre for Nuclear Research, Poland;

Aim:

- Cost effective total-body PET
- Light, modular, configurable and portable
- For large animals
- MR and CT compatible PET insert



Cracow, July 2016



crystals

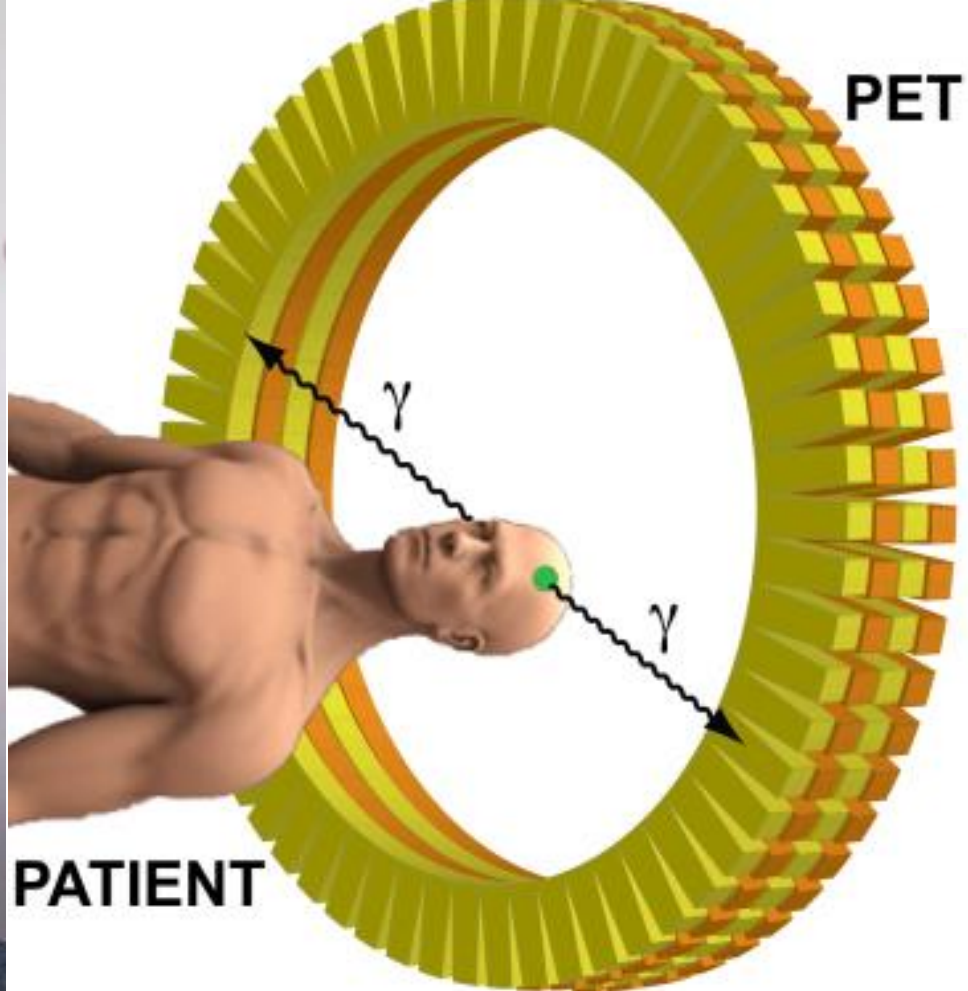


plastics



- **PET**

- **Jagiellonian-PET (J-PET)**
- **Positronium imaging (PET & PALS)**
- **Discrete symmetries**
- **Quantum Entanglement Tomography**
- **Hadrontherapy beam monitoring**



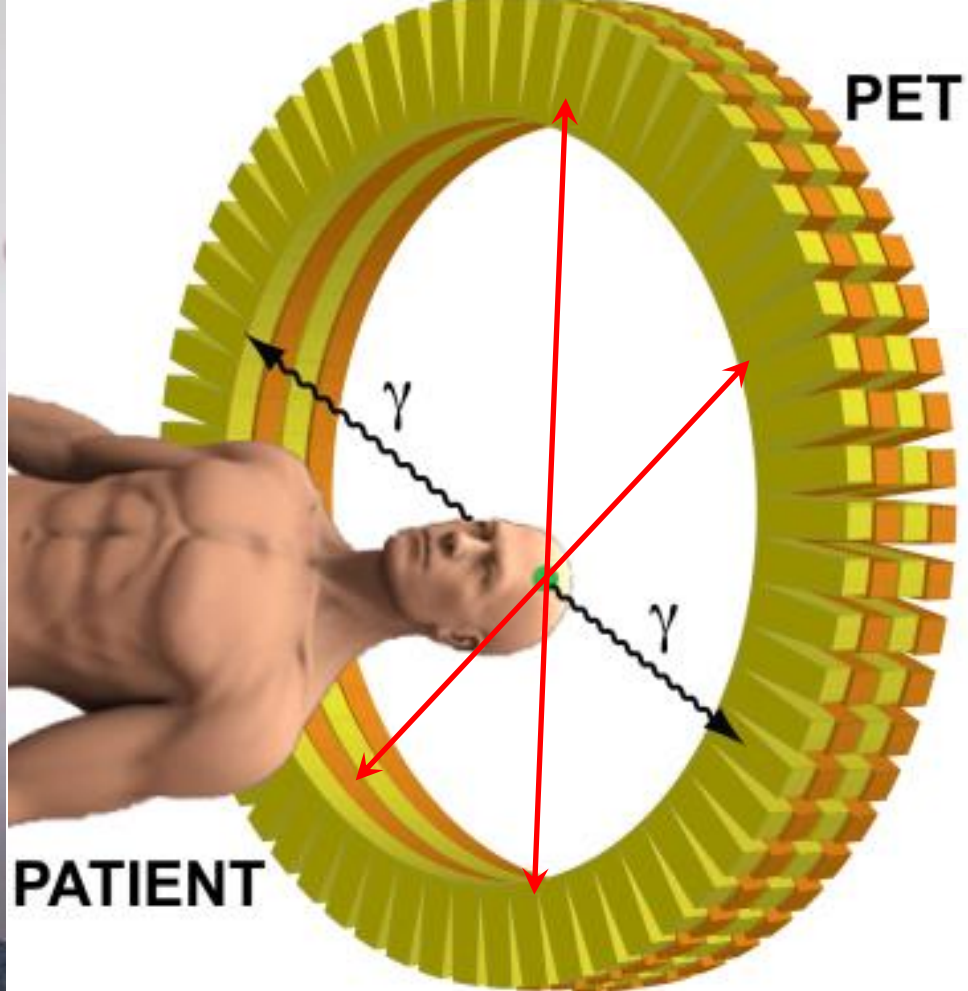
RADIOACTIVE SUGER

Fluoro-deoxy-glucose
(F-18 FDG)

~200 000 000
gamma per second



7 mSv PET/CT
~ 2.5 mSv PET
~3 mSv natural
background in Poland



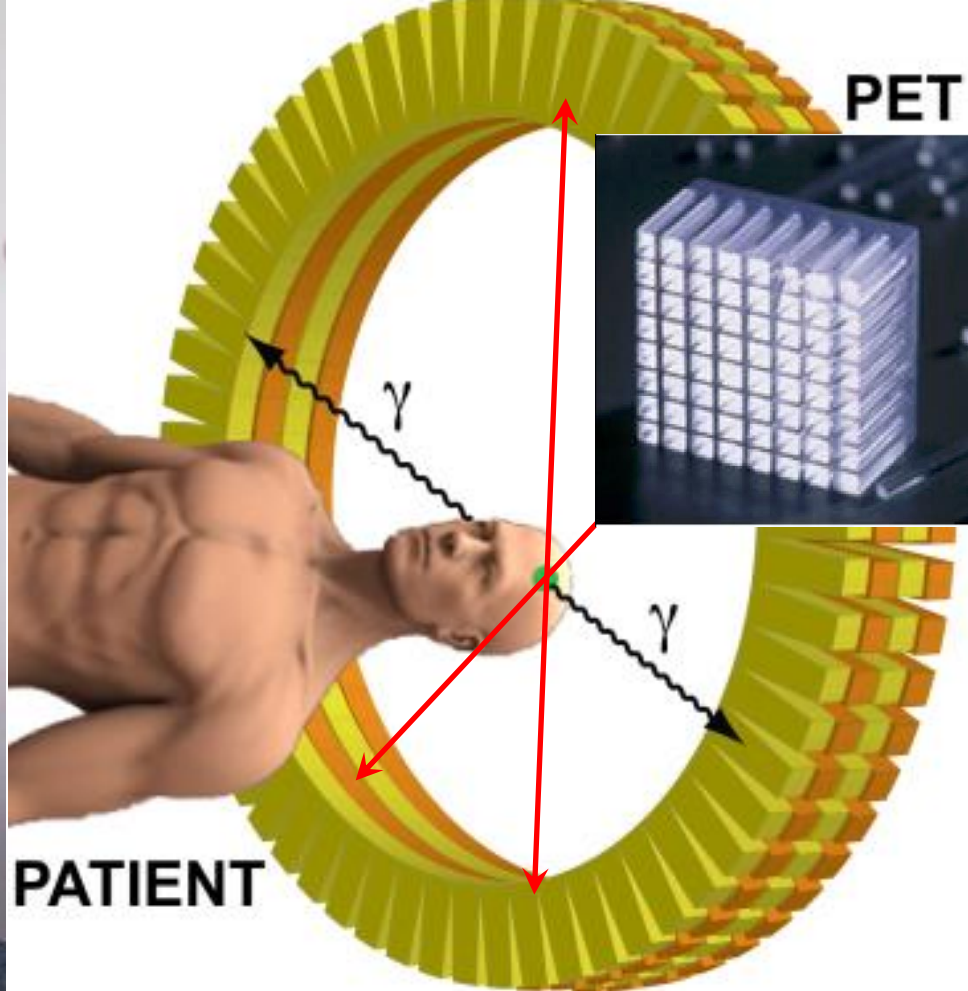
RADIOACTIVE SUGER

Fluoro-deoxy-glucose
(F-18 FDG)

~200 000 000
gamma per second



7 mSv PET/CT
~ 2.5 mSv PET
~3 mSv natural
background in Poland

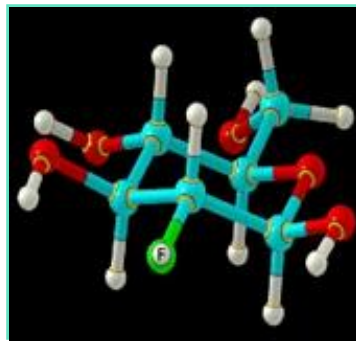


RADIOACTIVE SUGER

Fluoro-deoxy-glucose
(F-18 FDG)

~200 000 000

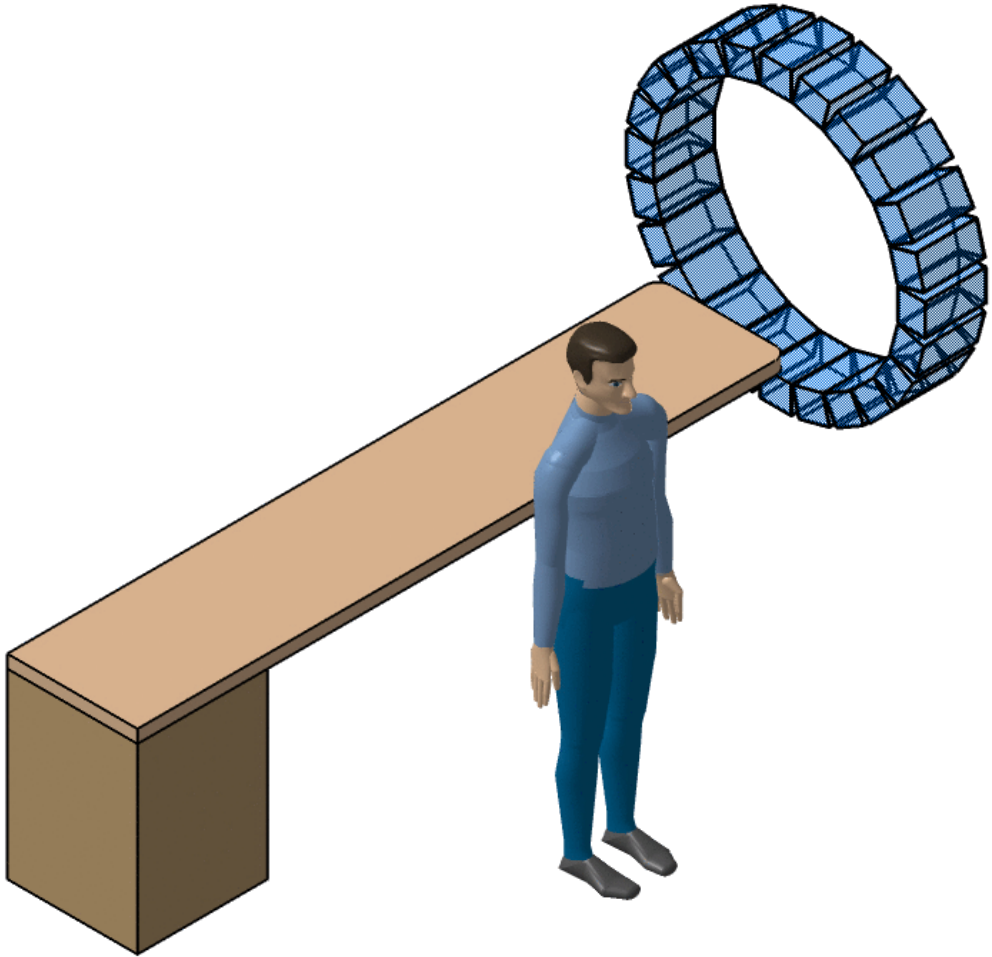
gamma per second



7 mSv PET/CT

~ 2.5 mSv PET

~3 mSv natural
background in Poland



EXPLORER PROJECT

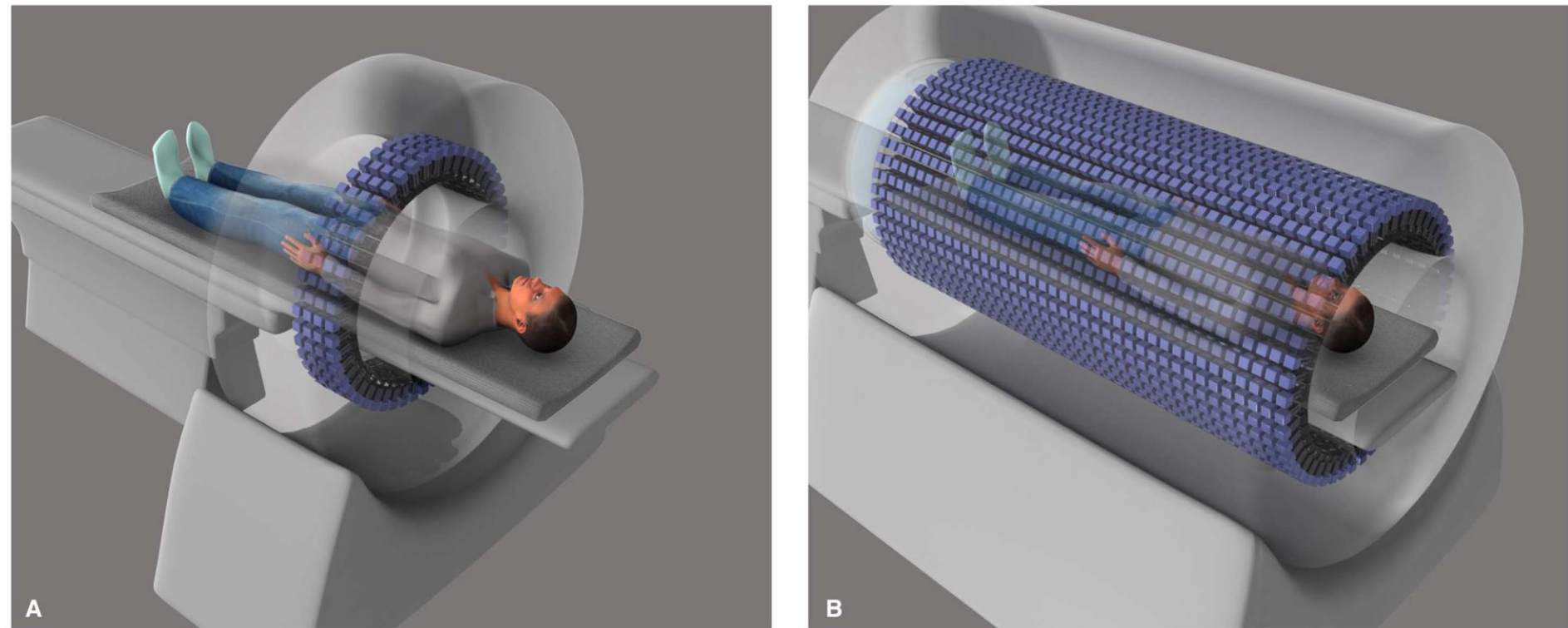


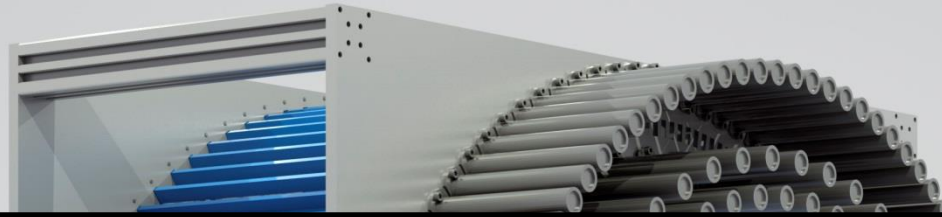
Fig. 1. Seeing into our future. Illustration depicting (A) a conventional PET scanner and (B) total-body PET (TB-PET) scanner. An x-ray computed tomography (CT) scanner will be mounted on the front of the TB-PET gantry for anatomical coregistration to ensure optimal integration of anatomical imaging with molecular imaging.

Simon R. Cherry,^{1*} Ramsey D. Badawi,¹ Joel S. Karp,² William W. Moses,³ Pat Price,⁴ Terry Jones¹

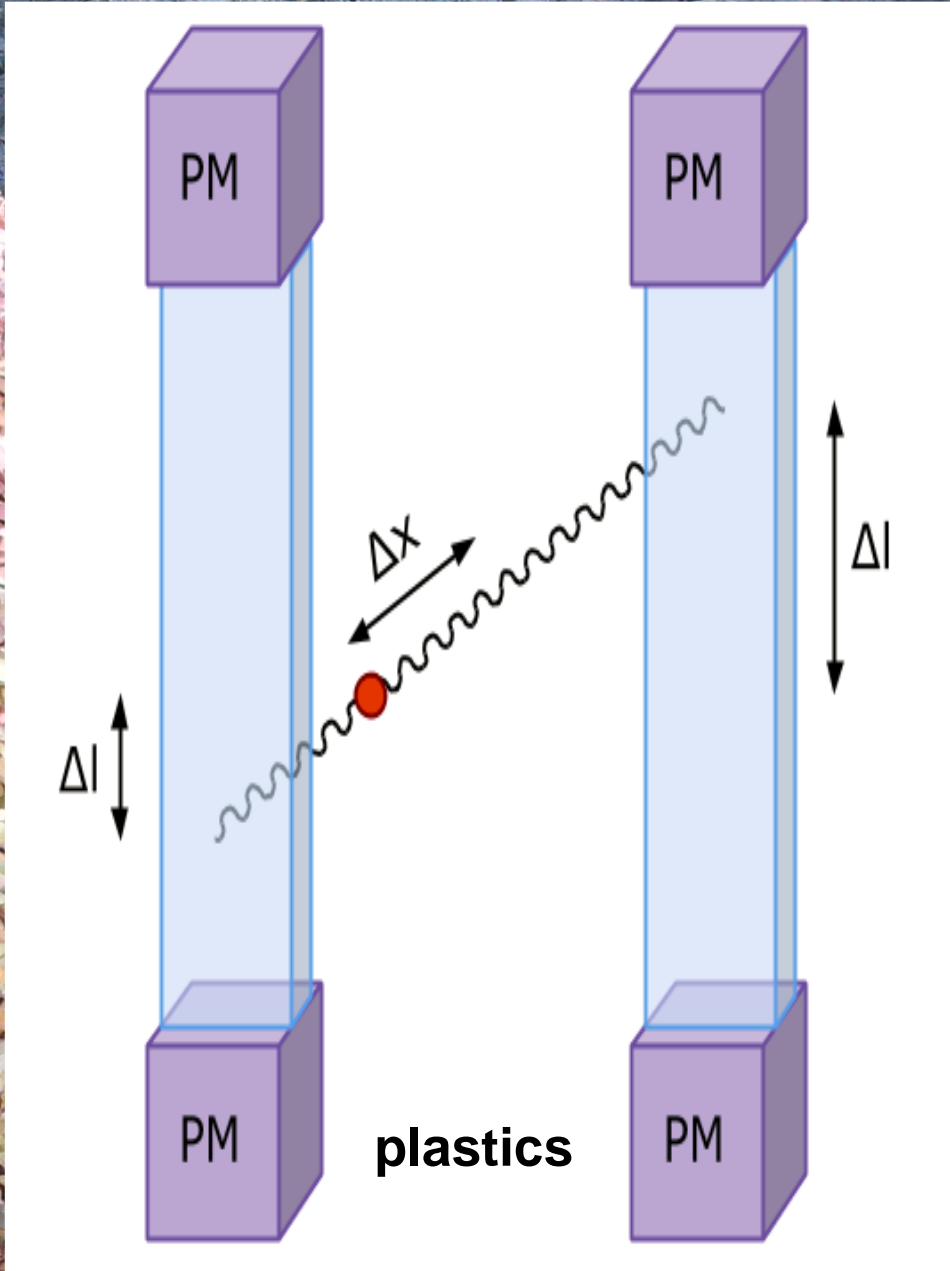
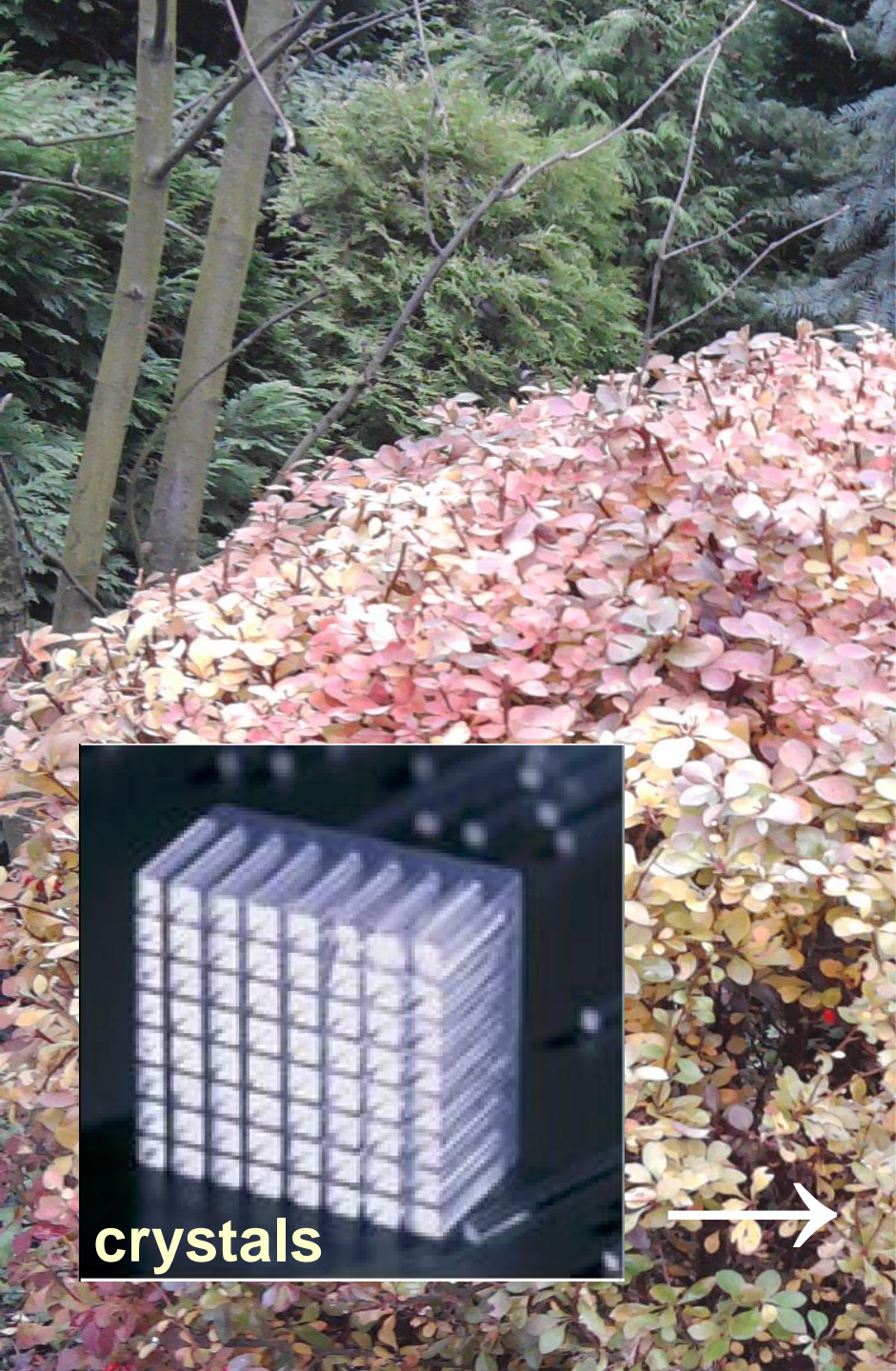
Cherry et al., Sci. Transl. Med. **9**, eaaf6169 (2017)

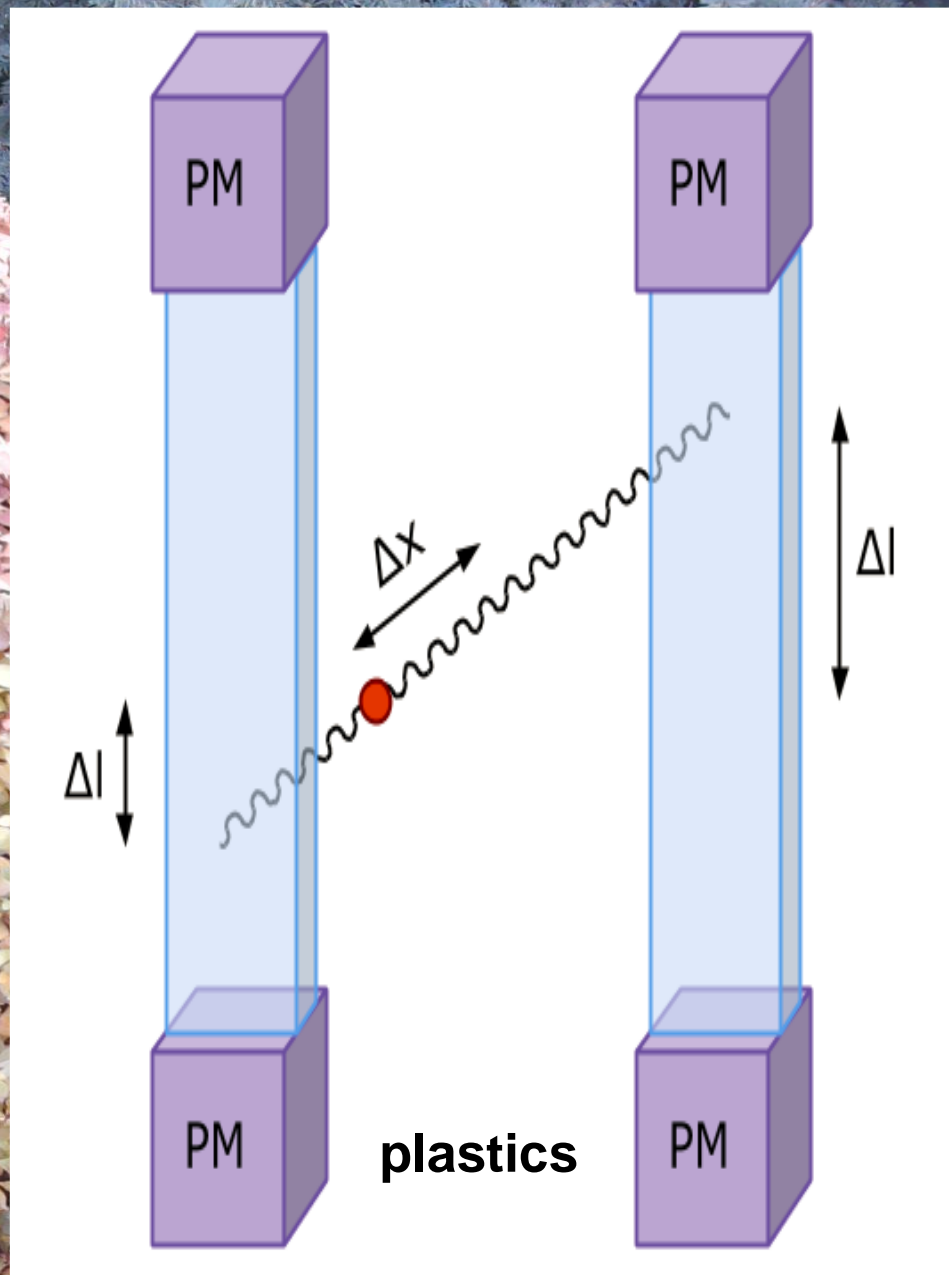
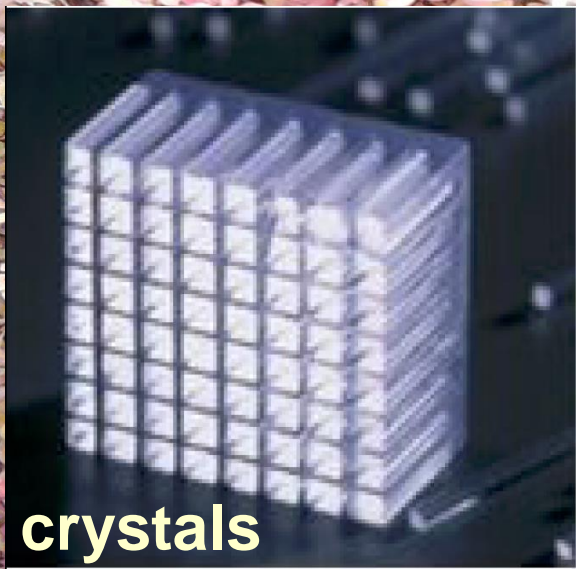
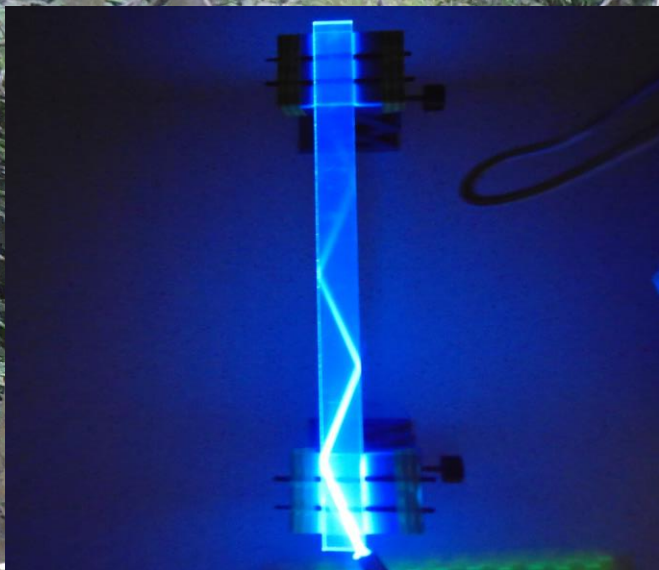
¹University of California, Davis, Davis, CA 95616, USA. ²University of Pennsylvania, Philadelphia, PA 19104, USA.

³Lawrence Berkeley National Laboratory, Berkeley, CA 94720, USA. ⁴Hammersmith Hospital, Imperial College London, London W12 0NN, U.K.



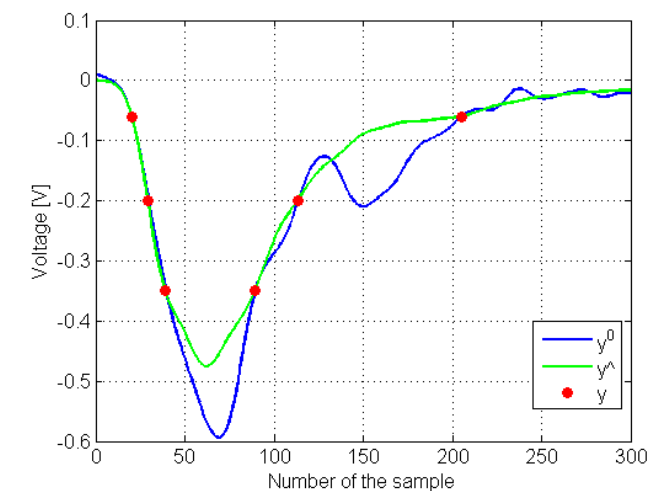
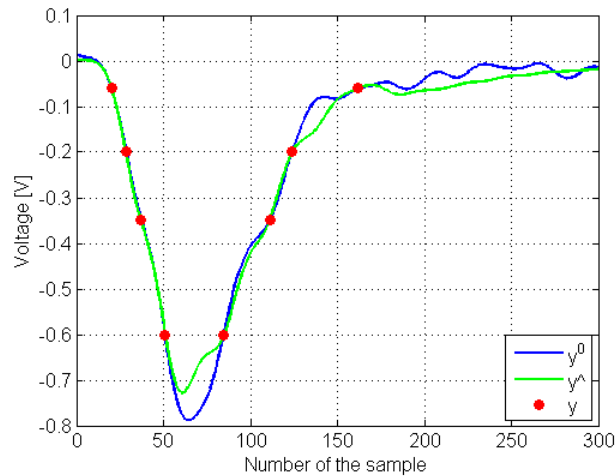
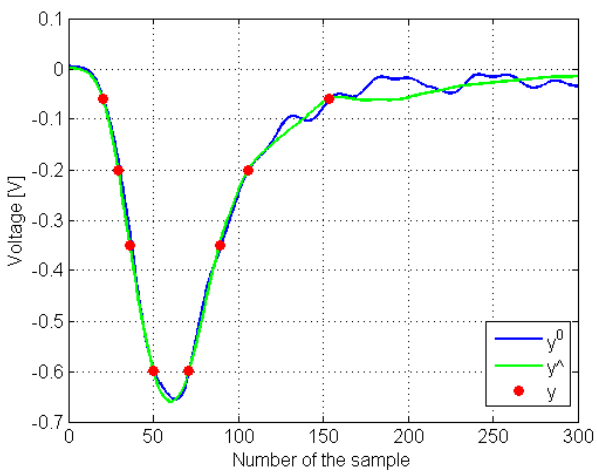
- **PET**
- **Jagiellonian-PET (J-PET)**
- **Positronium imaging (PET & PALS)**
- **Discrete symmetries**
- **Quantum Entanglement Tomography**
- **Hadrontherapy beam monitoring**







ONLY DIGITAL in triggerless mode
FFE sampling & Readout electronics
 precision of 21ps (sigma) for 10 Euro per sample
 M.Pałka, P.M., **PCT/EP2014/068367**
 G. Korcyl, P. M., M. Kajetanowicz, M. Pałka, **PCT/EP2014/068352**



Library of signals; Principal Component Analysis; Compressive Sensing;
 J-PET: L. Raczyński et al., Nucl. Instr. Meth. A786 (2015) 105
 J-PET: P. M. et al., Nucl. Instrum. Meth. A775 (2015) 54
 J-PET: L. Raczyński et al., Phys. Med. Biol. 62 (2017) 5076

Reconstruction



J-PET: M.Pałka et al., JINST 12 (2017) P08001 J-PET: W. Krzemień et al., Acta Phys. Pol. B47 (2016) 561
 J-PET: G. Korcyl et al., IEEE TMI 37 (2018) 2526 J-PET: P. Bialas et al., Bio-Alg. and Med-Sys. 10 (2014) 12



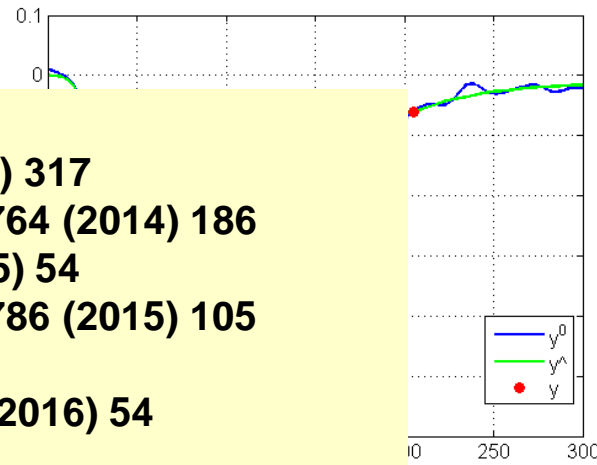
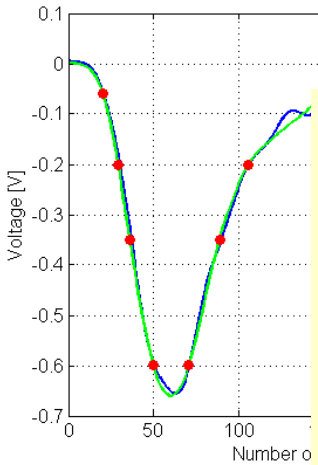
ONLY DIGITAL in triggerless mode

FFE sampling & Readout electronics

precision of 20ps (sigma) for 10 Euro per sample

M. Pałka, P. M., **PCT/EP2014/068367**

G. Korcyl, P. M., M. Kajetanowicz, M. Pałka, **PCT/EP2014/068352**



... > 80 articles ...

J-PET: P. M. et al., Nucl. Instrum. Meth. A764 (2014) 317

J-PET: L. Raczyński et al., Nucl. Instrum. Meth. A764 (2014) 186

J-PET: P. M. et al., Nucl. Instrum. Meth. A775 (2015) 54

J-PET: L. Raczyński et al., Nucl. Instrum. Meth. A786 (2015) 105

J-PET: P. M. et al., Phys. Med. Biol. 61 (2016) 2025

J-PET: A. Gajos et al., Nucl. Instrum. Meth. B 819 (2016) 54

J-PET: P. M. et al., Acta Phys. Pol. B 47 (2016) 509

J-PET: D. Kamińska et al., Eur. Phys. J. C76 (2016) 445

J-PET: J. Smyrski et al., Nucl. Instrum. Meth. A851 (2017) 39

J-PET: L. Raczyński et al., Phys. Med. Biol. 62 (2017) 5076

J-PET: M. Pałka et al., JINST 12 (2017) P08001

J-PET: P. Kowalski et al., Phys. Med. Biol. 63 (2018) 165008

J-PET: G. Korcyl et al., IEEE Trans. Med. Imaging 37 (2018) 2526

J-PET: A. Gajos et al., Adv. High Energy Phys. 2018 (2018) 8271280

J-PET: P. M. et al., Eur. Phys. J. C 78 (2018) 970

J-PET: P. M. et al., Phys. Med. Biol. 64 (2019) 055017

Library of signal
 J-PET: L. Raczyński
 J-PET: P. M. et al.
 J-PET: L. Raczyński

Detector

J-PET: M. Pałka et al.
 J-PET: G. Korcyl et al.

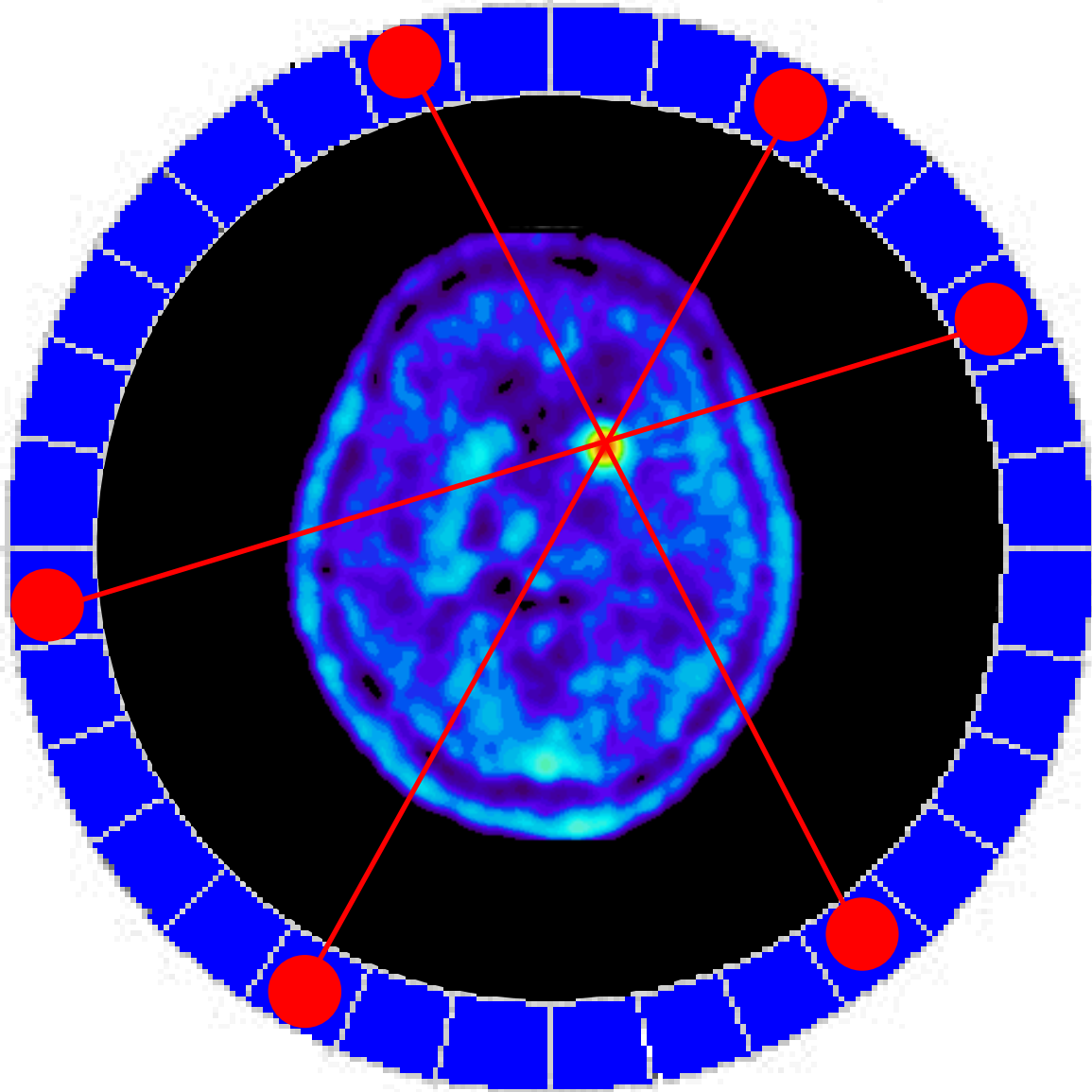
and 17 patents

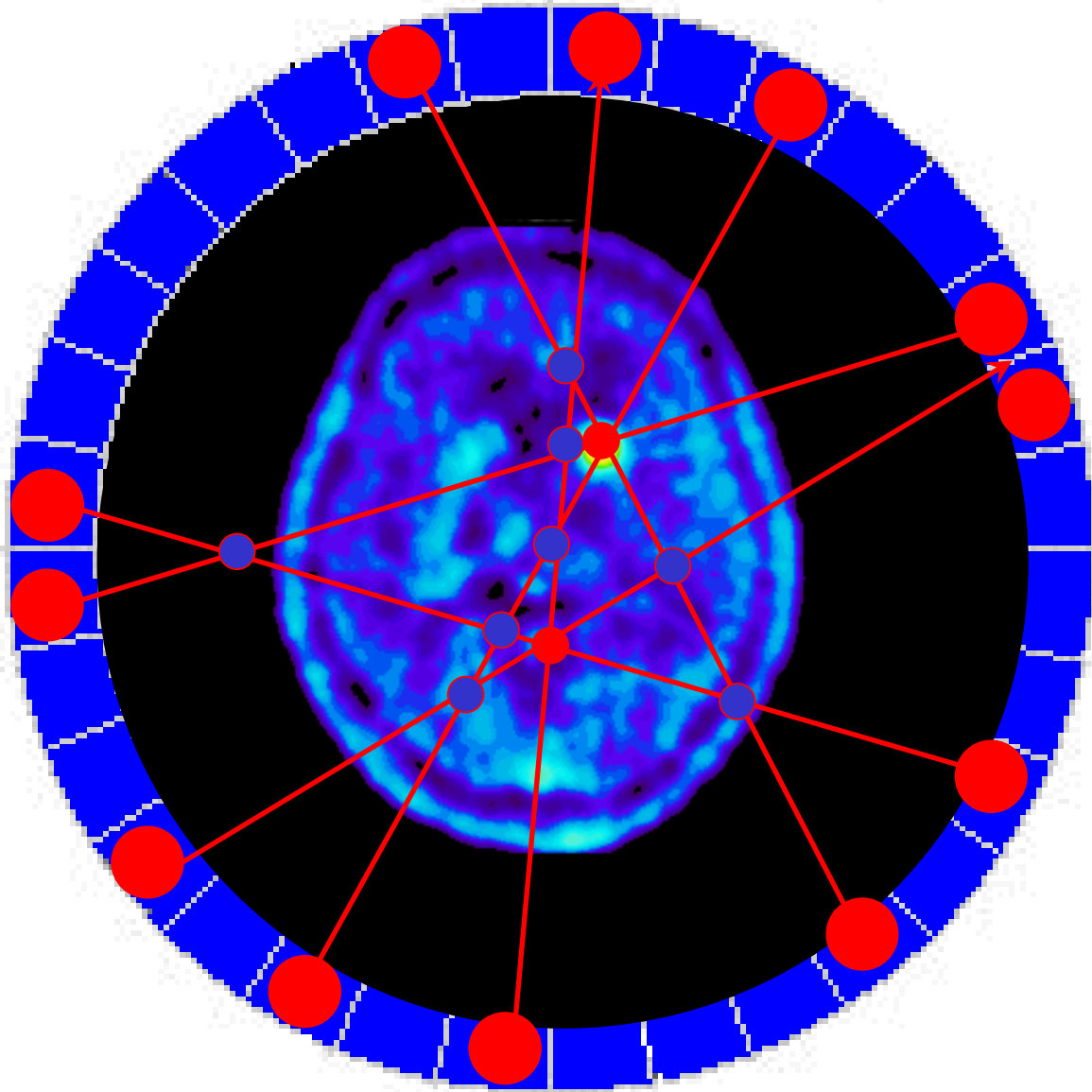
Image

(2016) 561
 0 (2014) 12

for the 2.5 cm layer the efficiency for the registration of events selected to reconstruct the image is for the plastic scintillator by
**a factor of about 20 smaller in relation to the BGO crystals
and about 40 times less compared to the LSO crystals**

name	type	density [g/cm³]	decay time [ns]	photons/ MeV	mean free path [cm]	light Attenuation length [cm]
BGO	crystal	7.13	300	6000	1.04	7.1
GSO	crystal	6.71	50	10000	1.49	6.7
LSO	crystal	7.40	40	29000	1.15	7.4
BC420	polymer	1.032	1.5	10000	10.2	110
BC404	polymer	1.032	1.8	10000	10.2	160
BC408	polymer	1.032	2.1	10000	10.2	380





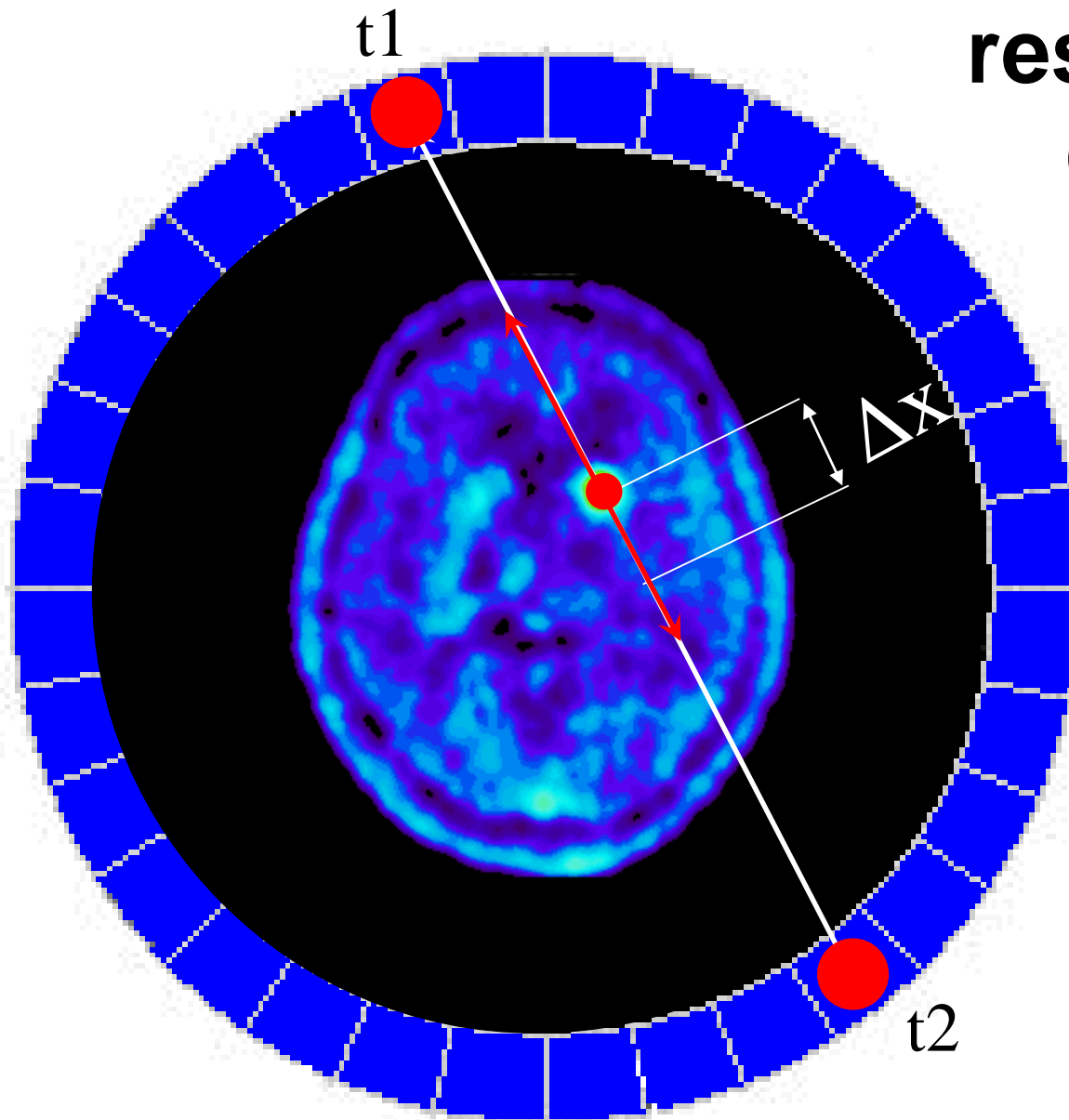
PET-TOF

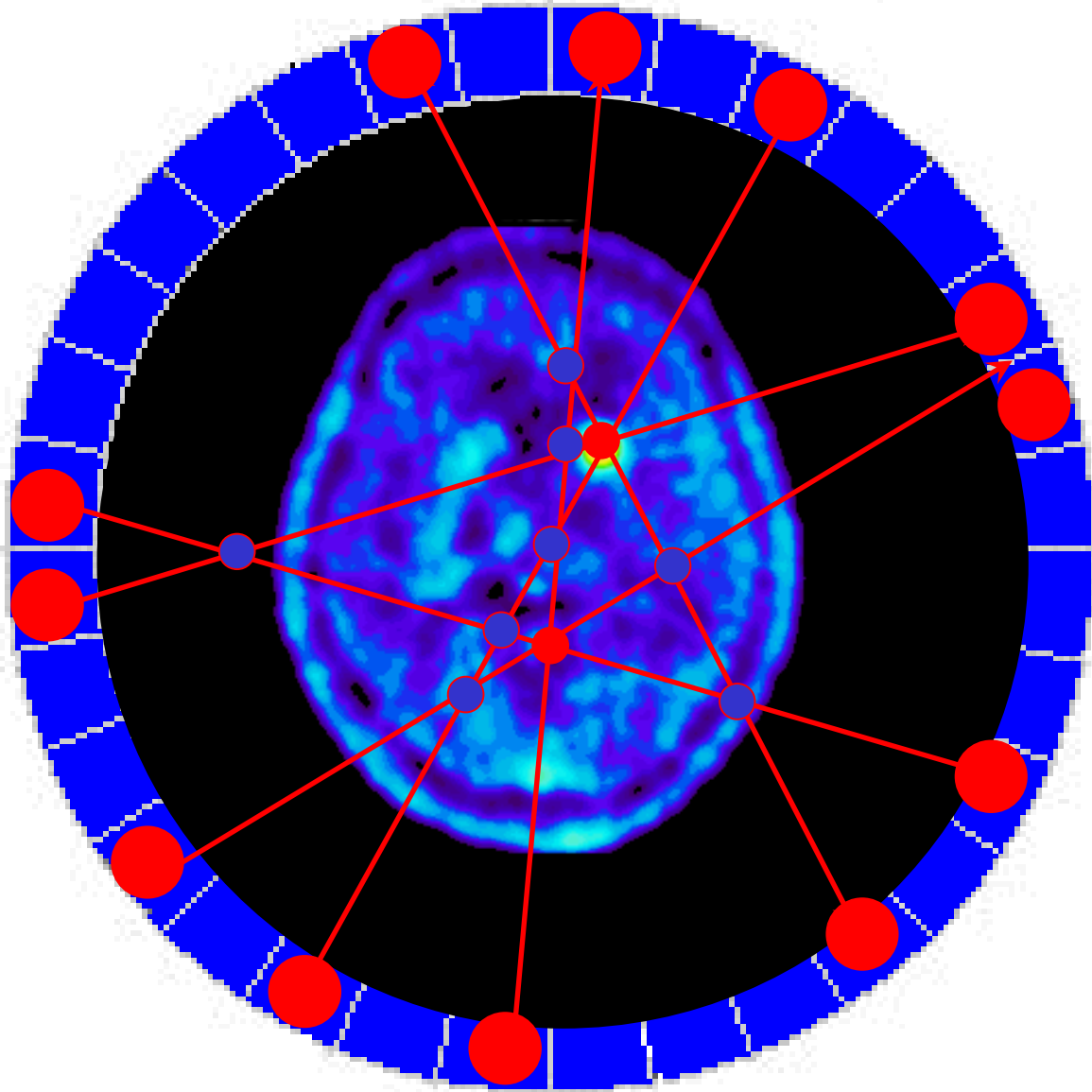
$$\Delta x = (t_2 - t_1) c / 2$$

resolution

600ps

CRT





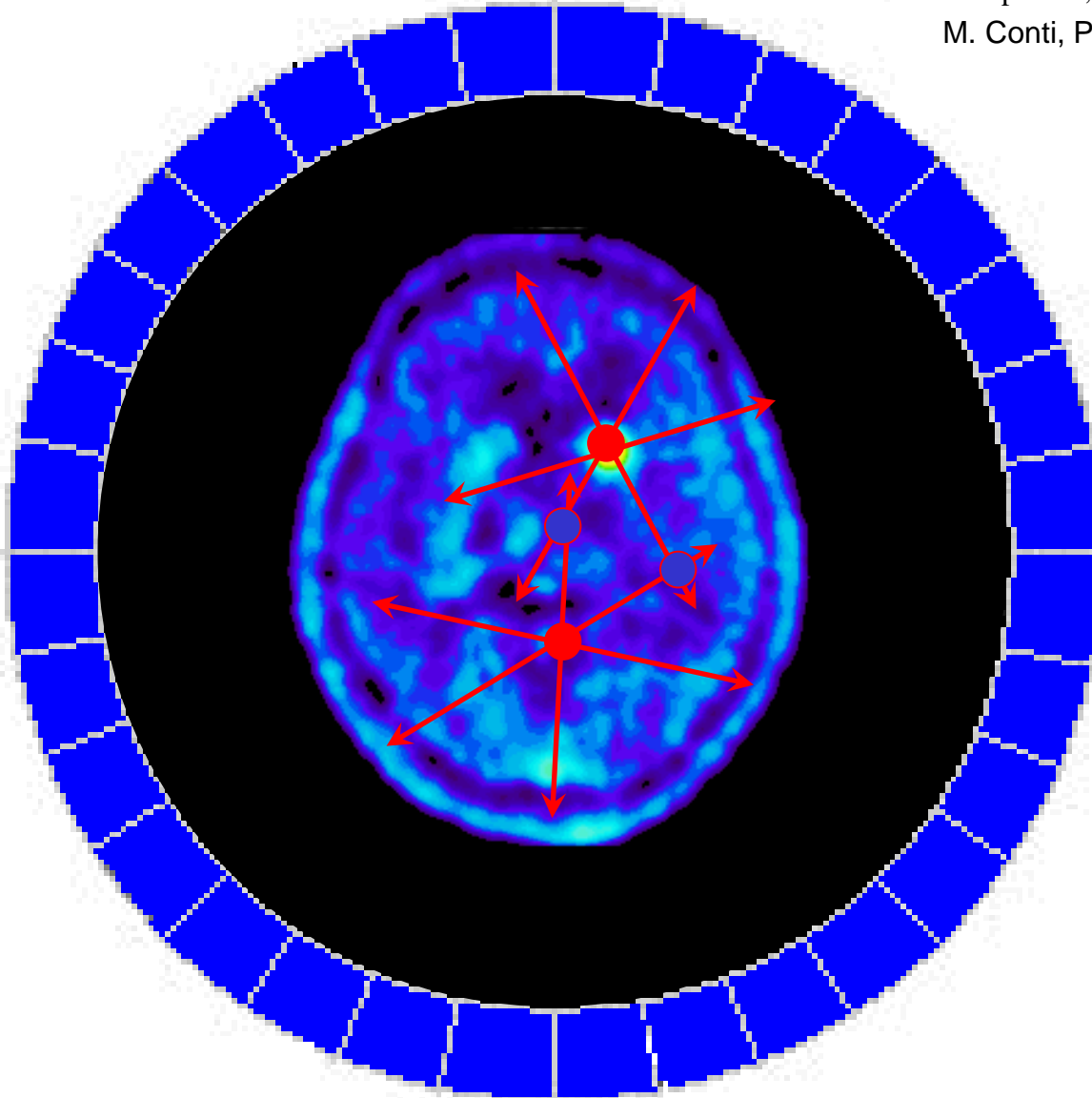
signal/noise

$$\sim D / \Delta t$$

40cm/600ps improvement by factor of 4

J. S. Karp et al., J Nucl Med 2008; 49: 462

M. Conti, Physica Medica 2009; 25: 1.



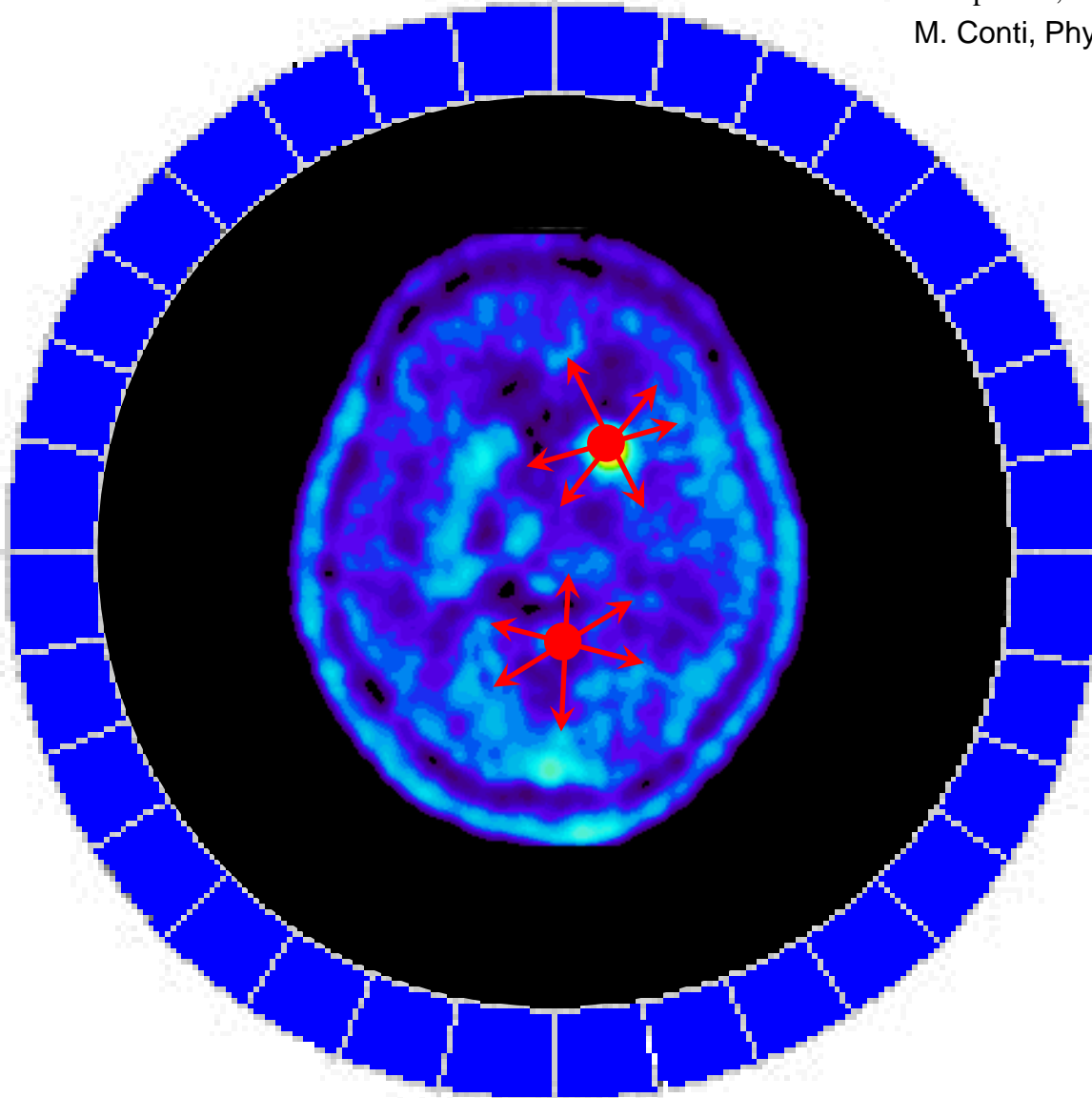
signal/background

40cm/200ps improvement by factor of 12

$$\sim D / \Delta t$$

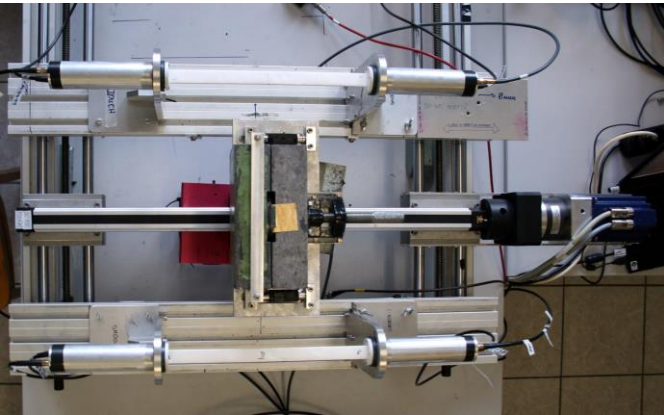
J. S. Karp et al., J Nucl Med 2008; 49: 462

M. Conti, Physica Medica 2009; 25: 1.



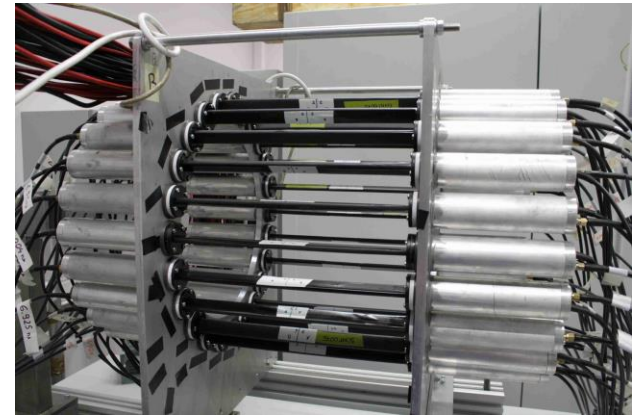
2012

2 strips

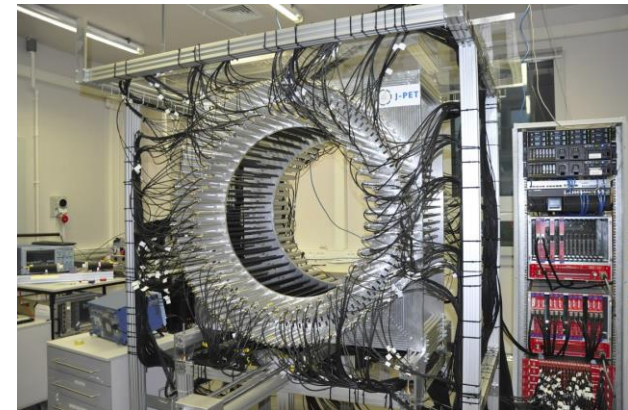


2014

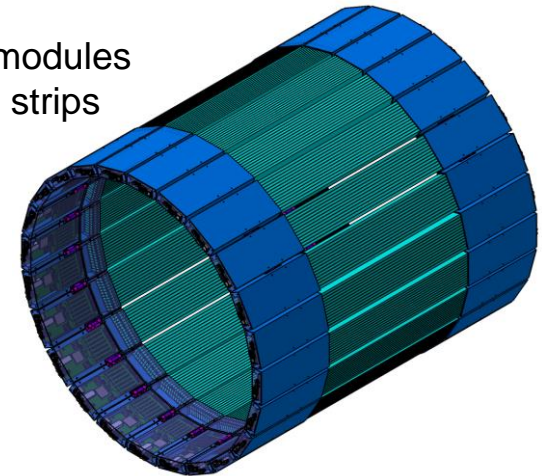
48 plastic strips



192 plastic strips



24 modules
312 strips



MODULAR

2019

2016

Funding:

Foundation for Polish Science (TEAM)

Polish National Centre for Development and Research

Polish Ministry for Science and Higher Education

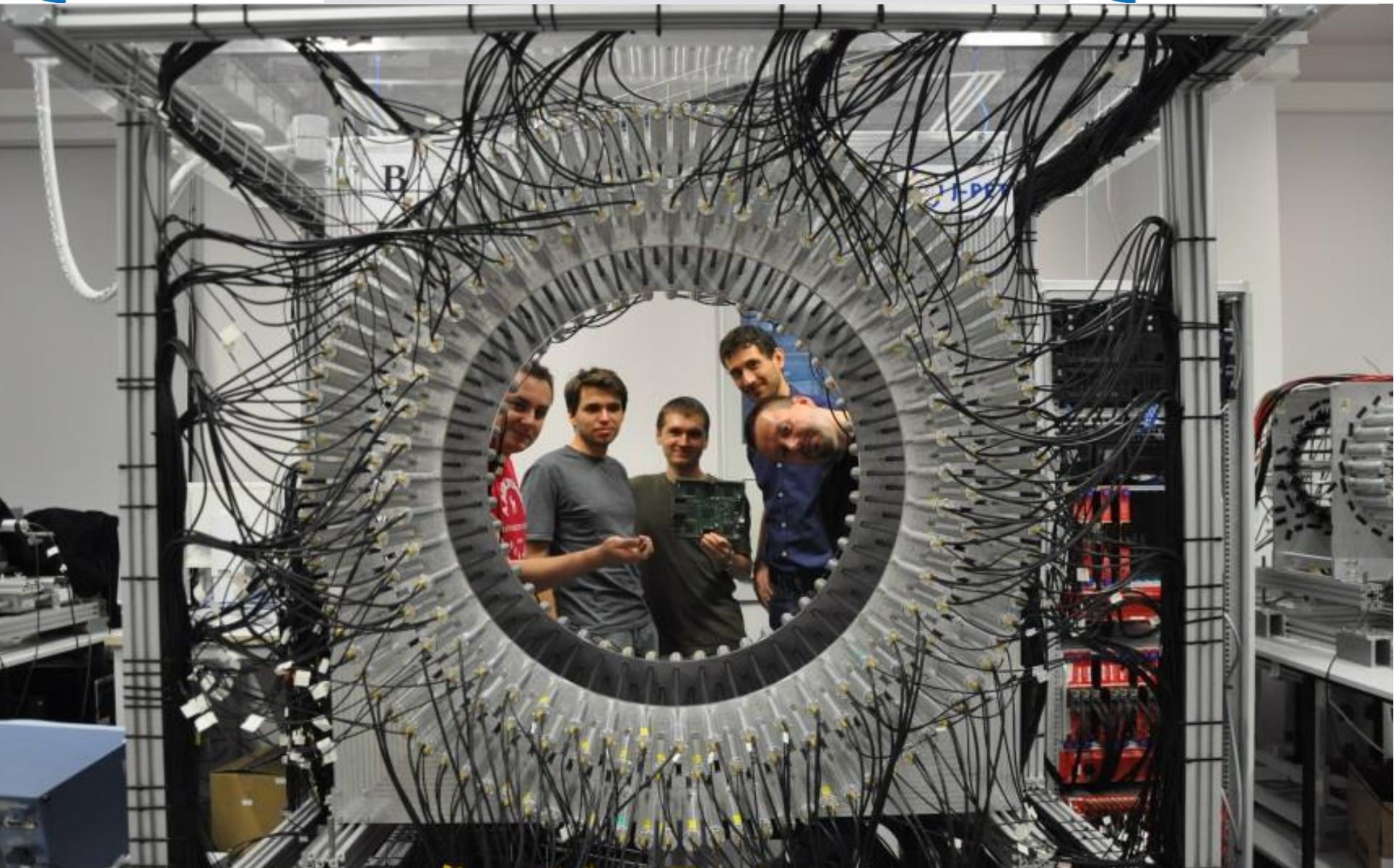


J-PET

Jagiellonian PET



J-PET



AFOV: 17 cm \rightarrow 50 cm ; TOF < 450 ps

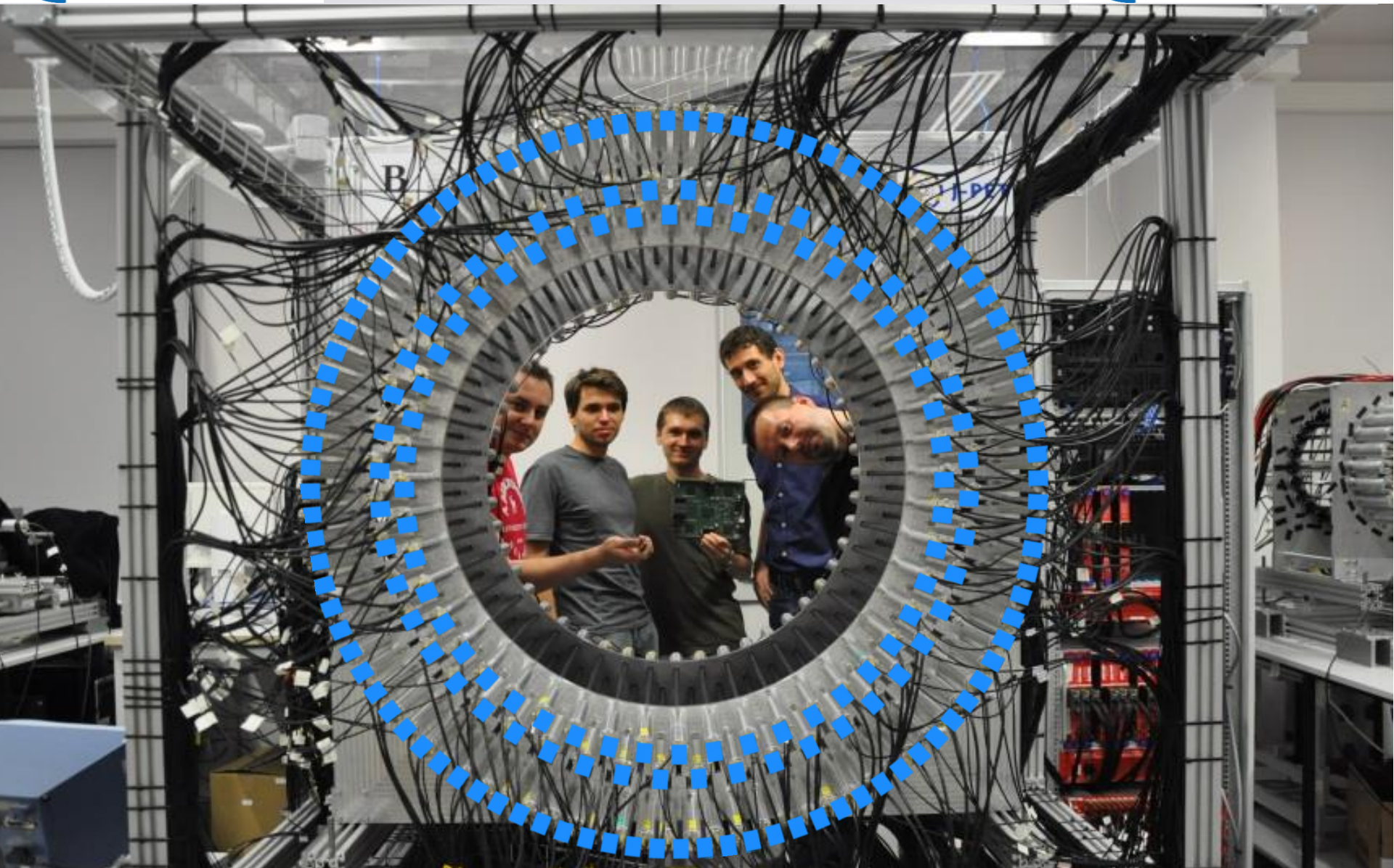


J-PET

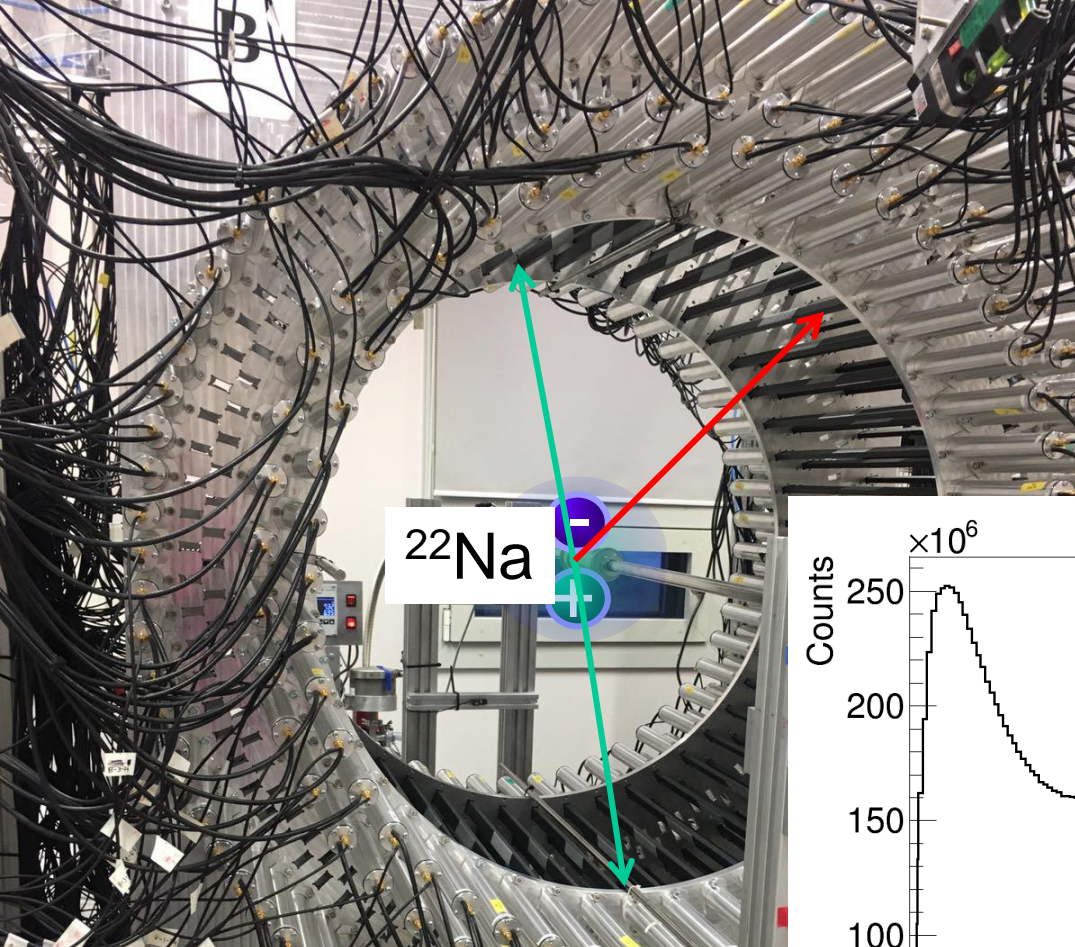
Jagiellonian PET



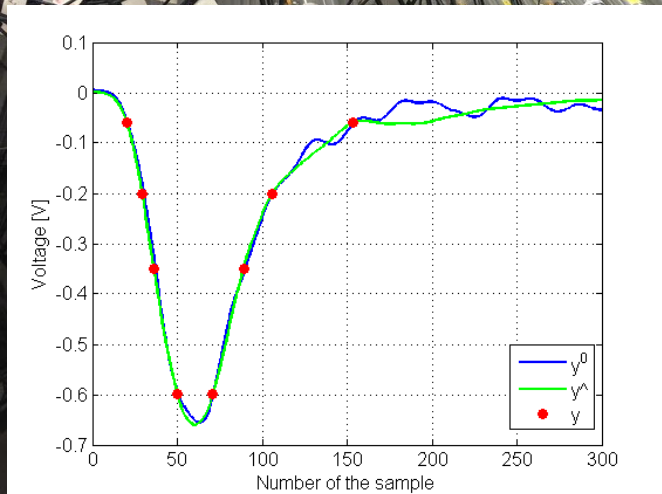
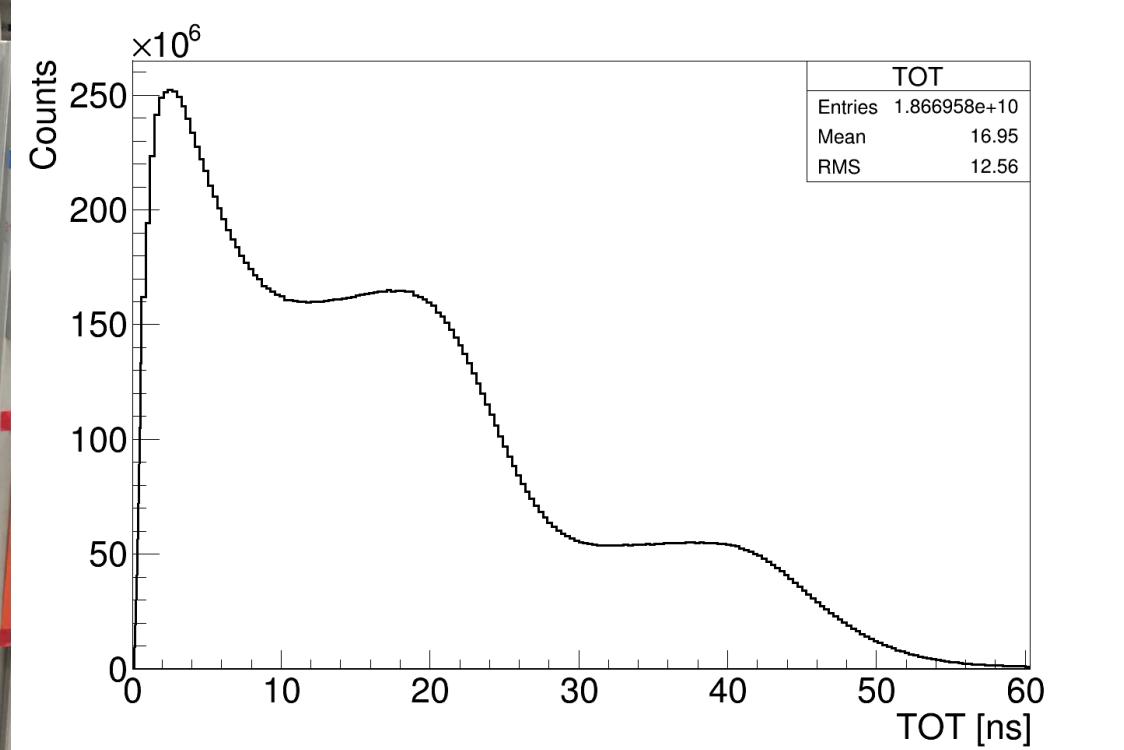
J-PET

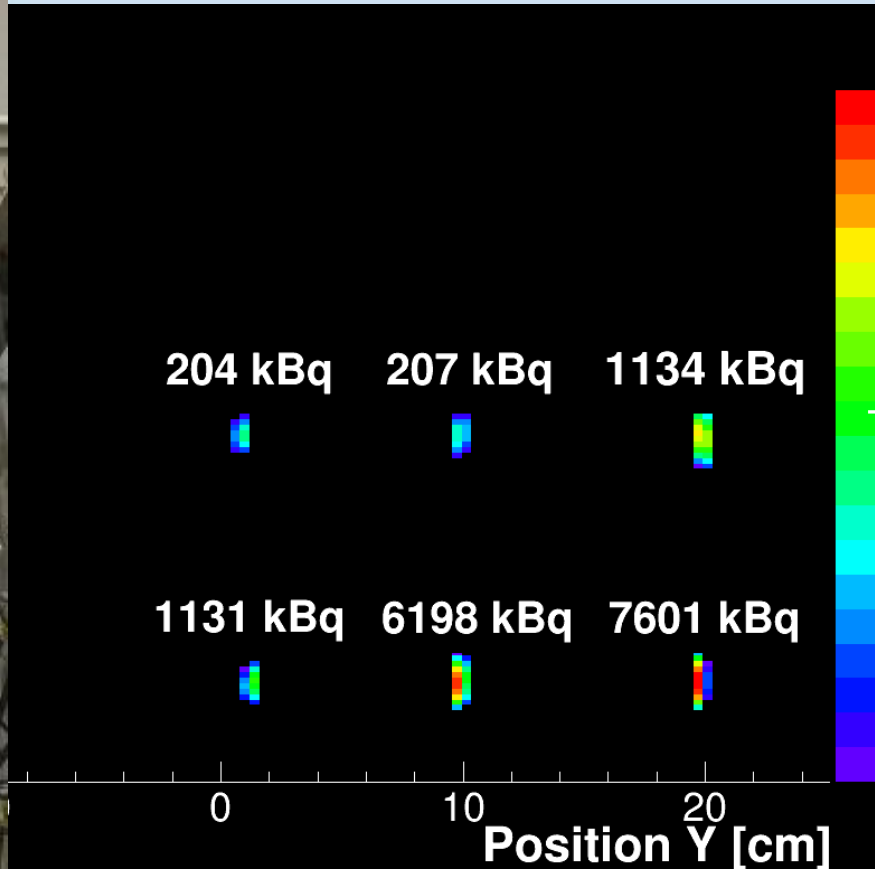
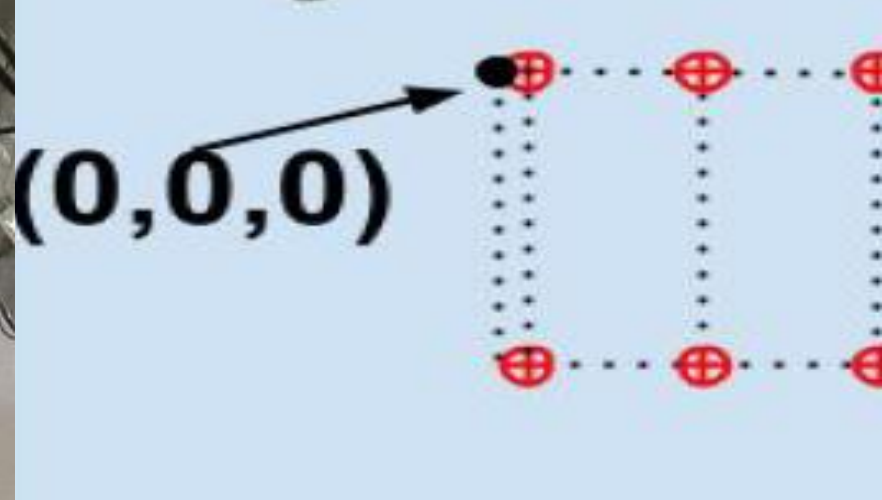


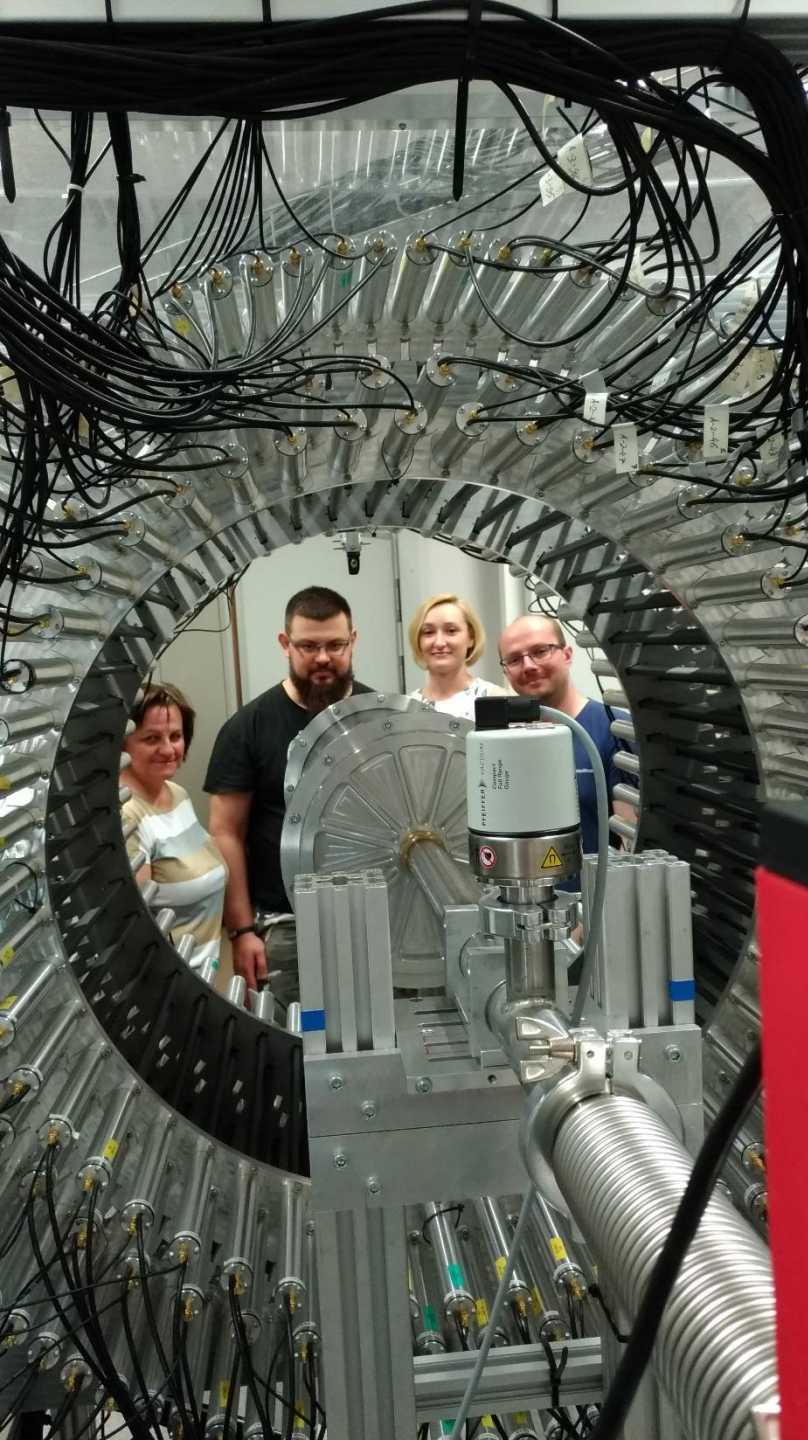
AFOV: 50 cm ; TOF < 450 ps (CRT)

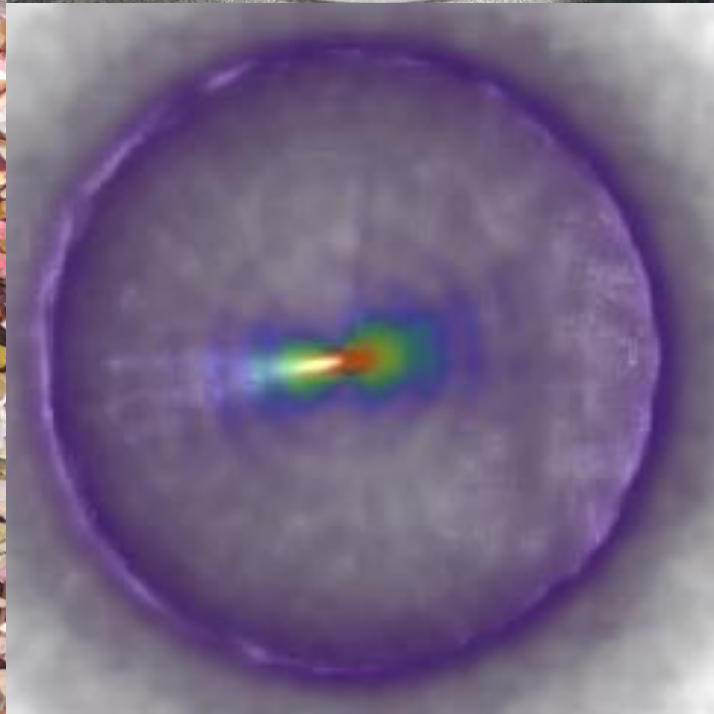
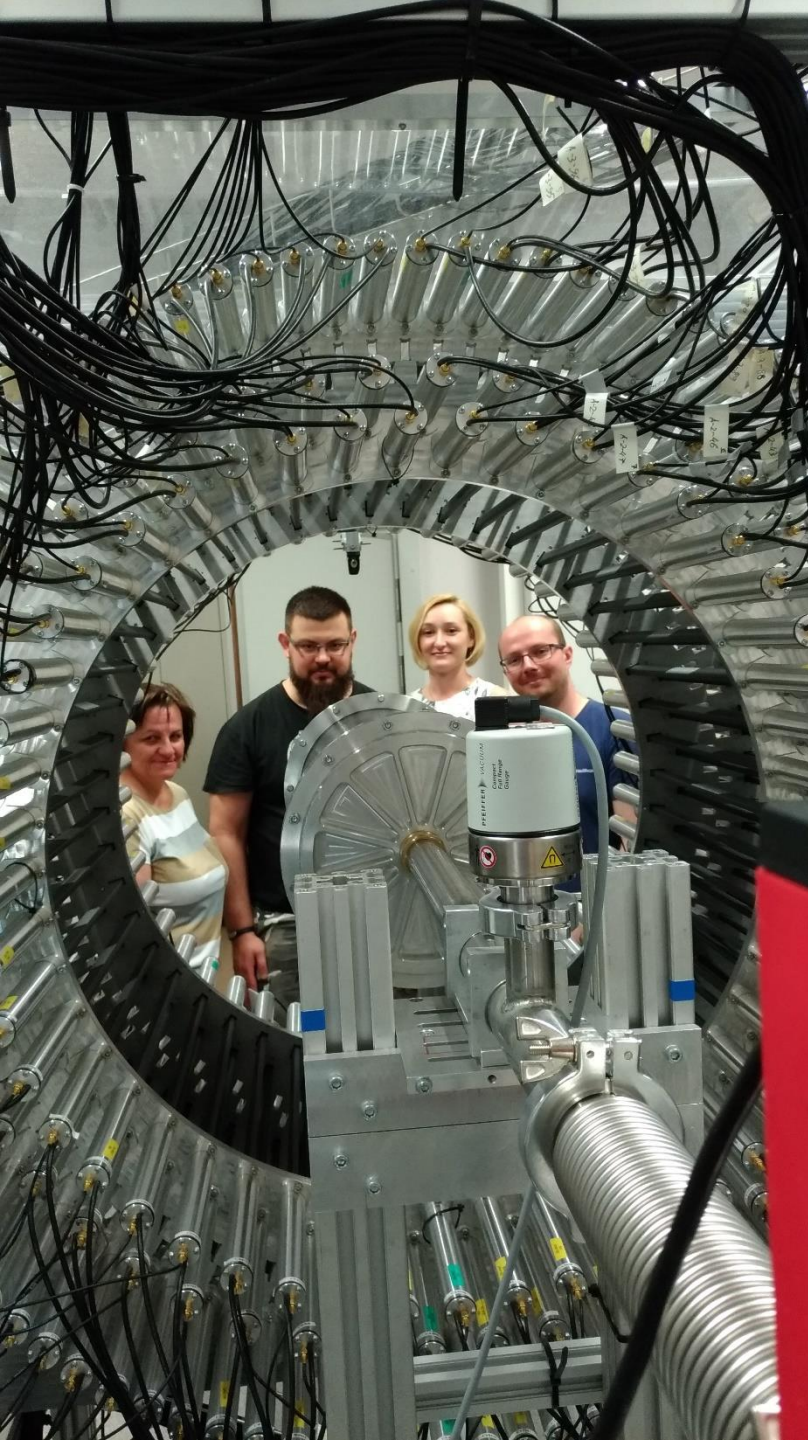


^{22}Na









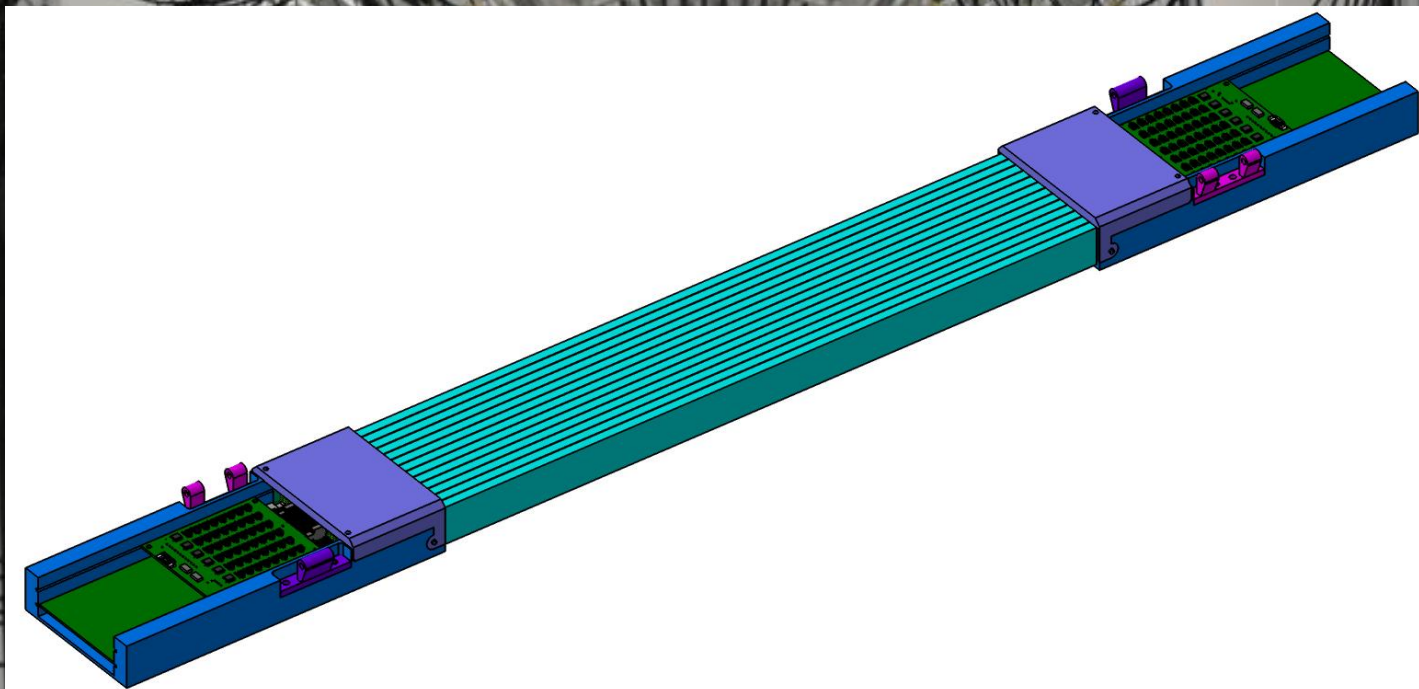


J-PET

Jagiellonian PET



J-PET



AFOV: 17 cm \rightarrow 50 cm ; TOF < 450 ps

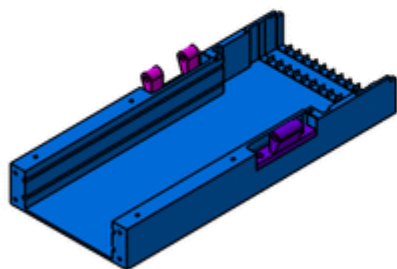


J-PET

Jagiellonian PET



J-PET



AFOV: 50 cm ; TOF < 450 ps (FWHM)

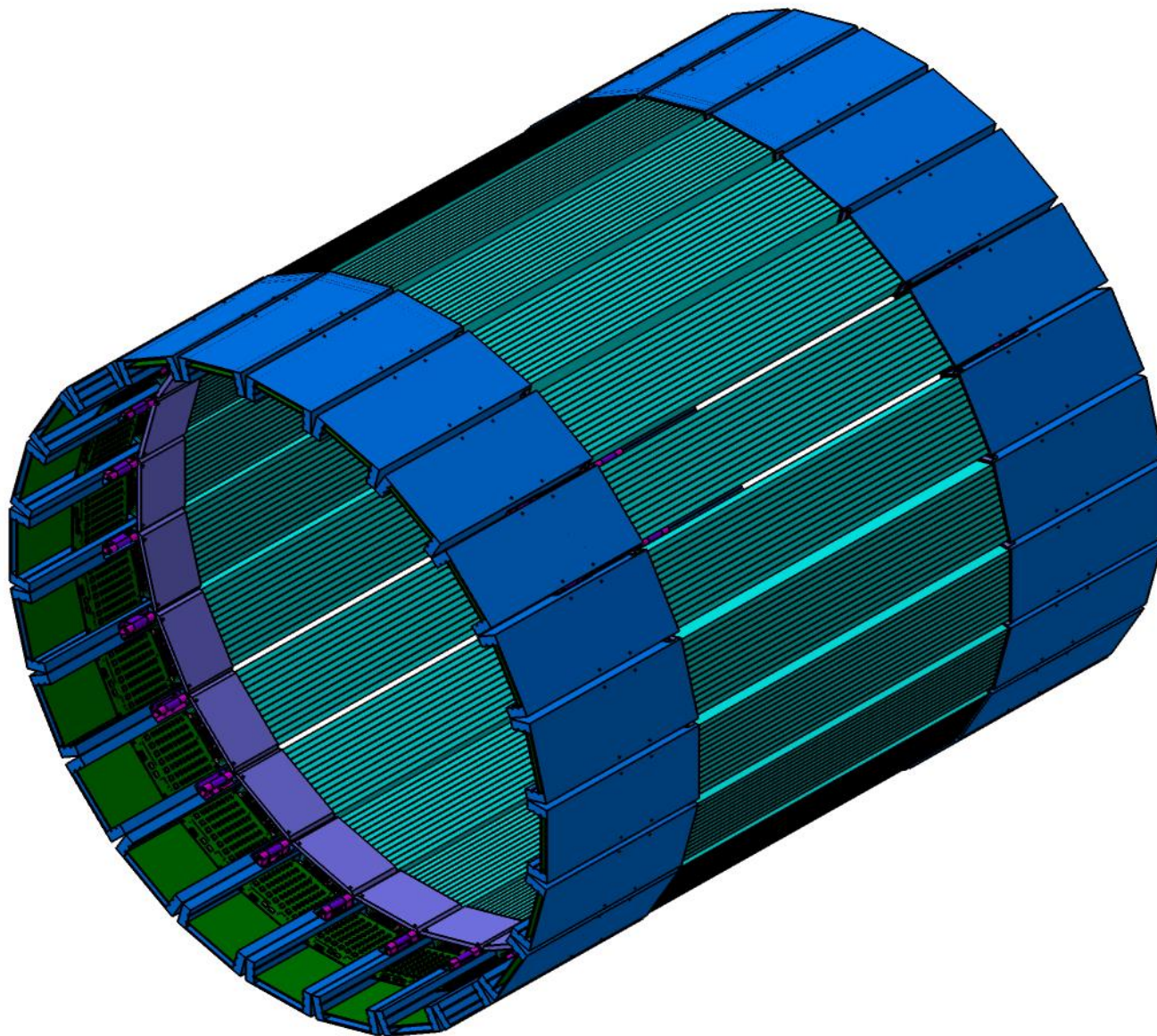


J-PET

Jagiellonian PET



J-PET



AFOV: 50 cm ; TOF < 450 ps (FWHM)

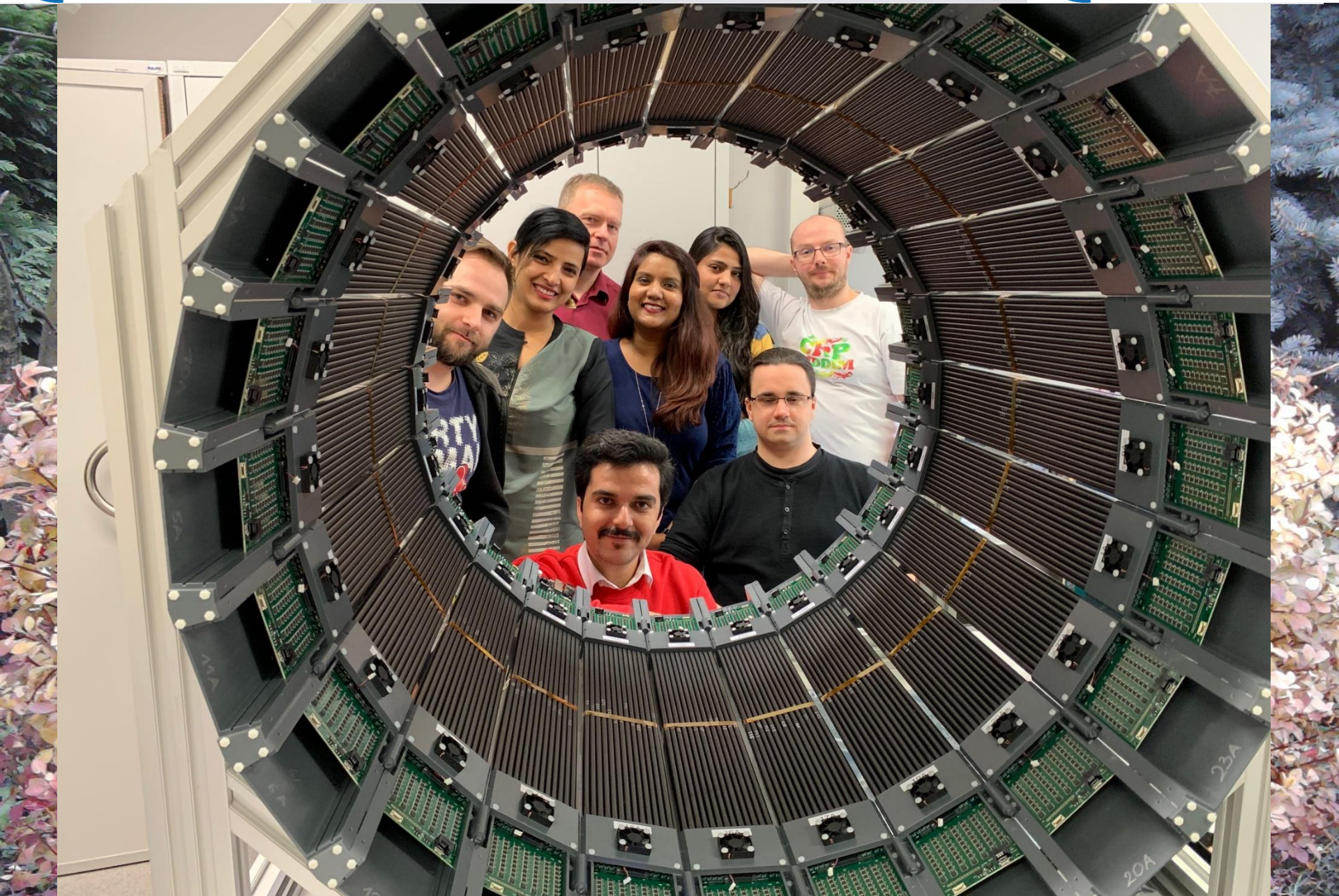


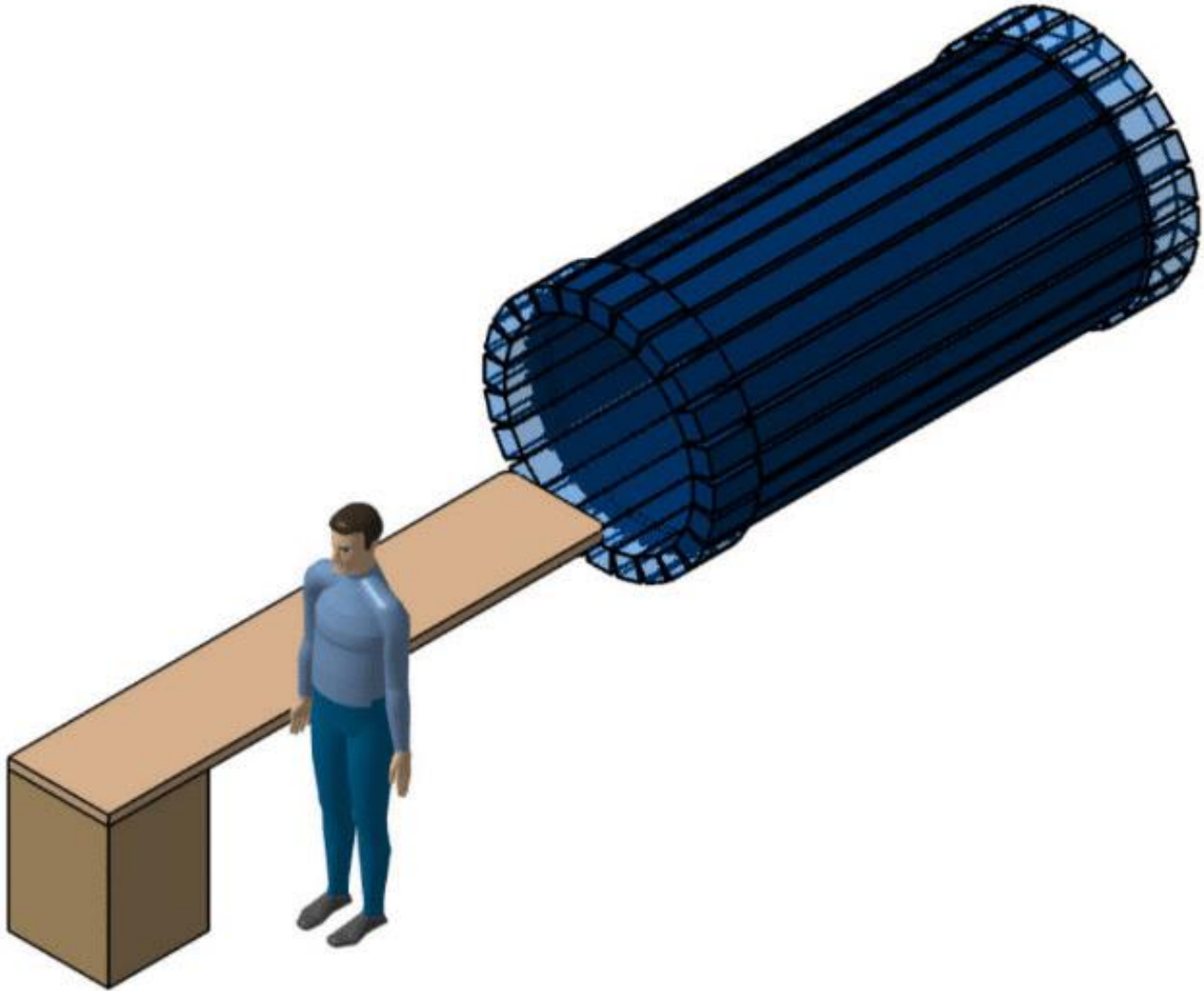
J-PET

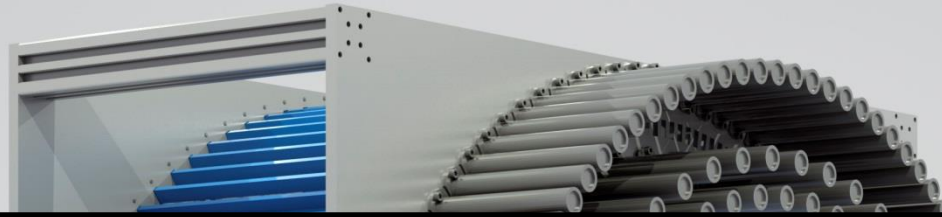
Jagiellonian PET



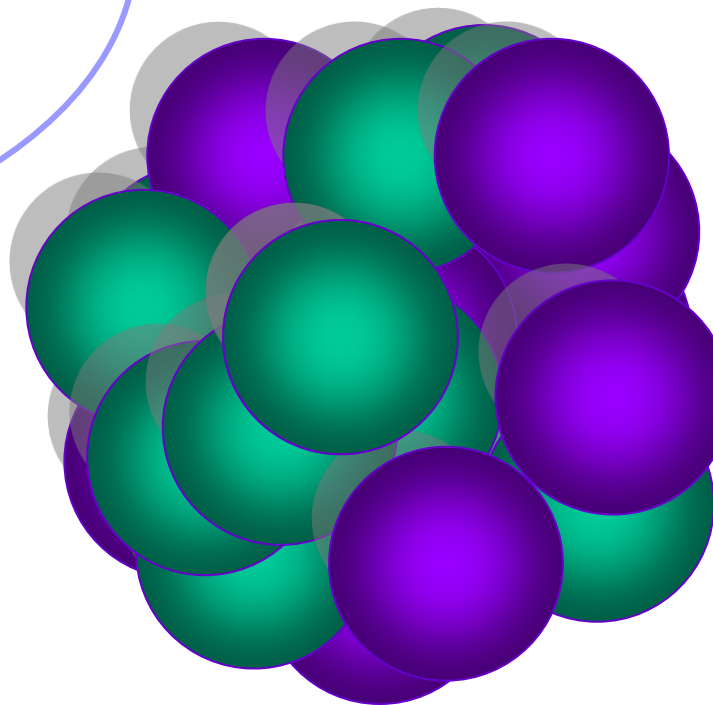
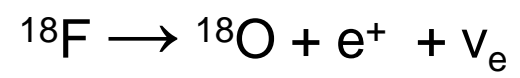
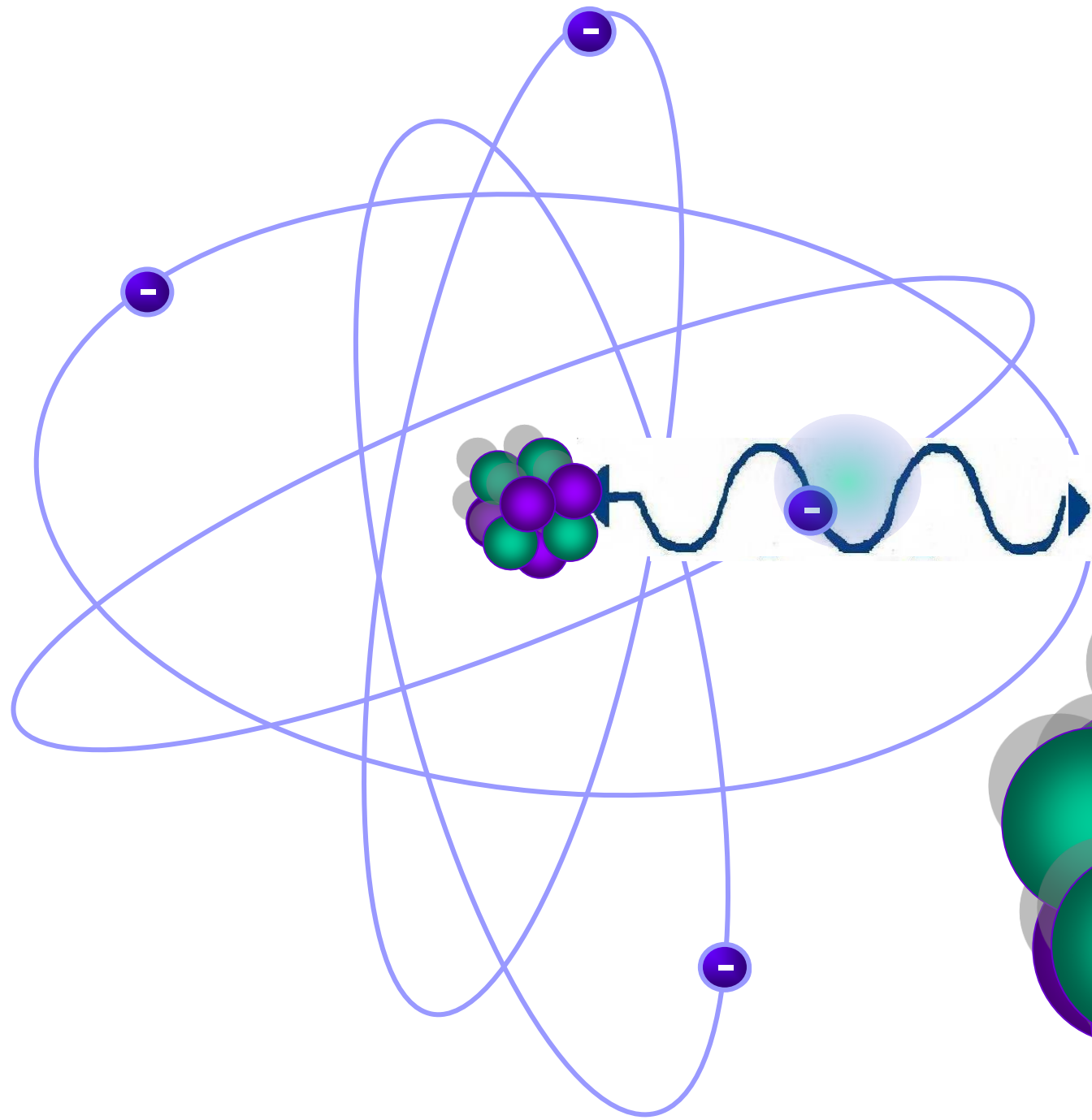
J-PET





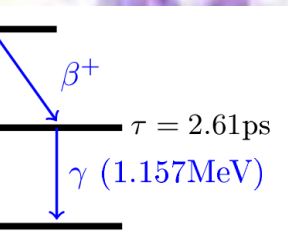
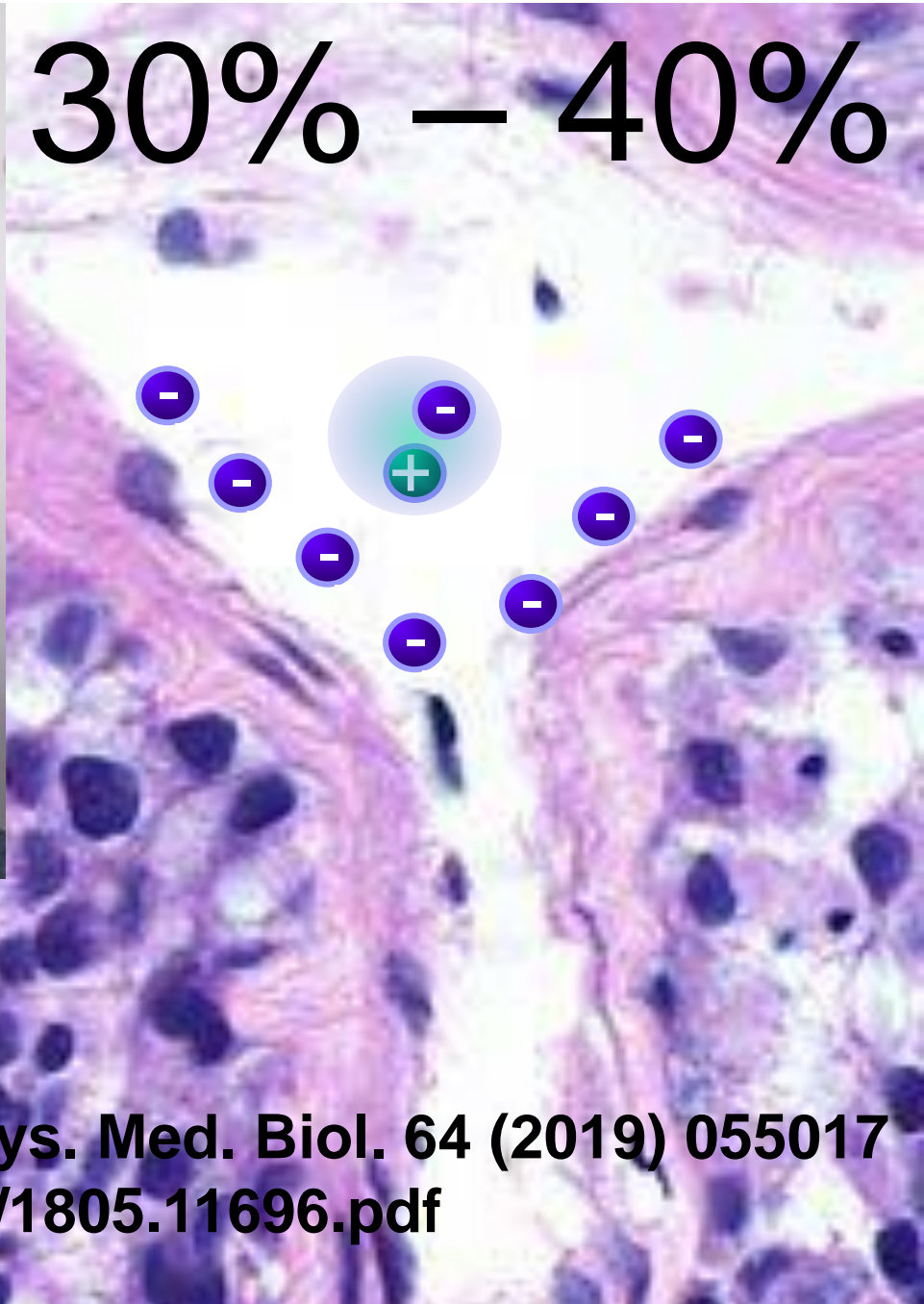


- **PET**
- **Jagiellonian-PET (J-PET)**
- **Positronium imaging (PET & PALS)**
- **Discrete symmetries**
- **Quantum Entanglement Tomograph**
- **Hadrontherapy beam monitoring**



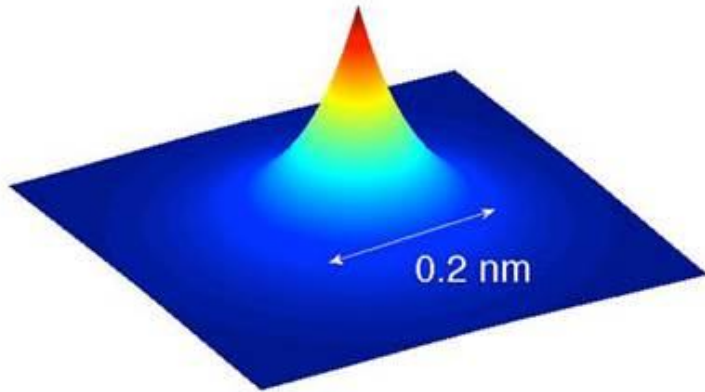


30% – 40%

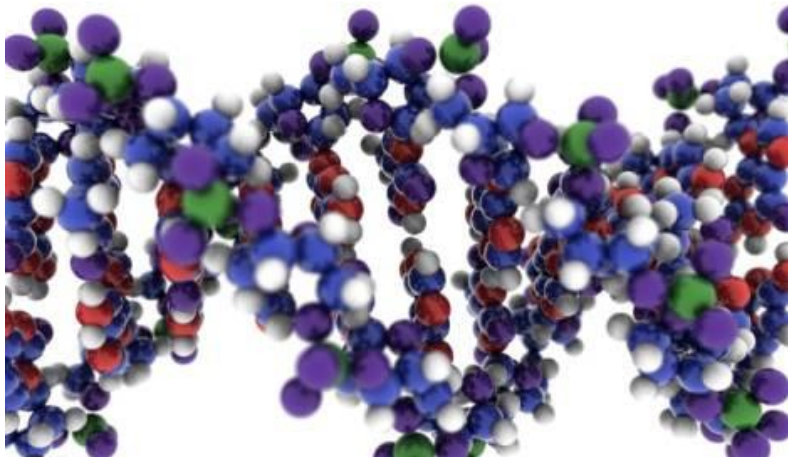


J-PET: P. M et al., Phys. Med. Biol. 64 (2019) 055017
<https://arxiv.org/pdf/1805.11696.pdf>

positronium



Y.H. Wang et al., Phys. Rev. A 89 (2014) 043624,
<http://www.chem-eng.kyushu-u.ac.jp/e/research.html>





	1S_0	3S_1
L	0	0



	1S_0	3S_1
L	0	0
S	0	1

$$S = 0 \quad \downarrow\uparrow - \uparrow\downarrow$$

$$S = 1 \quad \begin{matrix} \uparrow\uparrow \\ \uparrow\downarrow + \downarrow\uparrow \\ \downarrow\downarrow \end{matrix}$$



	1S_0	3S_1
L	0	0
S	0	1
C	+	-

$$S = 0 \quad \downarrow\uparrow - \uparrow\downarrow$$

$$S = 1 \quad \begin{matrix} \uparrow\uparrow \\ \downarrow\uparrow + \uparrow\downarrow \\ \downarrow\downarrow \end{matrix}$$



		1S_0	3S_1
	L	0	0
	S	0	1
	C	+	-
$L=0 \rightarrow$	P	-	-
	CP	-	+

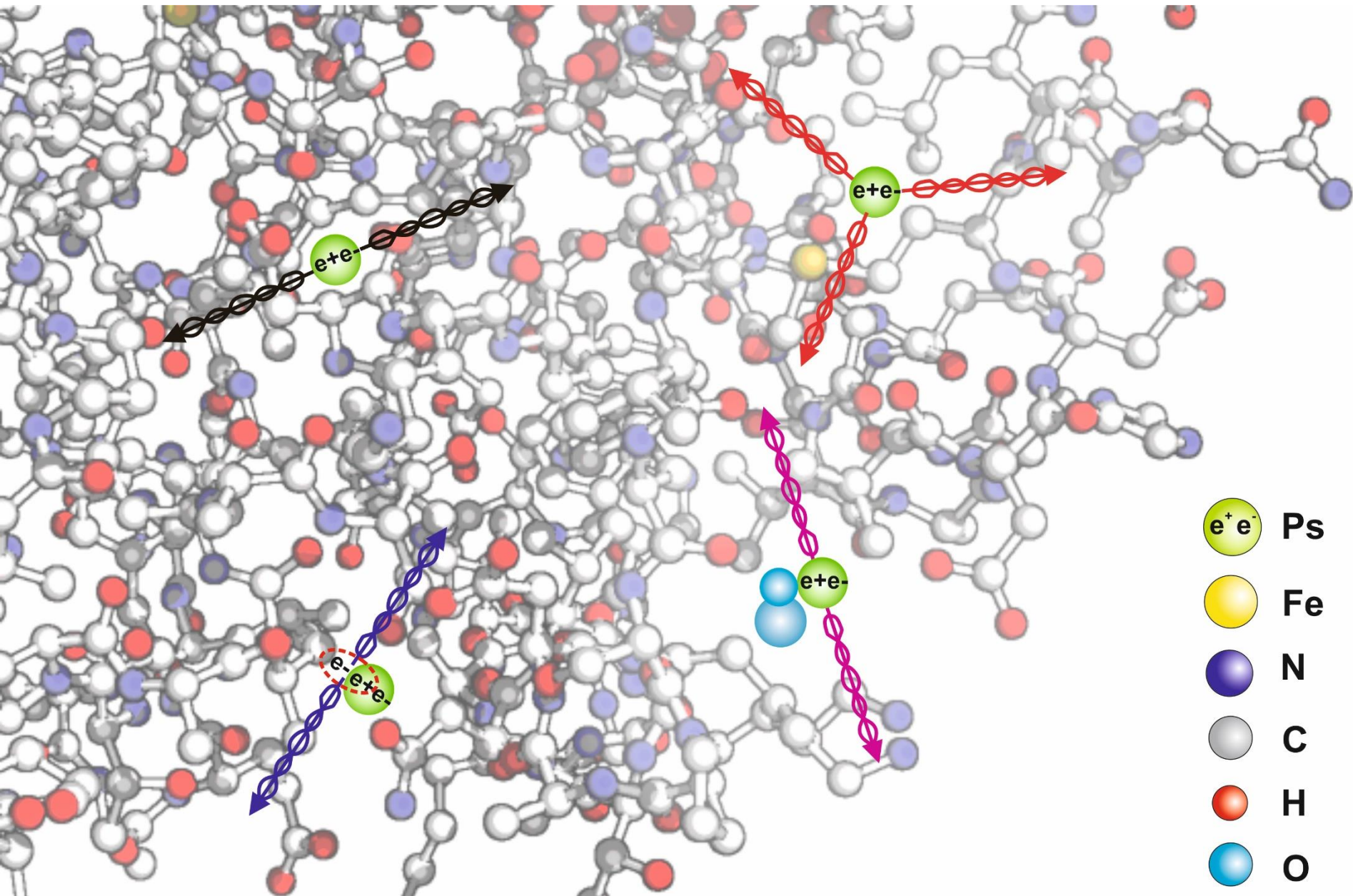
$$S = 0 \quad \downarrow\uparrow - \uparrow\downarrow$$

$$S = 1 \quad \uparrow\uparrow$$

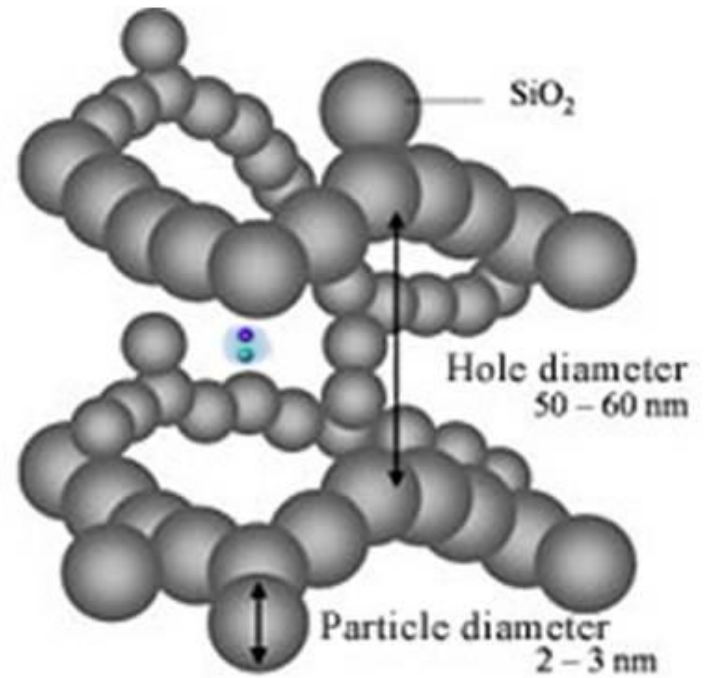
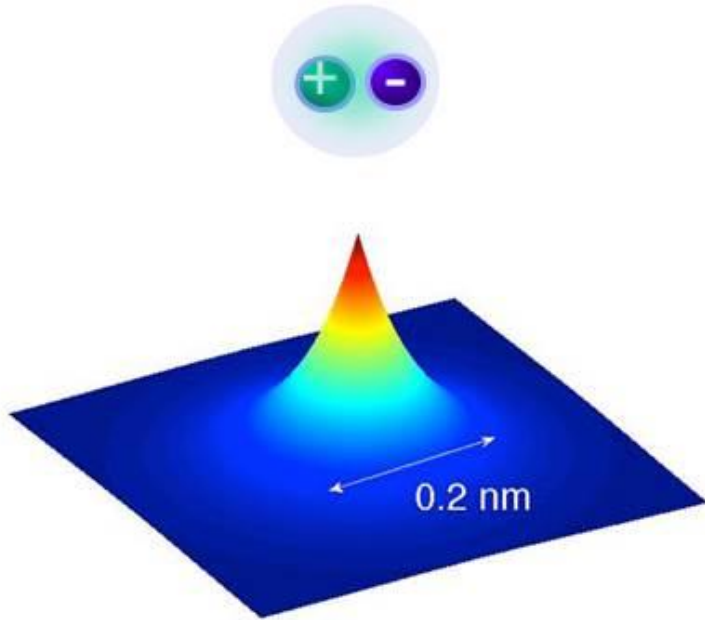
$$S = 1 \quad \downarrow\uparrow + \uparrow\downarrow$$

$$S = 1 \quad \downarrow\downarrow$$

Model of the hemoglobin molecule



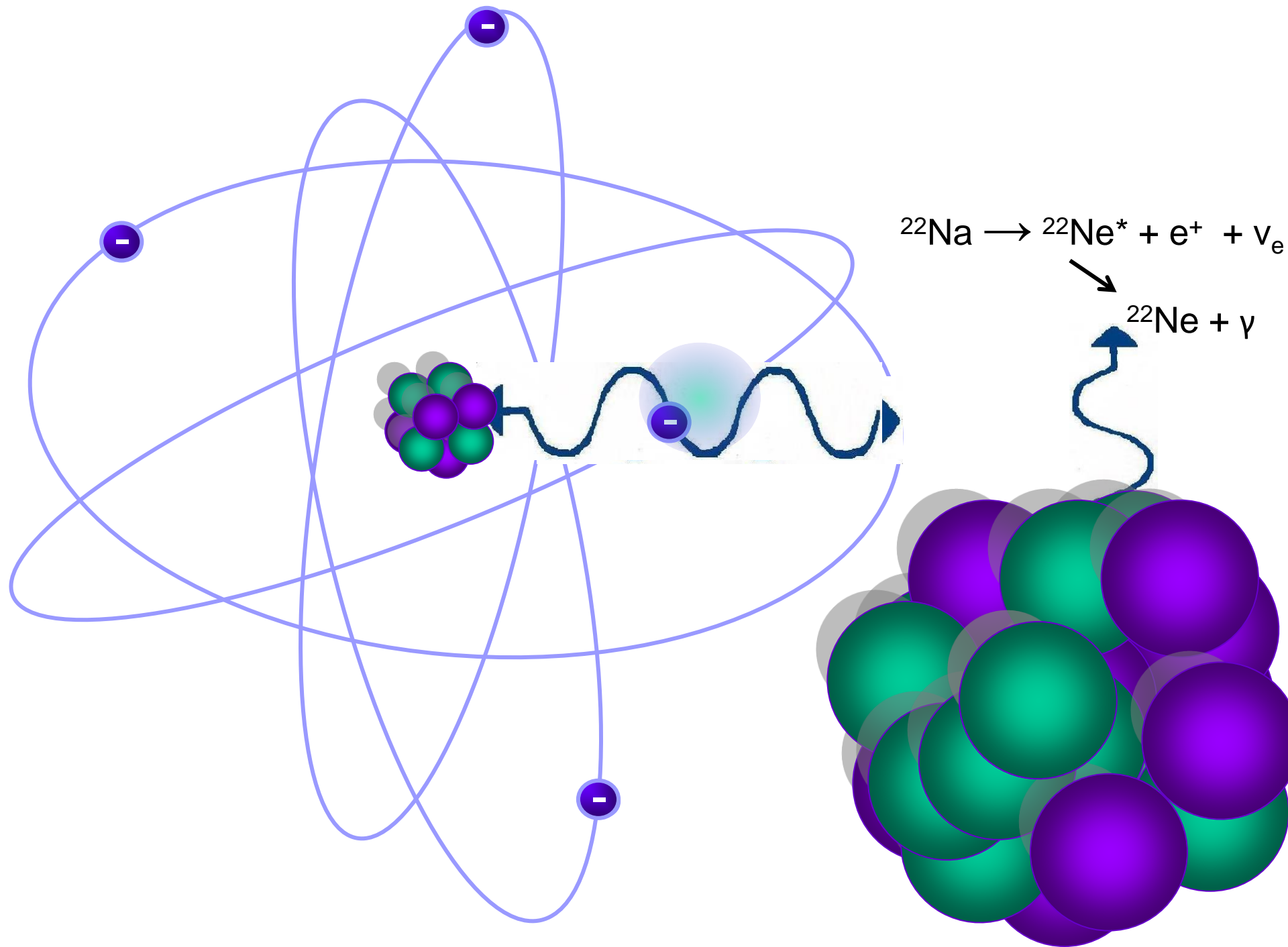
positronium

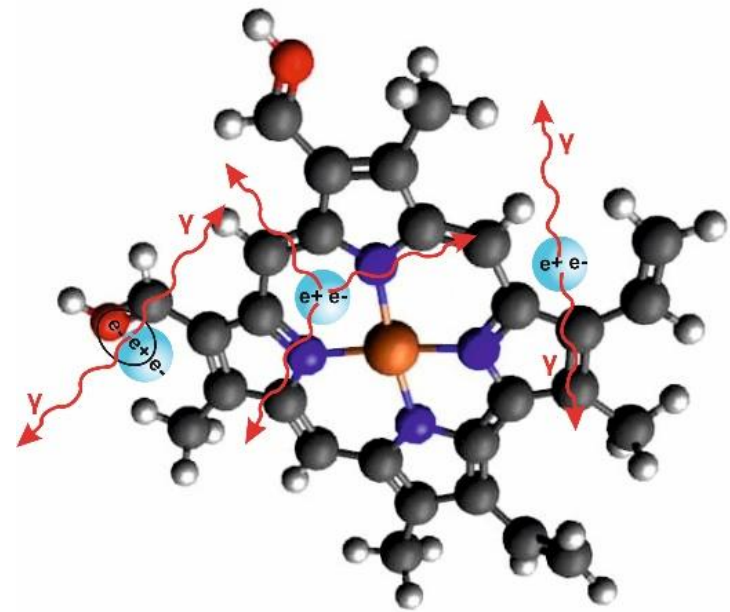
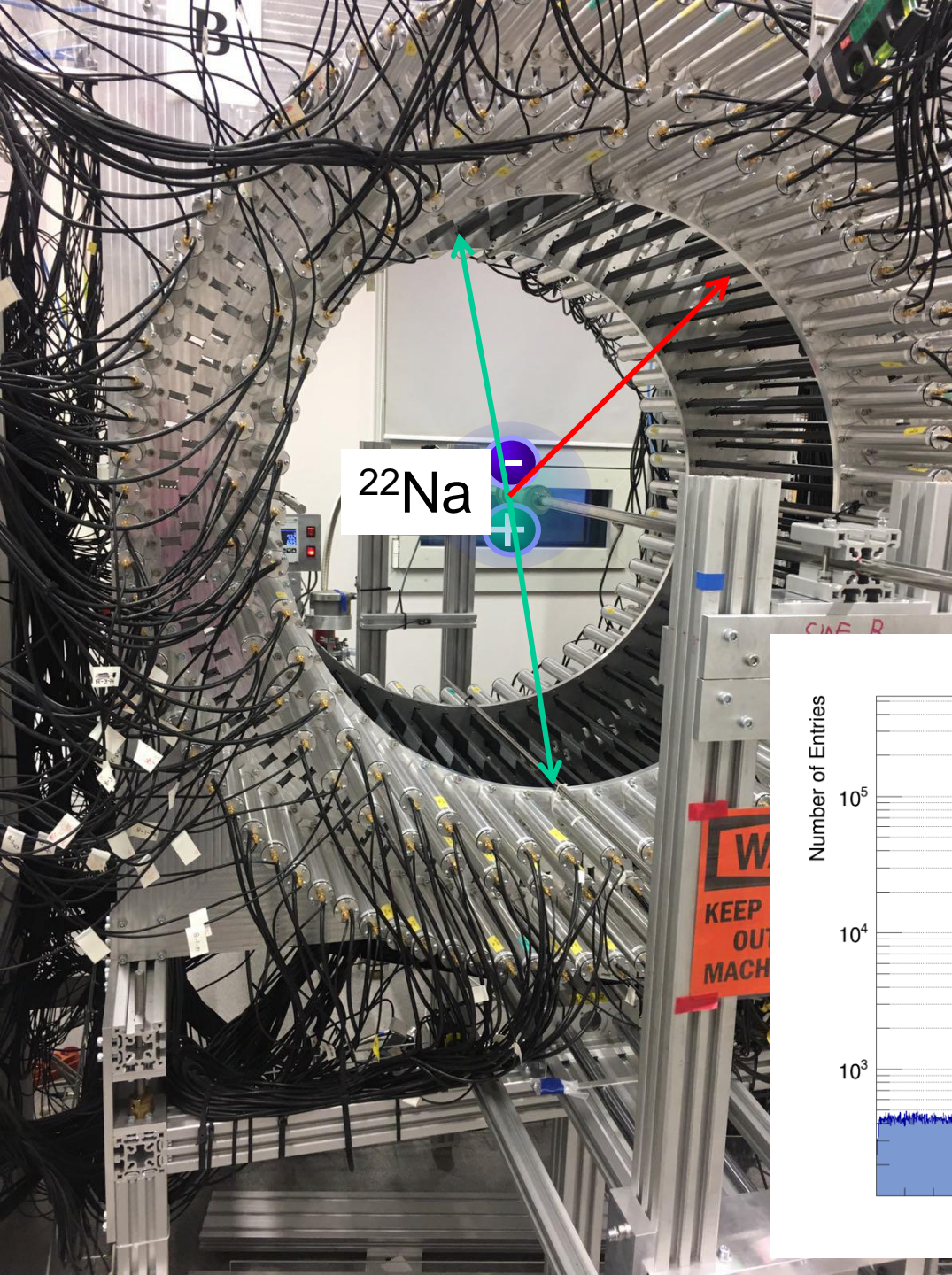


Y.H. Wang et al., Phys. Rev. A 89 (2014) 043624,
<http://www.chem-eng.kyushu-u.ac.jp/e/research.html>

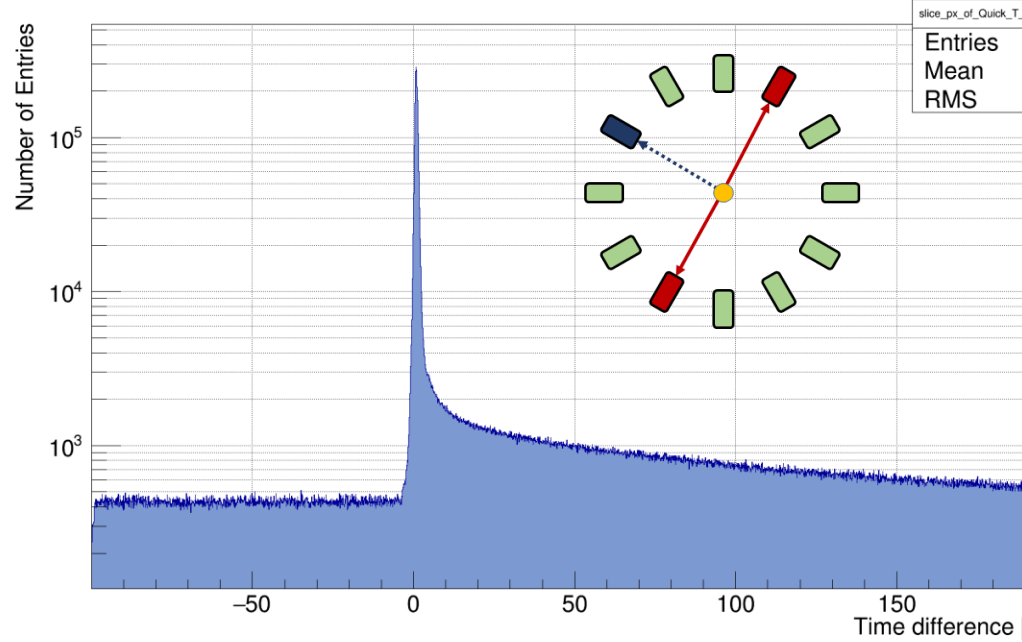


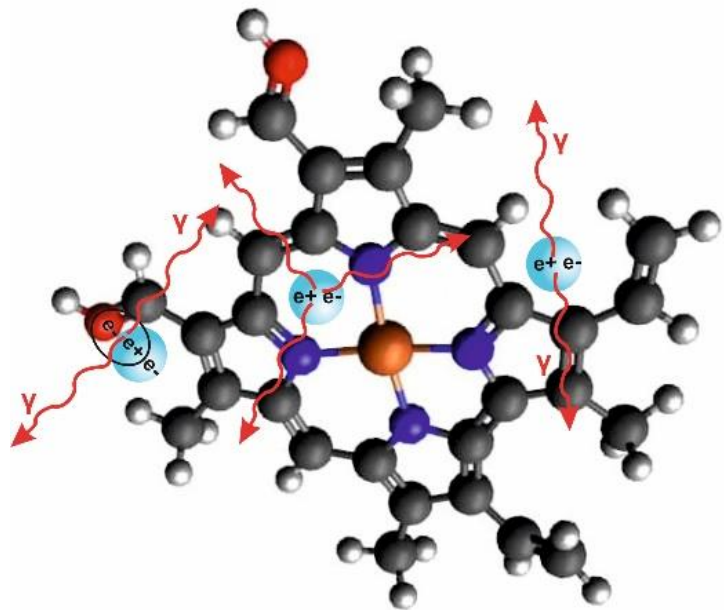
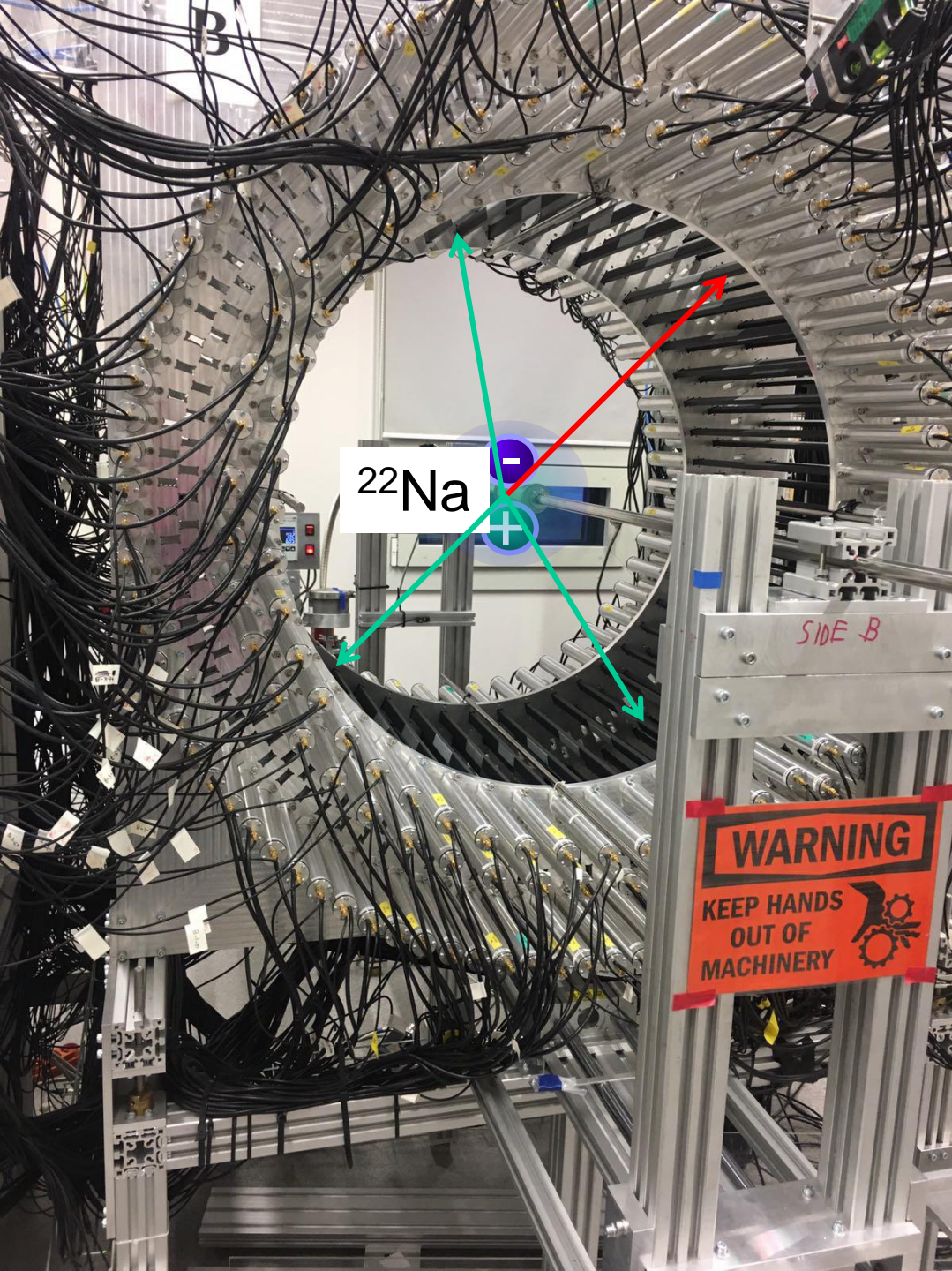


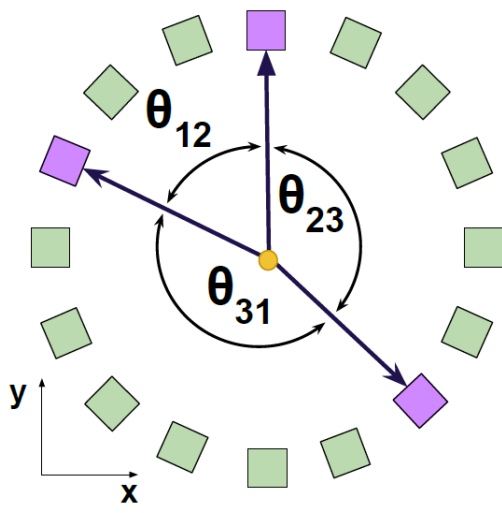




ProjectionX of biny=[1,200] [y=-0.5..199.5]

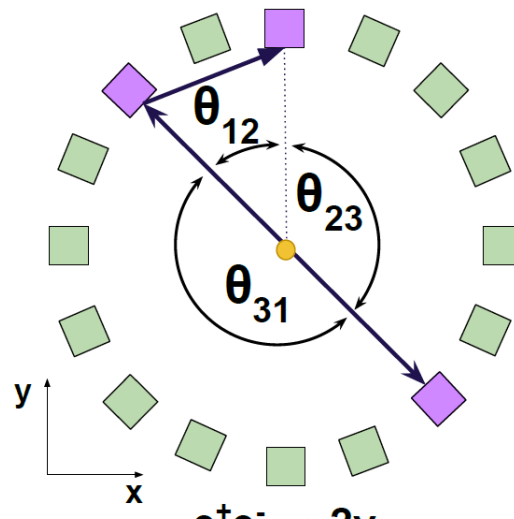






$o\text{-Ps} \rightarrow 3\gamma$

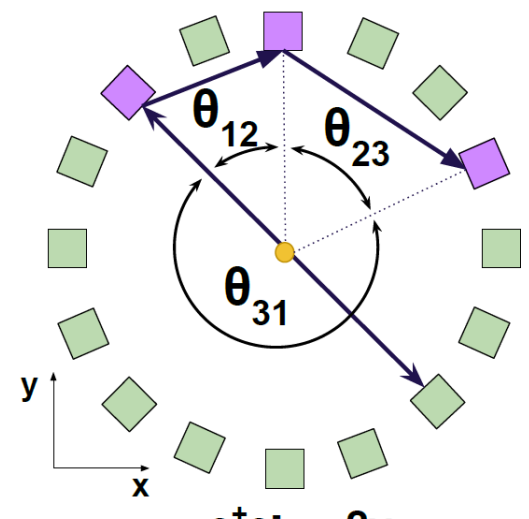
$$\theta_{23} + \theta_{12} > 180$$



$e^+e^- \rightarrow 2\gamma$

single scattered

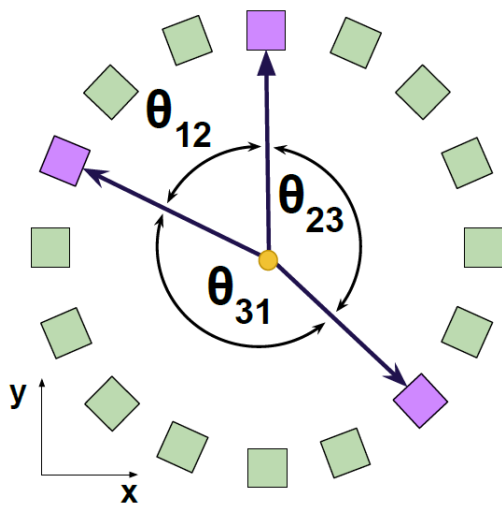
$$\theta_{23} + \theta_{12} = 180$$



$e^+e^- \rightarrow 2\gamma$

double scattered

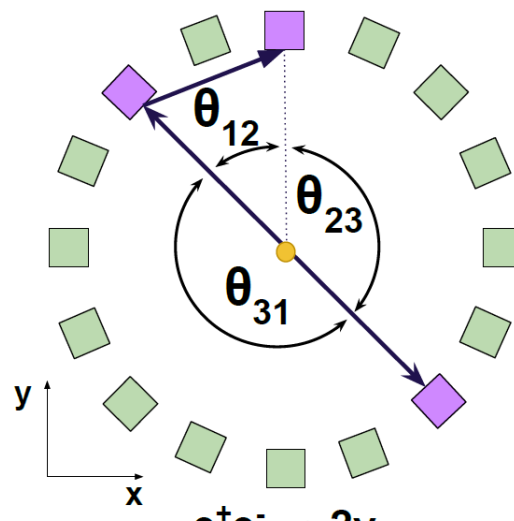
$$\theta_{23} + \theta_{12} < 180$$



$o\text{-Ps} \rightarrow 3\gamma$

$$\theta_{23} + \theta_{12} > 180$$

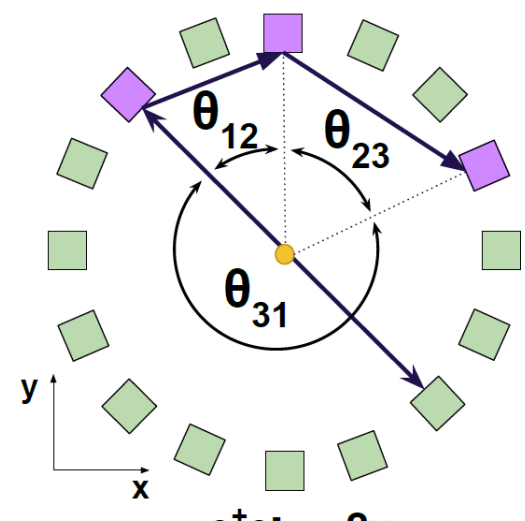
3 Hit angles



$e^+e^- \rightarrow 2\gamma$

single scattered

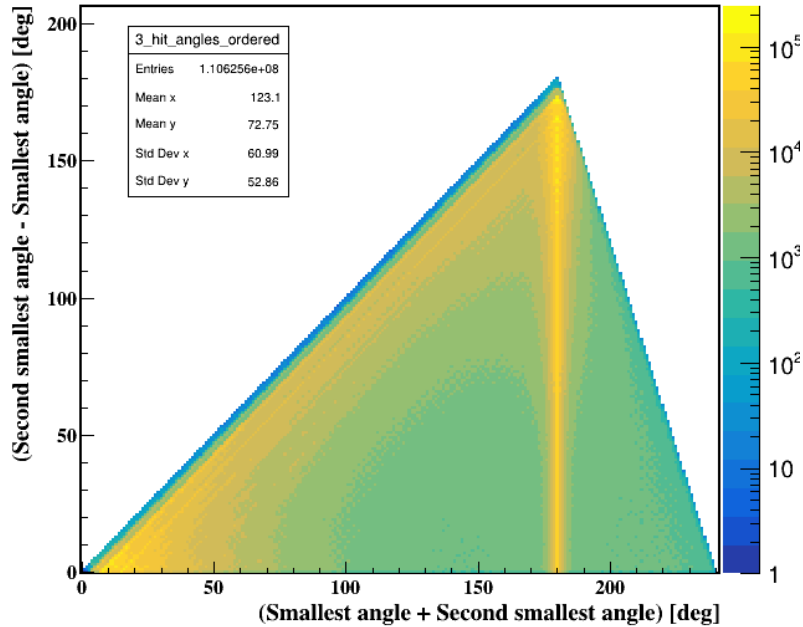
$$\theta_{23} + \theta_{12} = 180$$

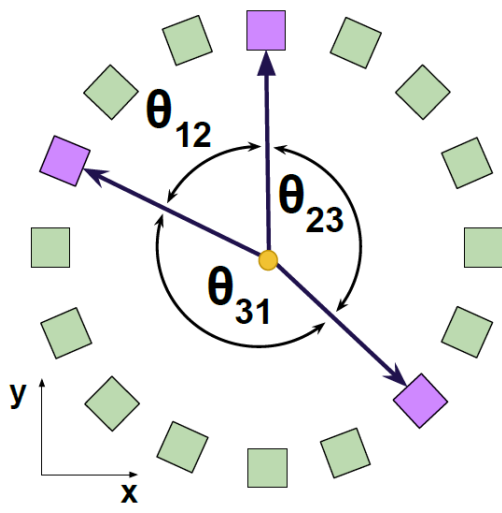


$e^+e^- \rightarrow 2\gamma$

double scattered

$$\theta_{23} + \theta_{12} < 180$$

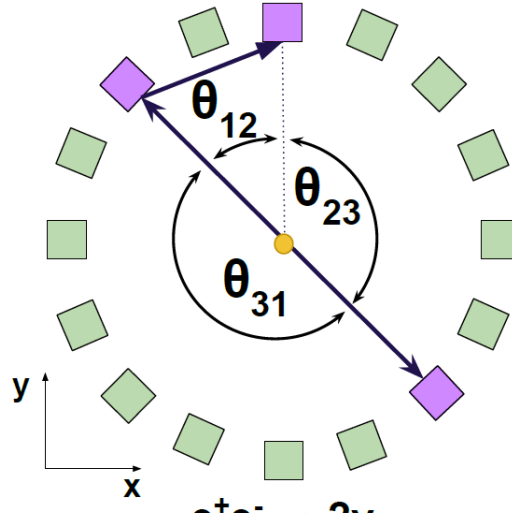




$o\text{-Ps} \rightarrow 3\gamma$

$$\theta_{23} + \theta_{12} > 180$$

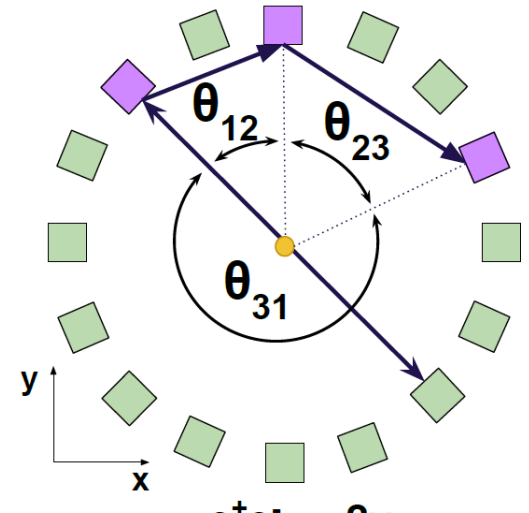
3 Hit angles



$e^+e^- \rightarrow 2\gamma$

single scattered

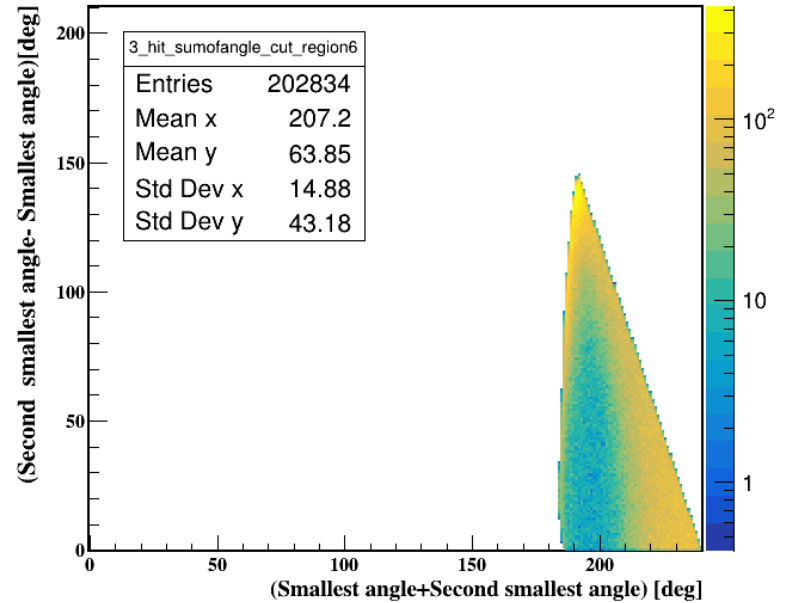
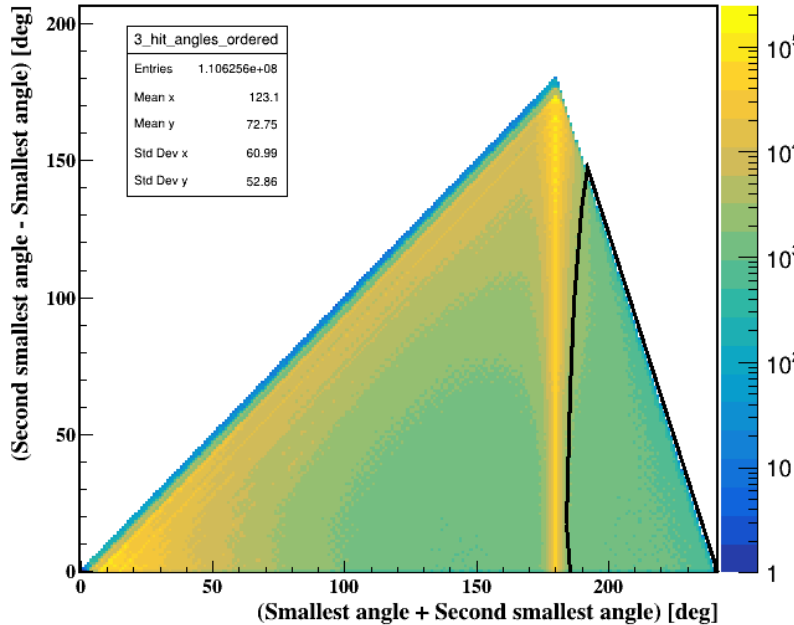
$$\theta_{23} + \theta_{12} = 180$$

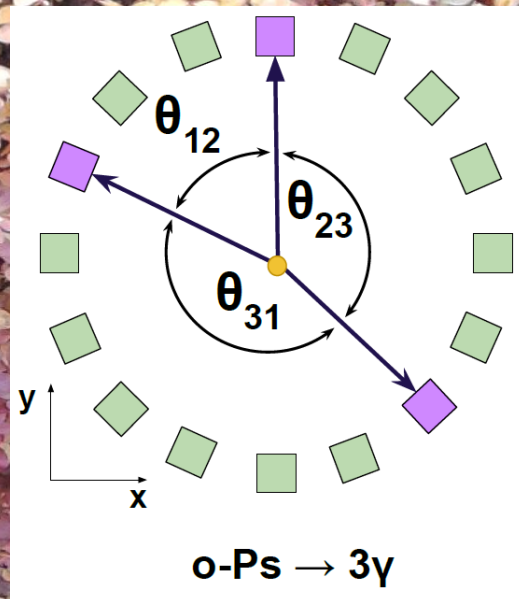
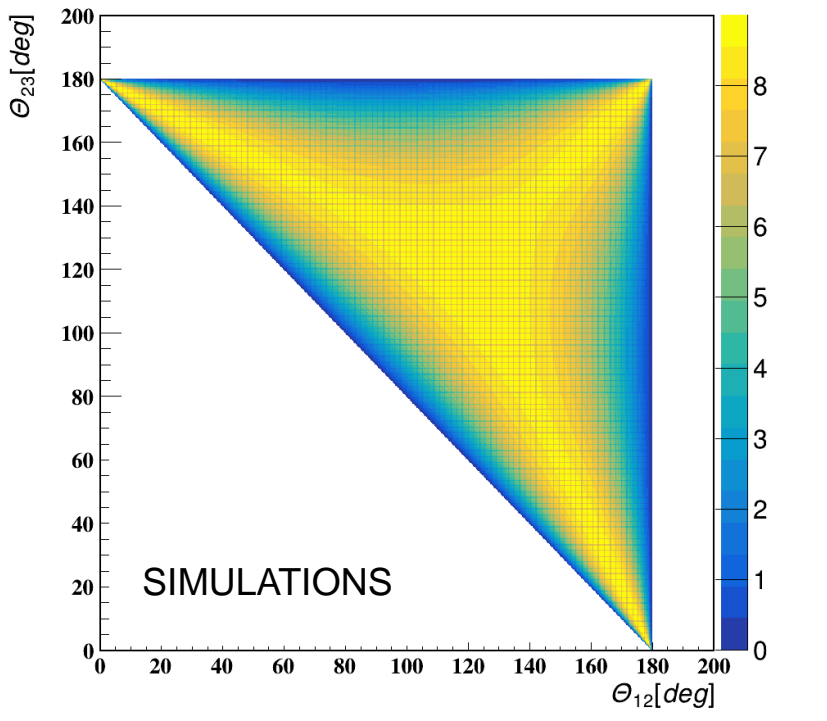
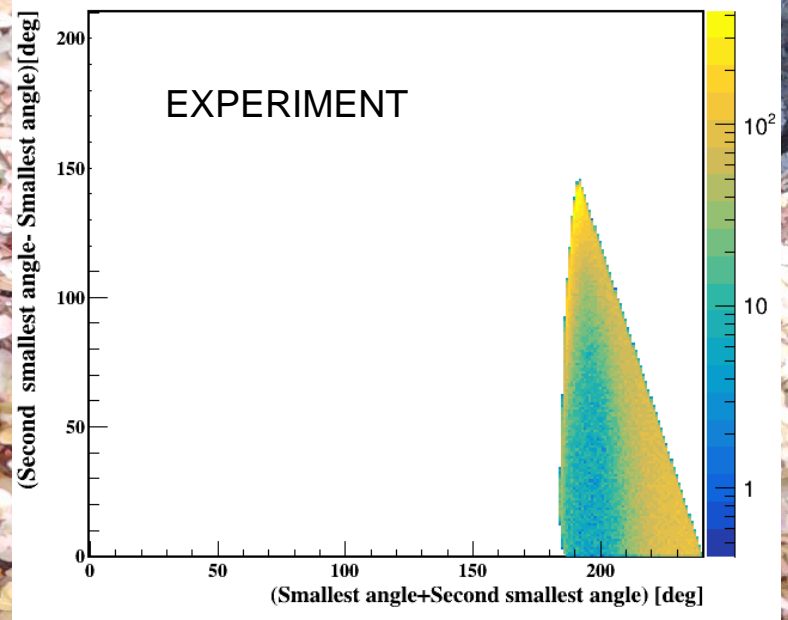
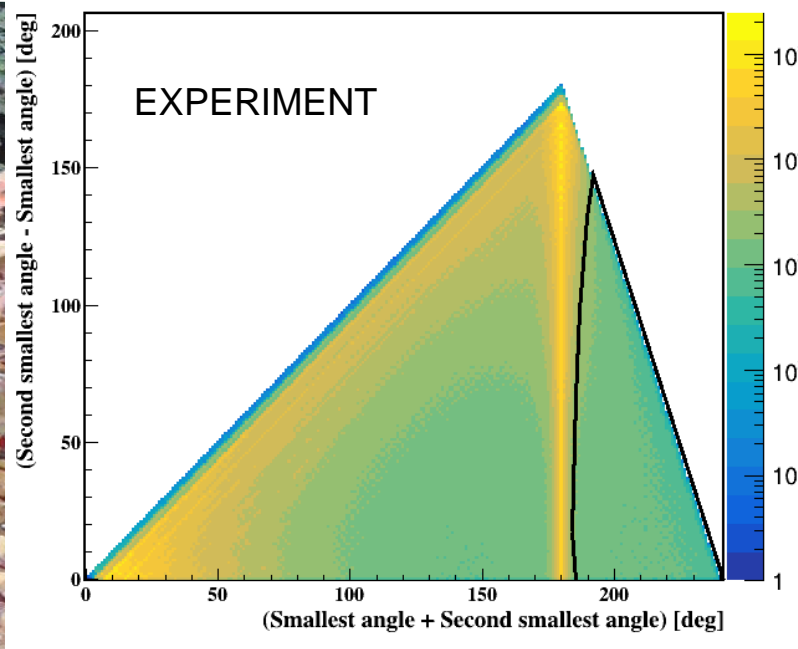


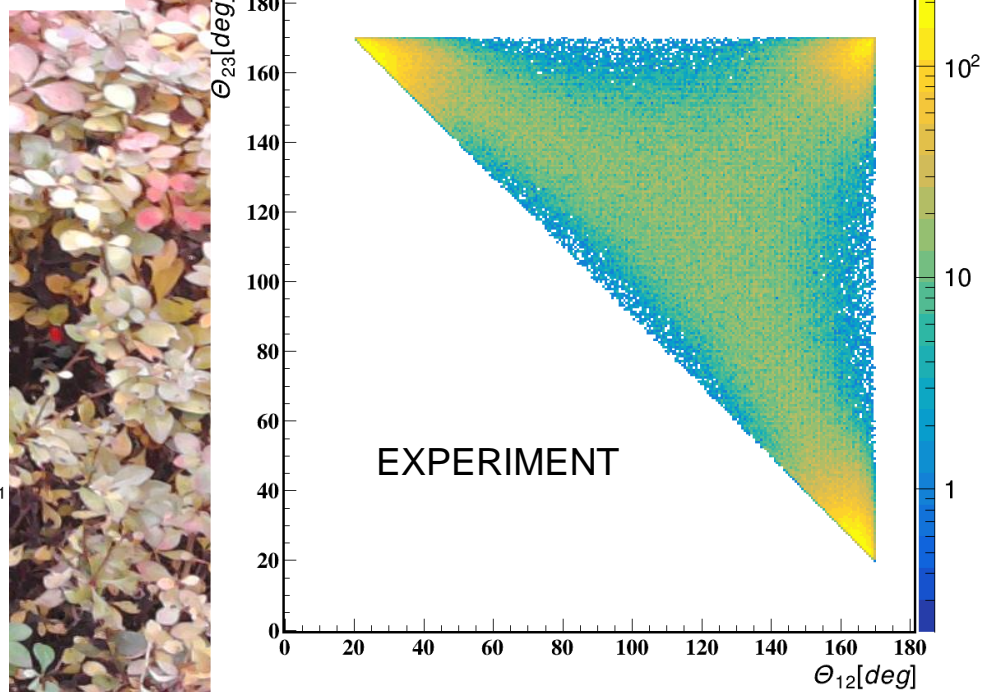
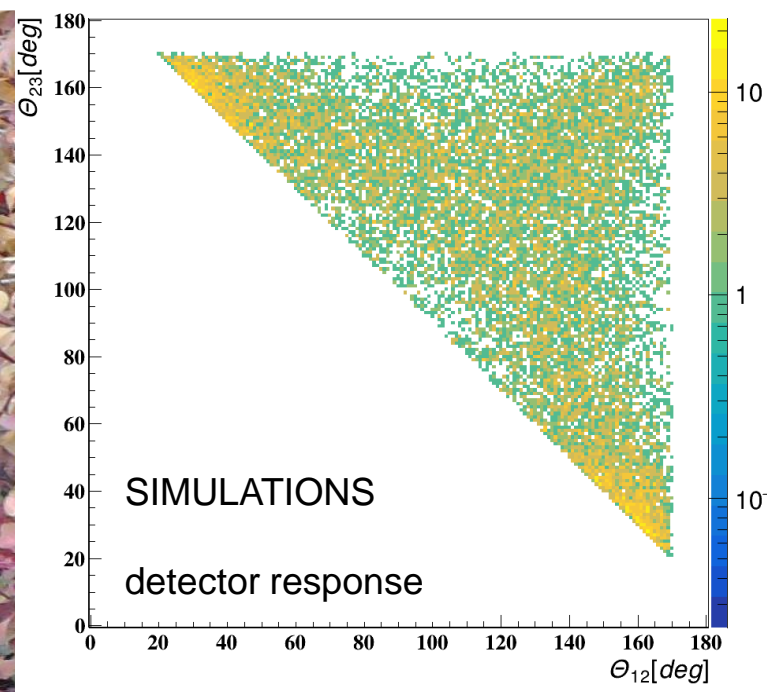
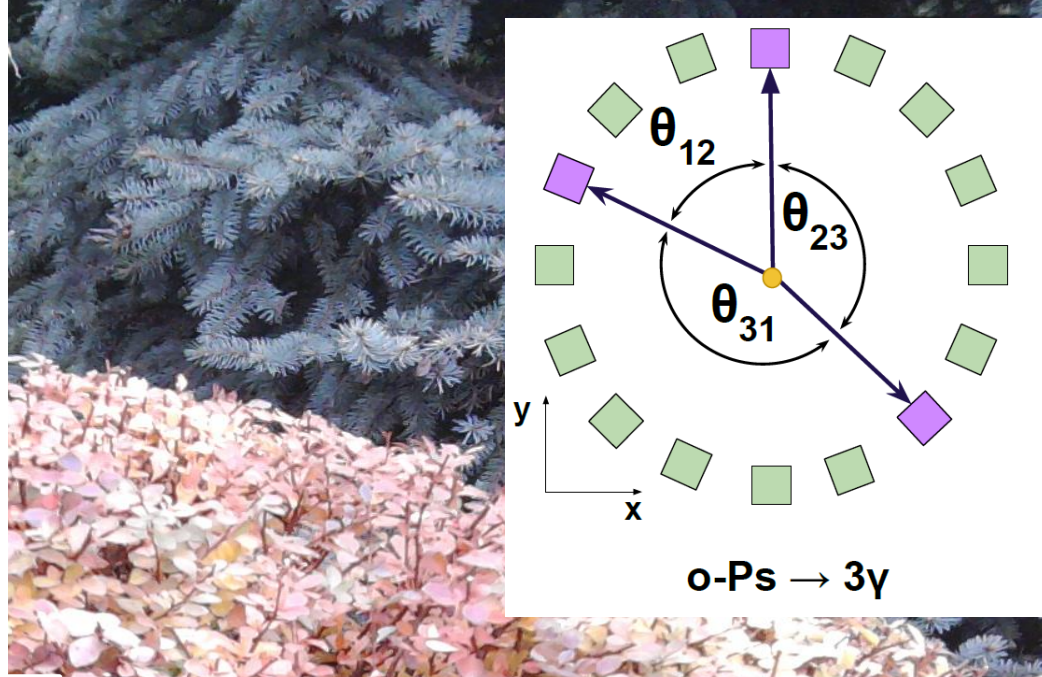
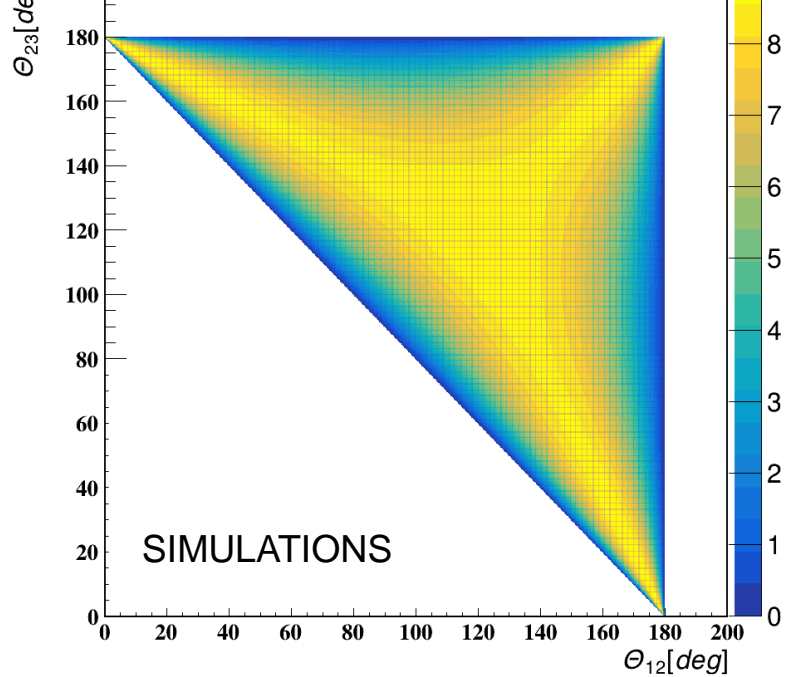
$e^+e^- \rightarrow 2\gamma$

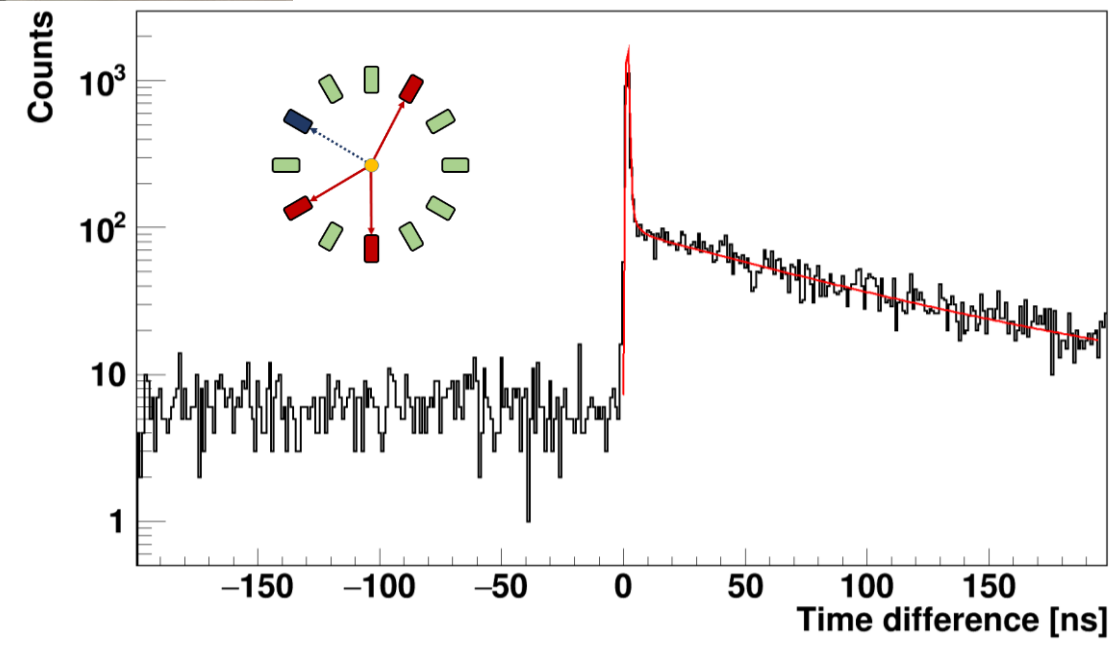
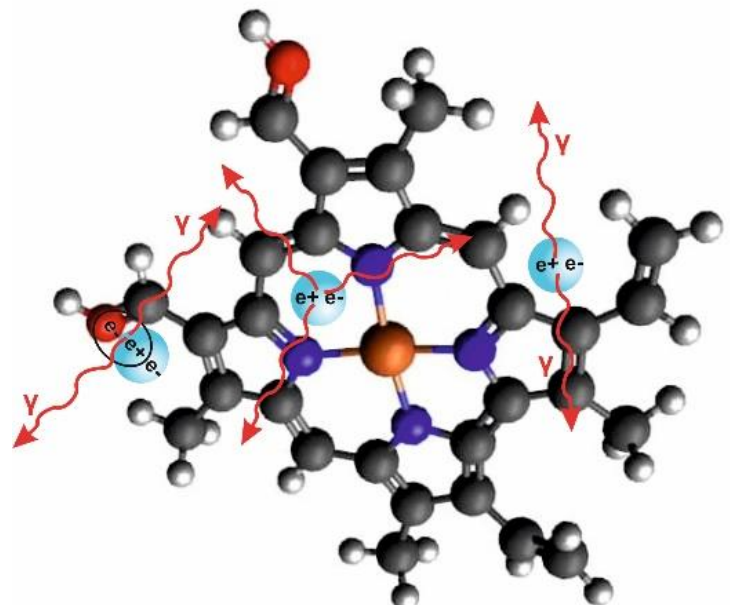
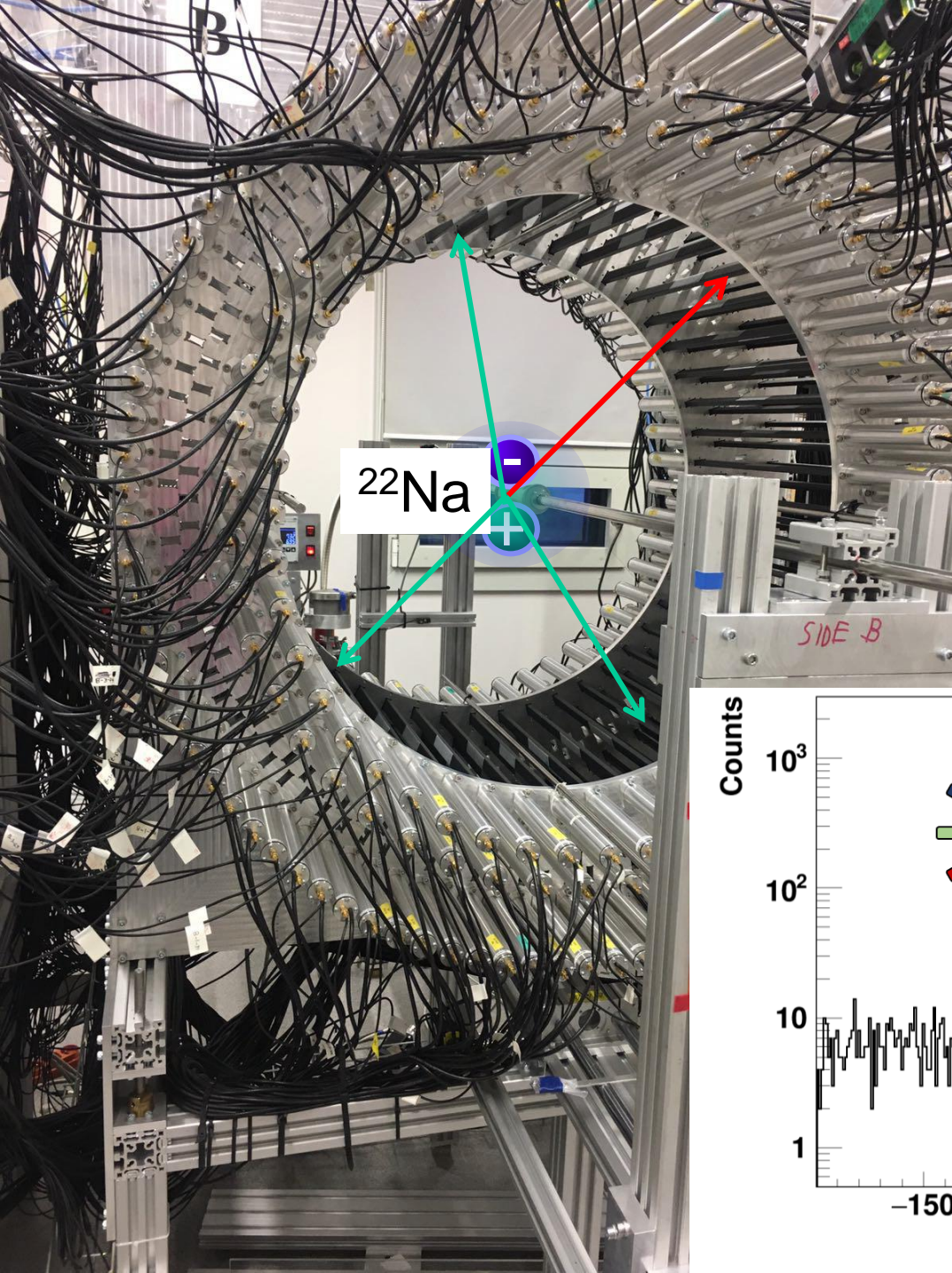
double scattered

$$\theta_{23} + \theta_{12} < 180$$



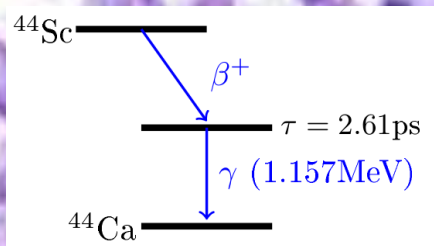
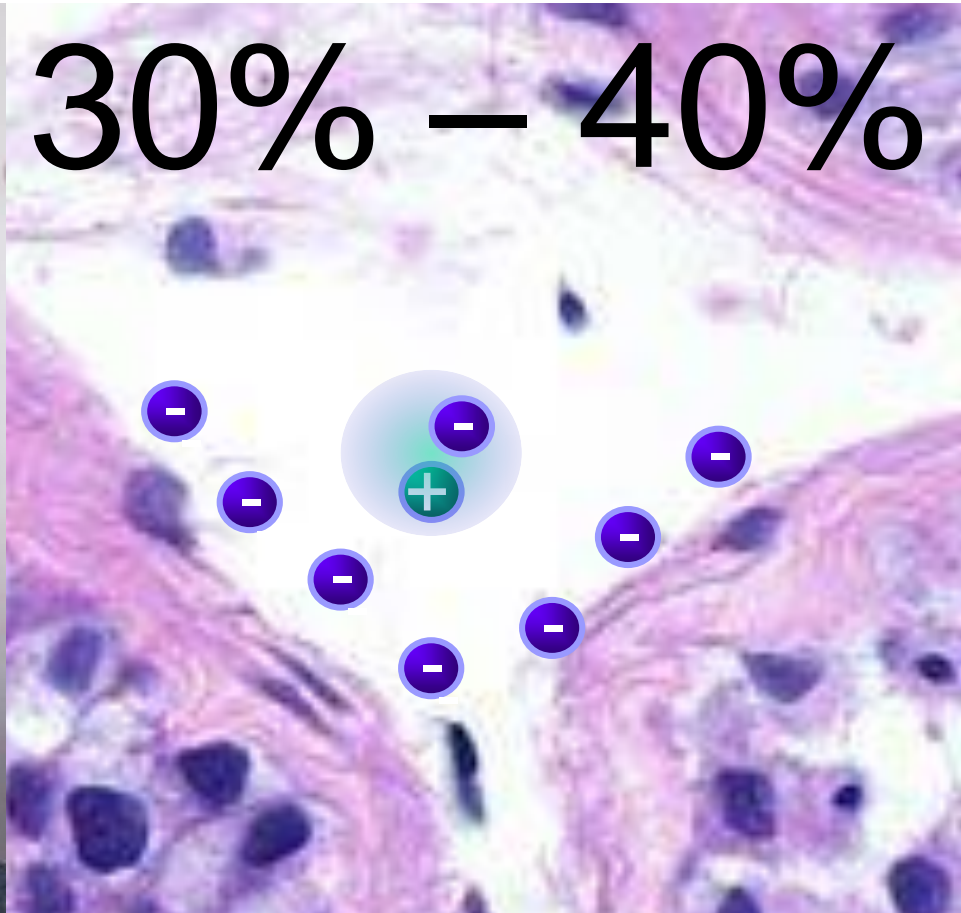








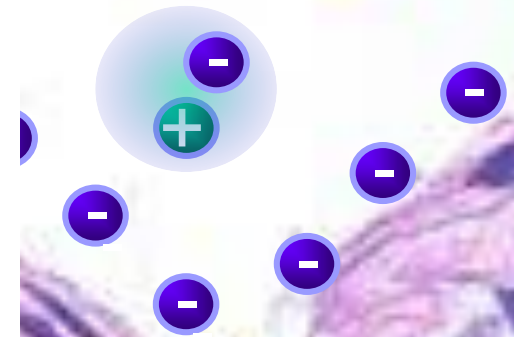
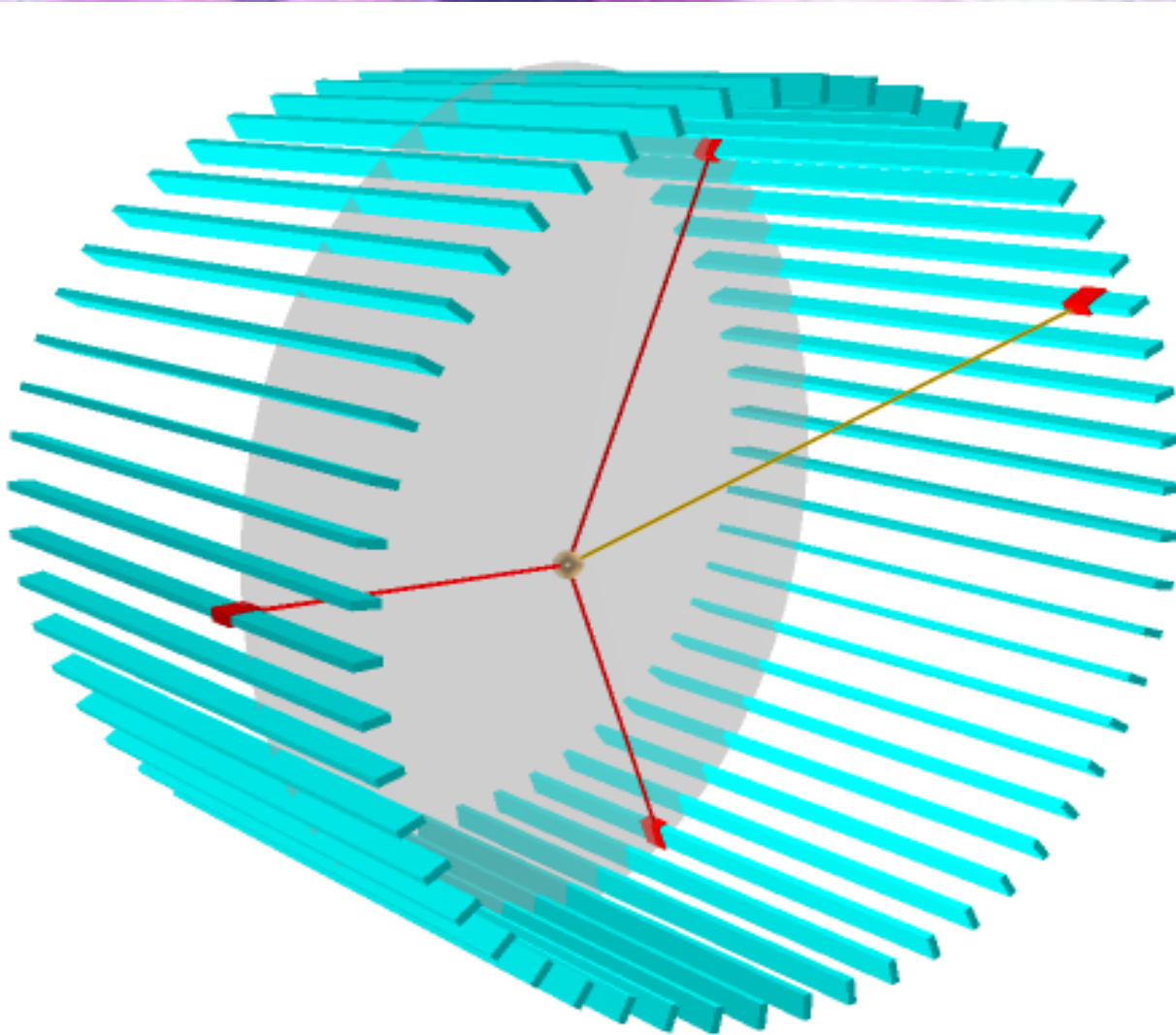
30% – 40%



J-PET: P. M et al., Phys. Med. 64 (2019) 055017
<https://arxiv.org/pdf/1805.11696.pdf>

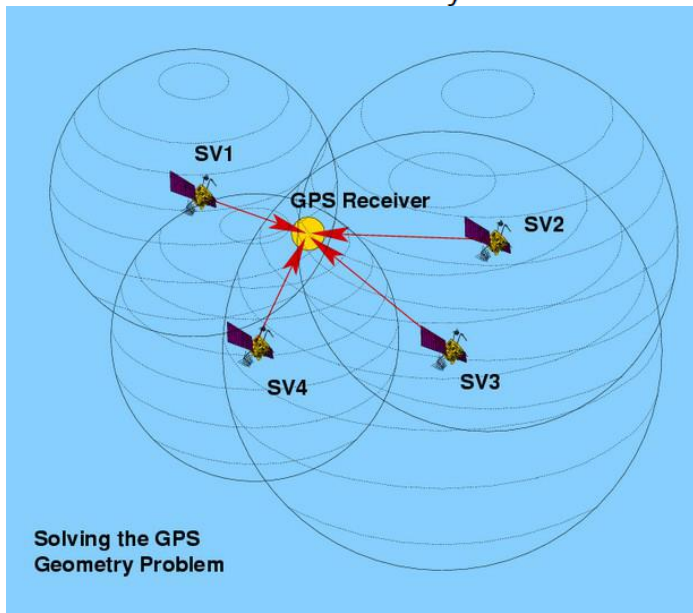
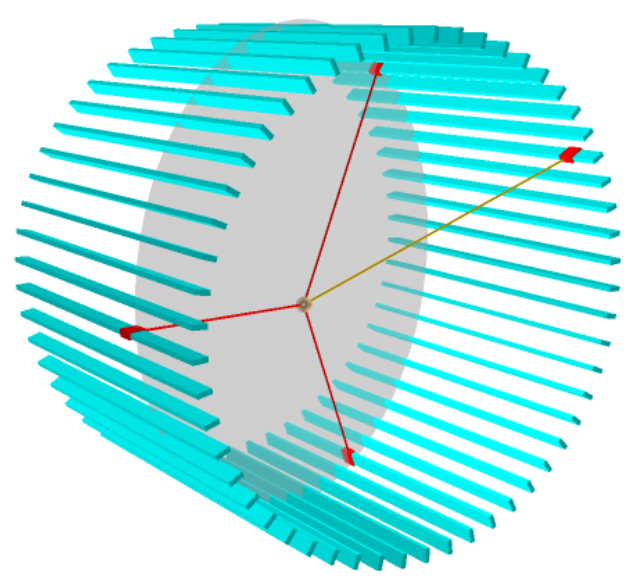
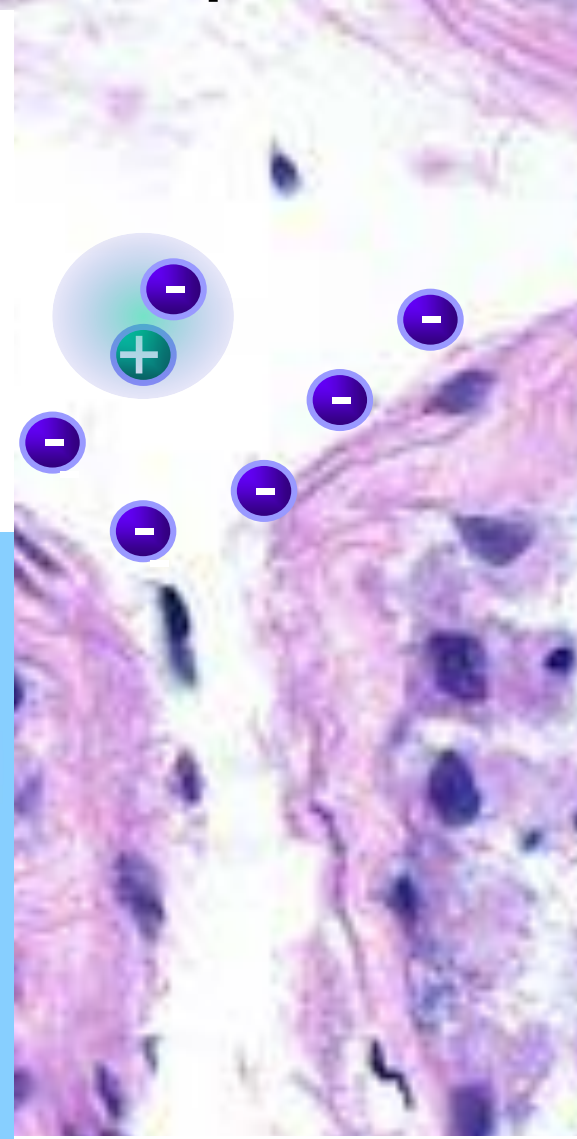
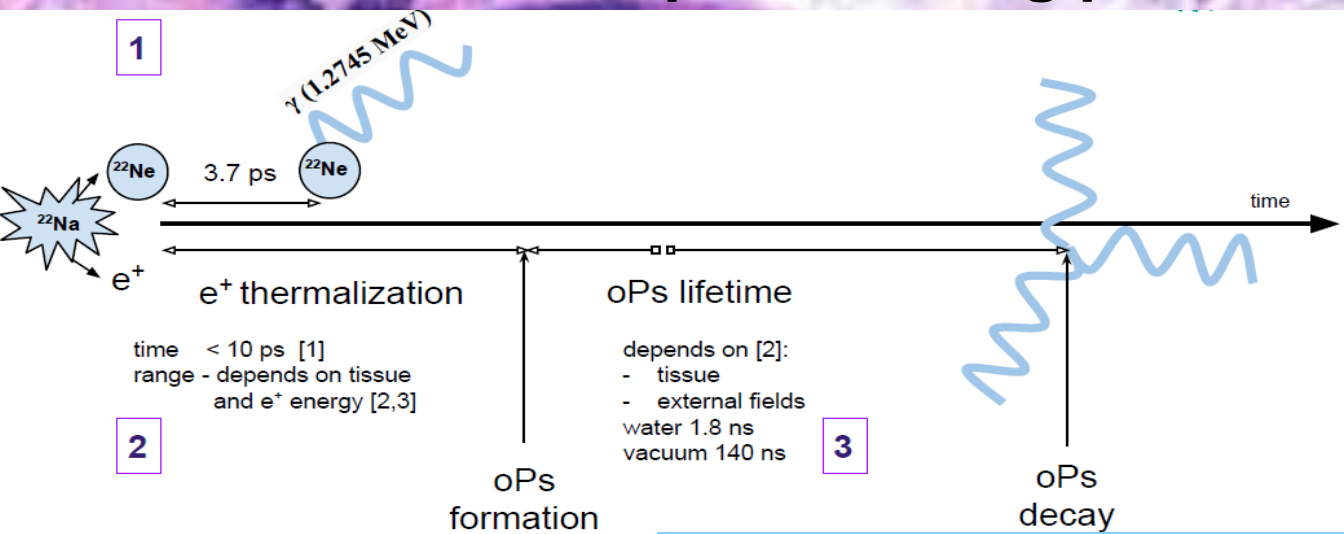
Ortho-positronium life-time tomography

P. M., Patent US 9,851,456, PCT/EP2014/068374

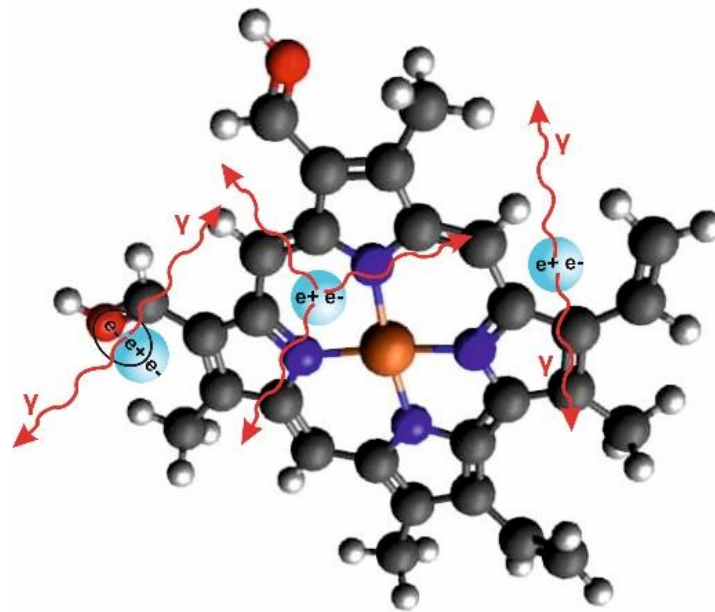
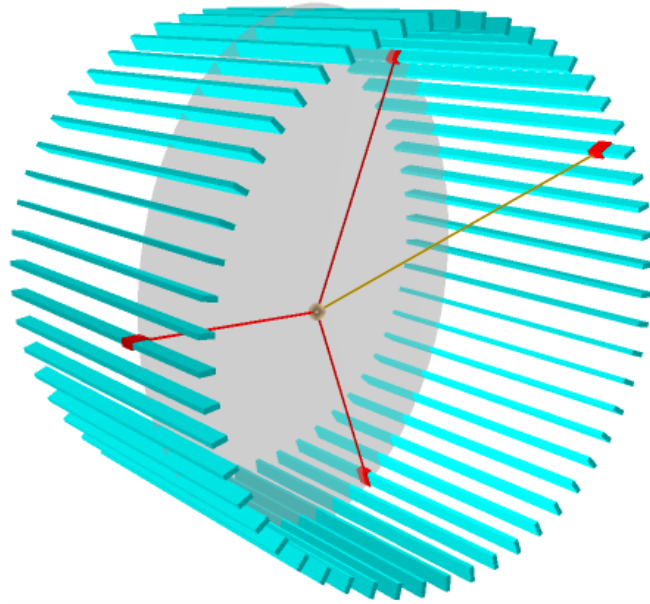


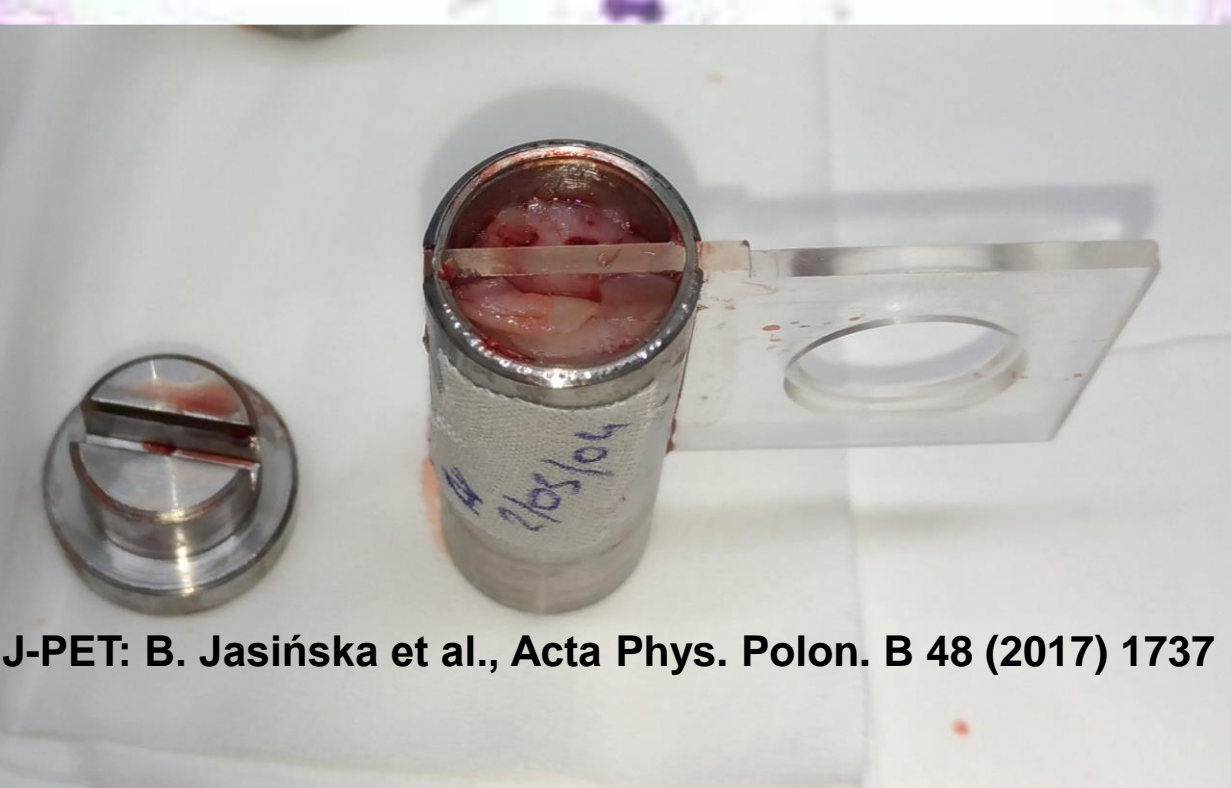
Ortho-positronium life-time tomography

J-PET: P. M et al., Phys. Med. Biol. 64 2019 055017
<https://arxiv.org/pdf/1805.11696.pdf>

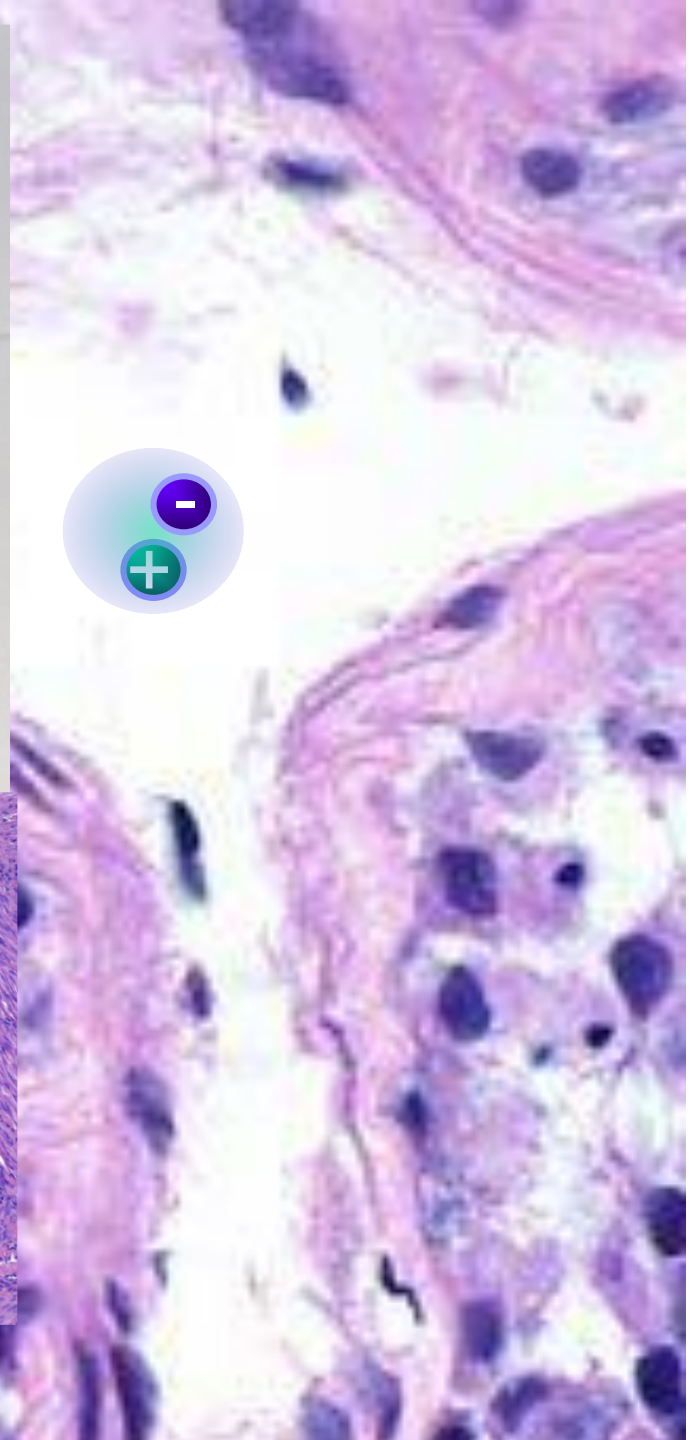
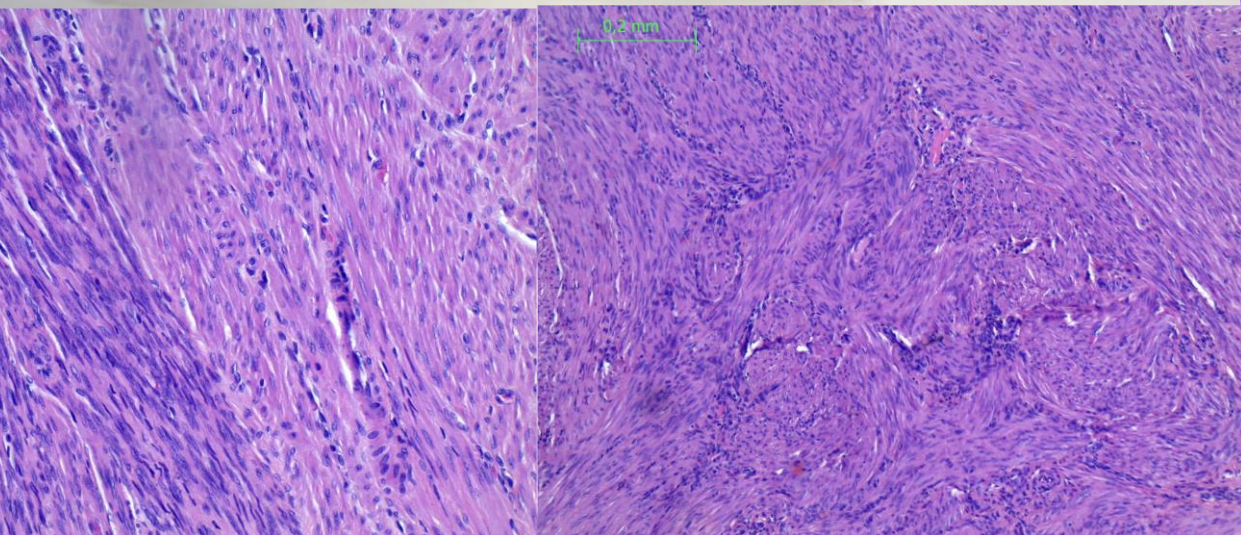
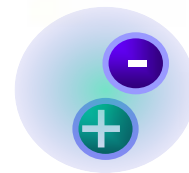


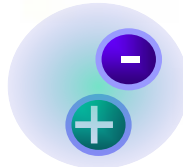
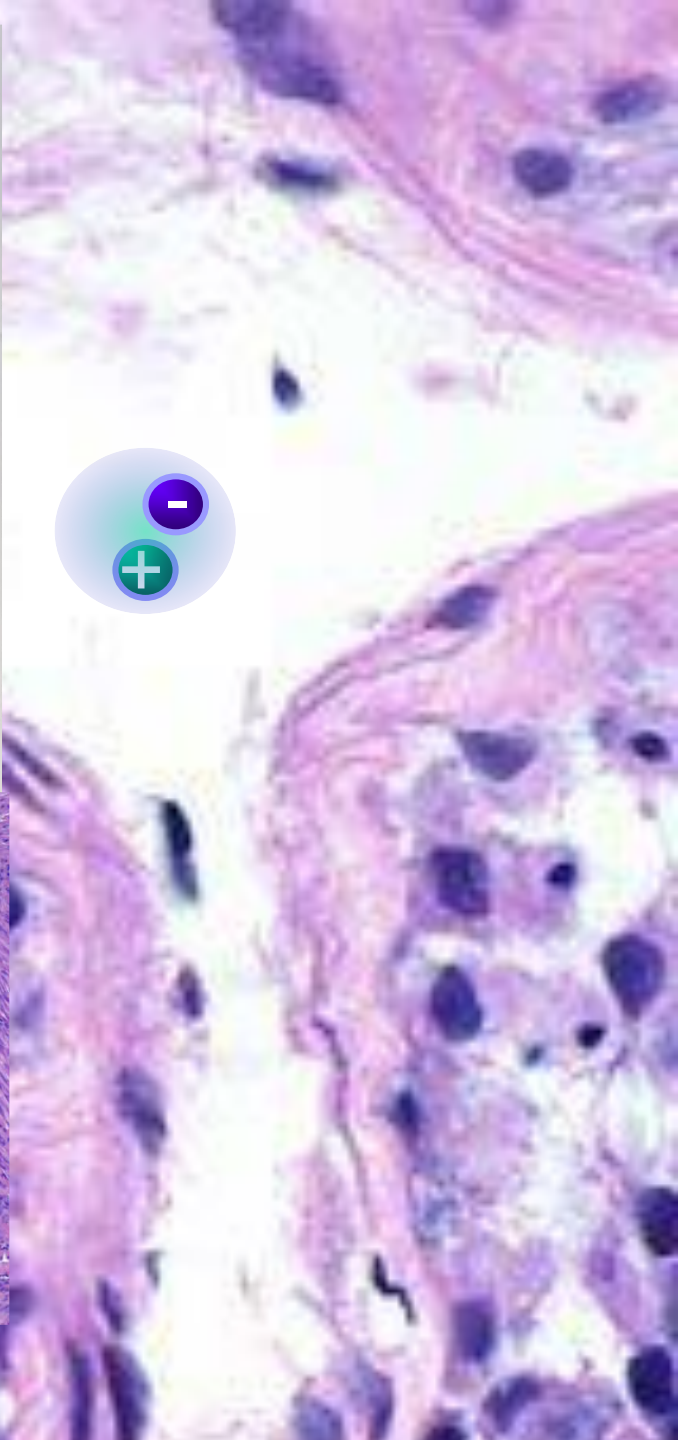
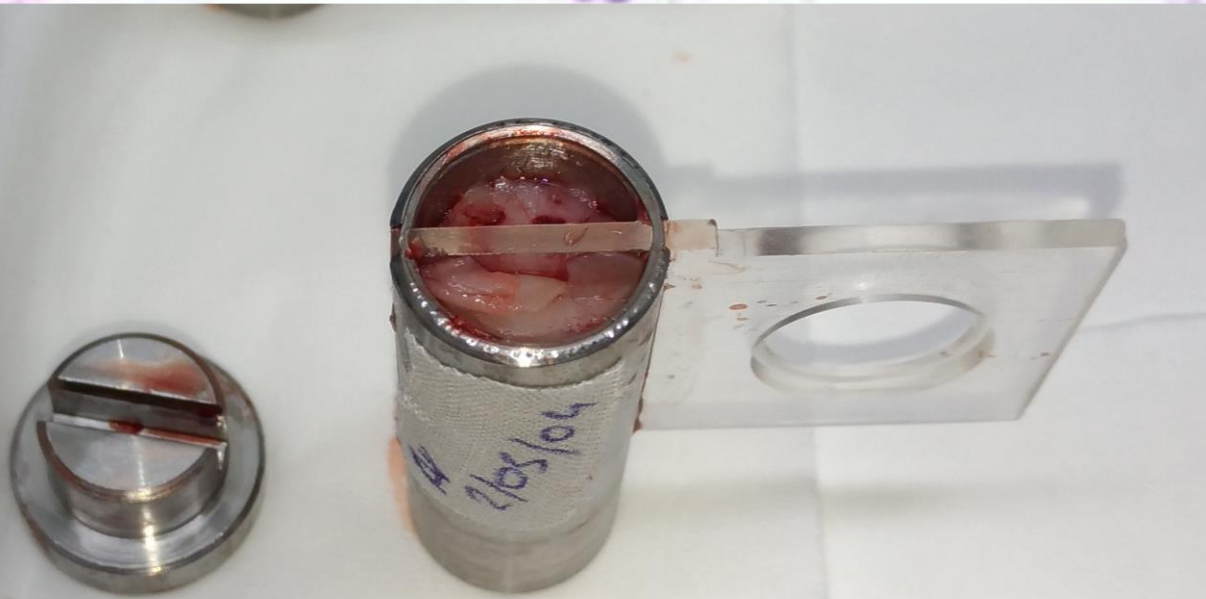
3g/2g tomography



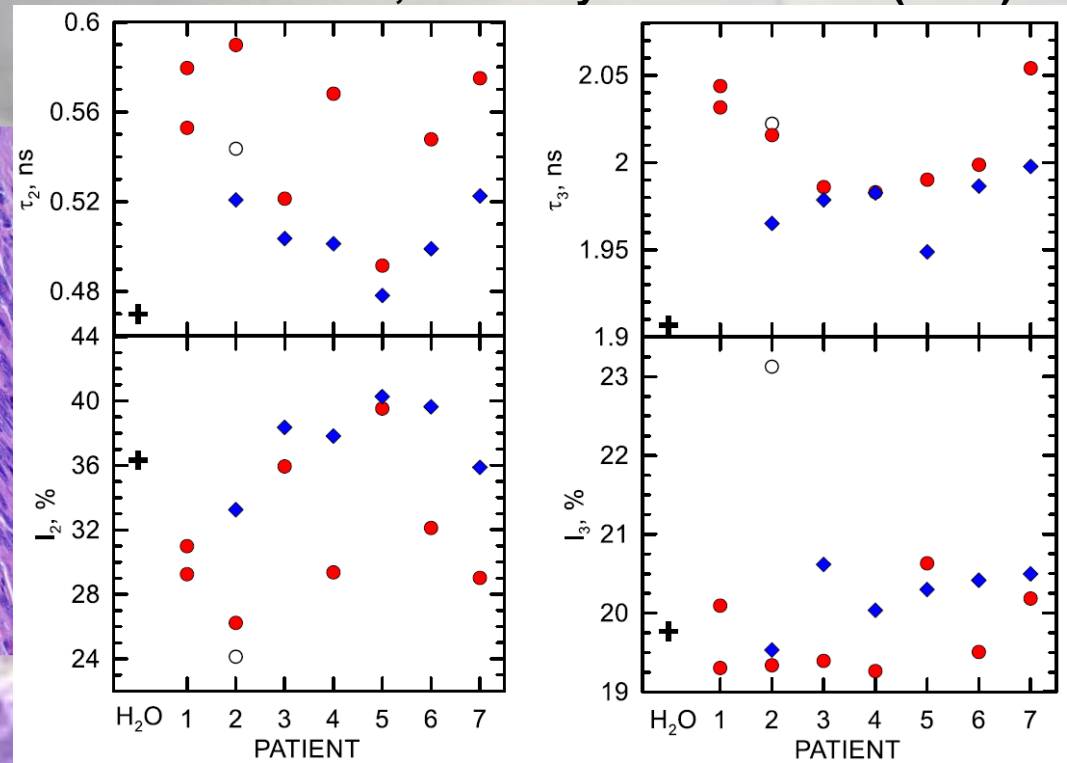


J-PET: B. Jasińska et al., Acta Phys. Polon. B 48 (2017) 1737

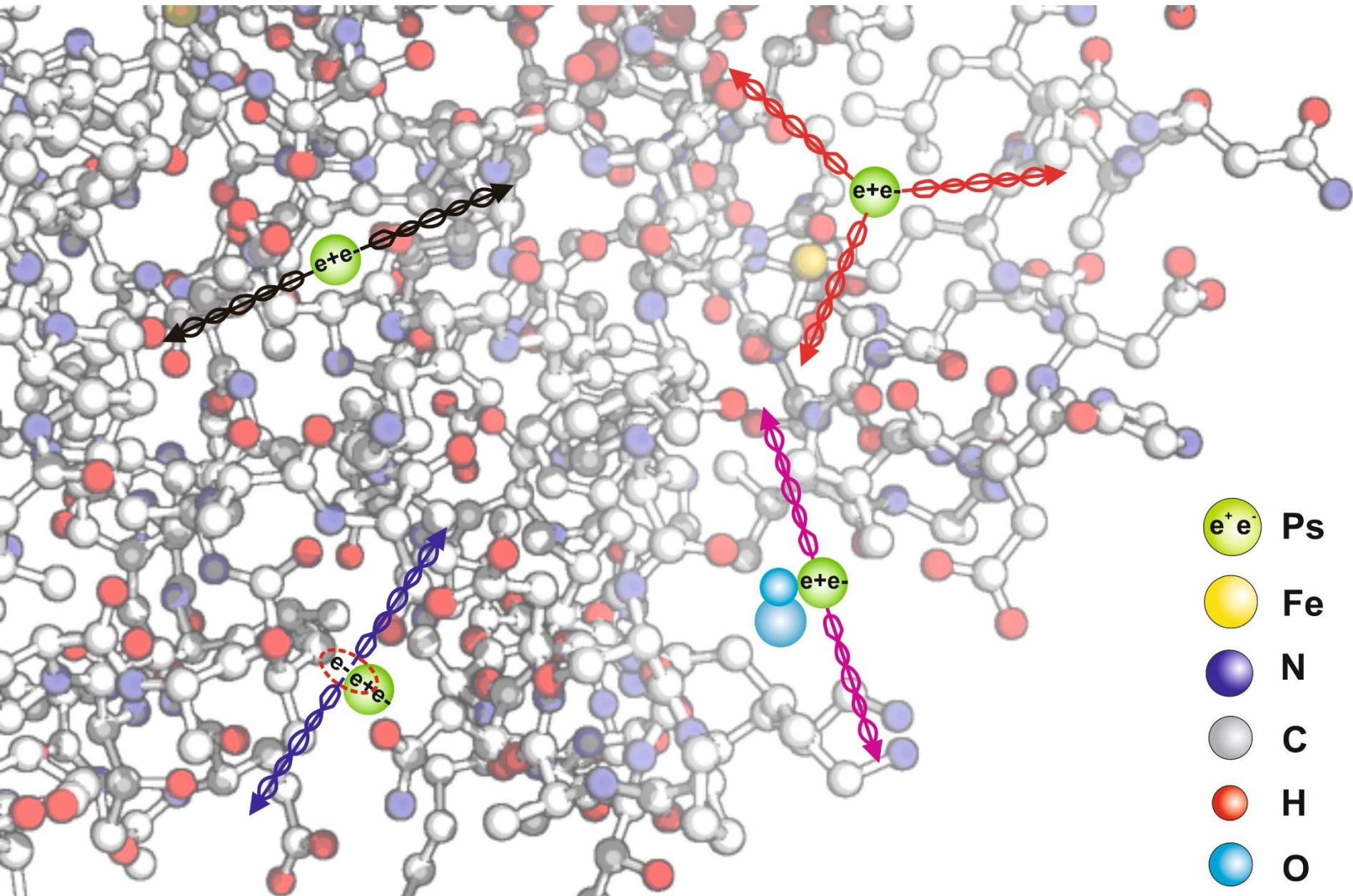


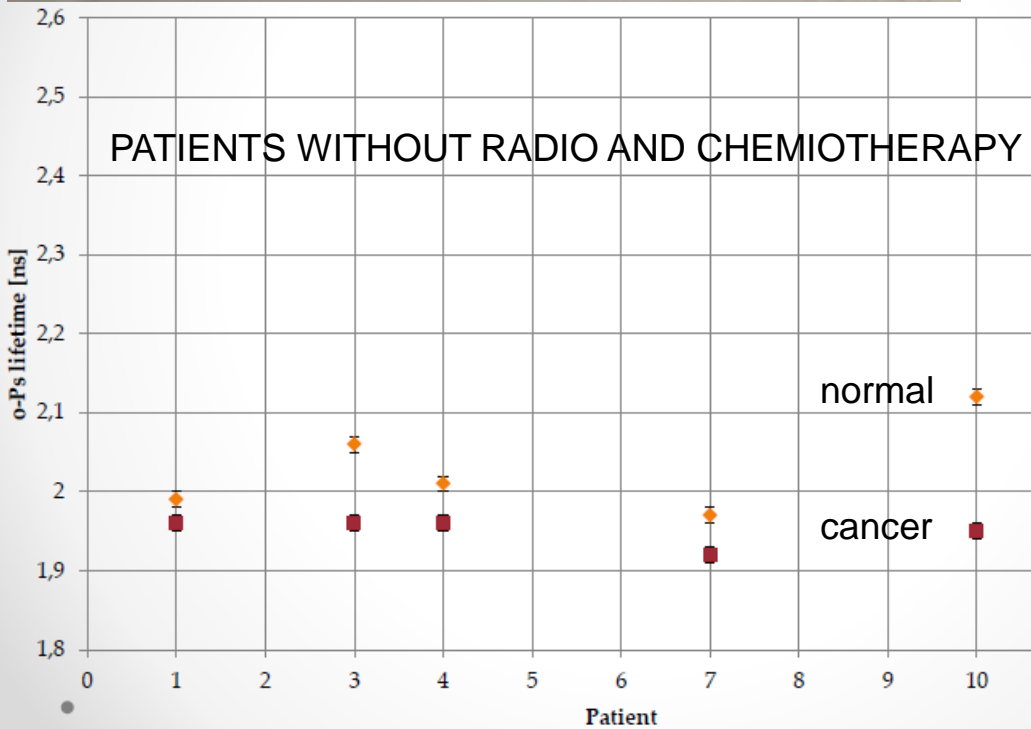


J-PET: B. Jasińska et al., Acta Phys. Polon. B 48 (2017) 1737

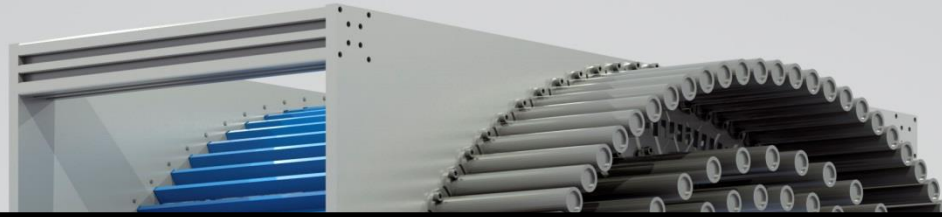


Model of the hemoglobin molecule





COLON CANCER
(CANCER OF LARGE INTENSTINE)

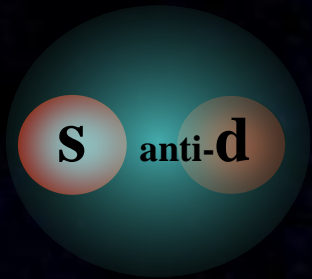


- **PET**
- **Jagiellonian-PET (J-PET)**
- **Positronium imaging (PET & PALS)**
- **Discrete symmetries**
- **Quantum Entanglement Tomograph**
- **Hadrontherapy beam monitoring**

Discrete symmetries

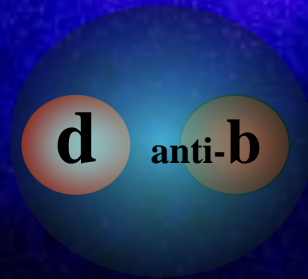
P	reflection in space	$(x,y,z \rightarrow -x,-y-z)$
C	charge conjugation	(particles \rightarrow anti-particle)
T	reversal in time	$(A \rightarrow B \Rightarrow B \rightarrow A)$
CP		
CPT		

Violation of CP and T
confirmed experimentally
for hadrons only



meson K

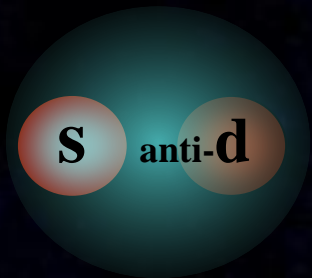
1964



meson B

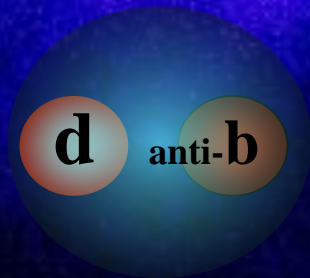
2012

Violation of CP and T confirmed experimentally for hadrons only



meson K

1964



meson B

2012

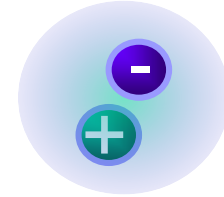


positronium

?

ODE TO POSITRONIUM

Eigen-state of Hamiltonian and P, C, CP operators



The lightest known atom and at the same time anti-atom which undergoes self-annihilation as flavor neutral mesons

The simplest atomic system with charge conjugation eigenstates.

Electrons and positron are the lightest leptons so they can not decay into lighter particles via weak interaction ...

effects due the weak interaction can lead to the violation at the order of 10^{-14} .

M. Sozzi, Discrete Symmetries and CP Violation, Oxford University Press (2008)

No charged particles in the final state (radiative corrections very small $2 * 10^{-10}$)

Light by light contributions to various correlations are small

B. K. Arbic et al., Phys. Rev. A 37, 3189 (1988).

W. Bernreuther et al., Z. Phys. C 41, 143 (1988).

Purely Leptonic state !

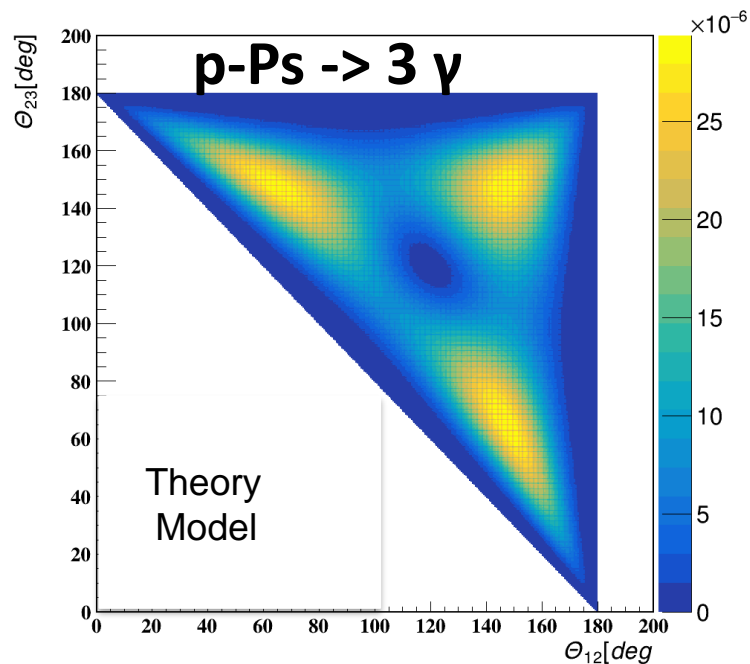
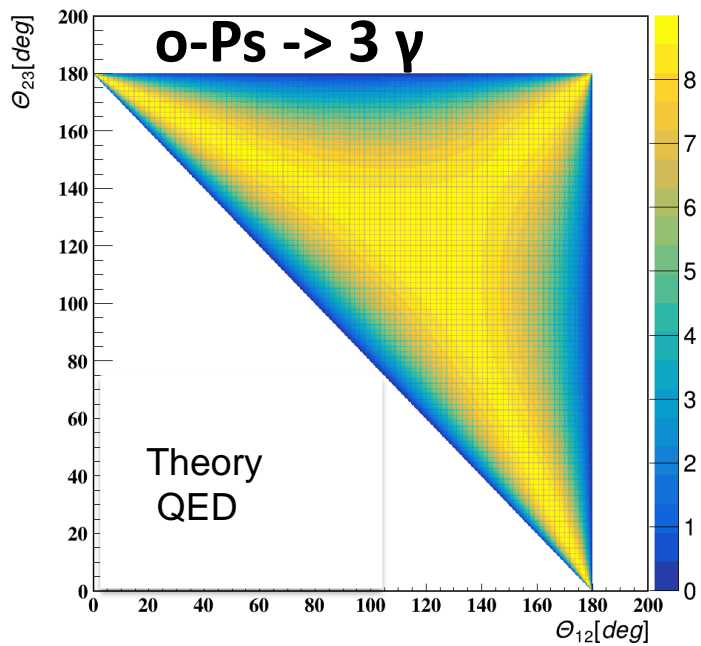
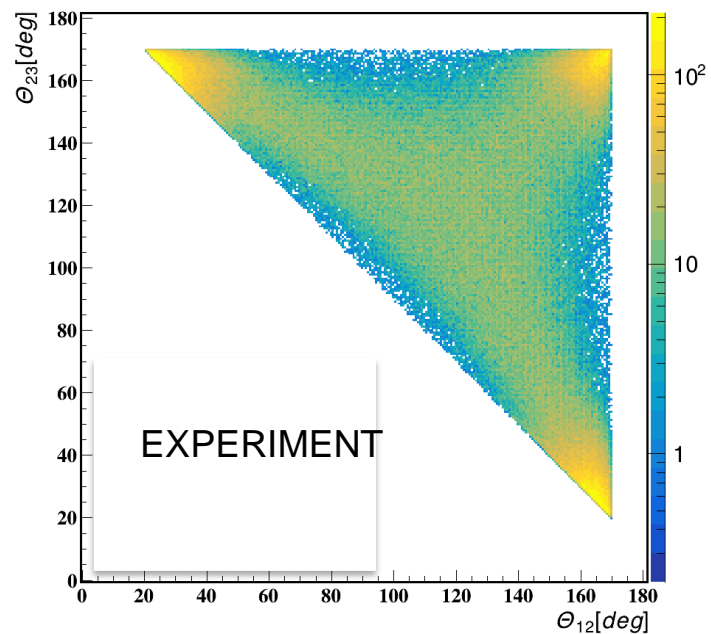
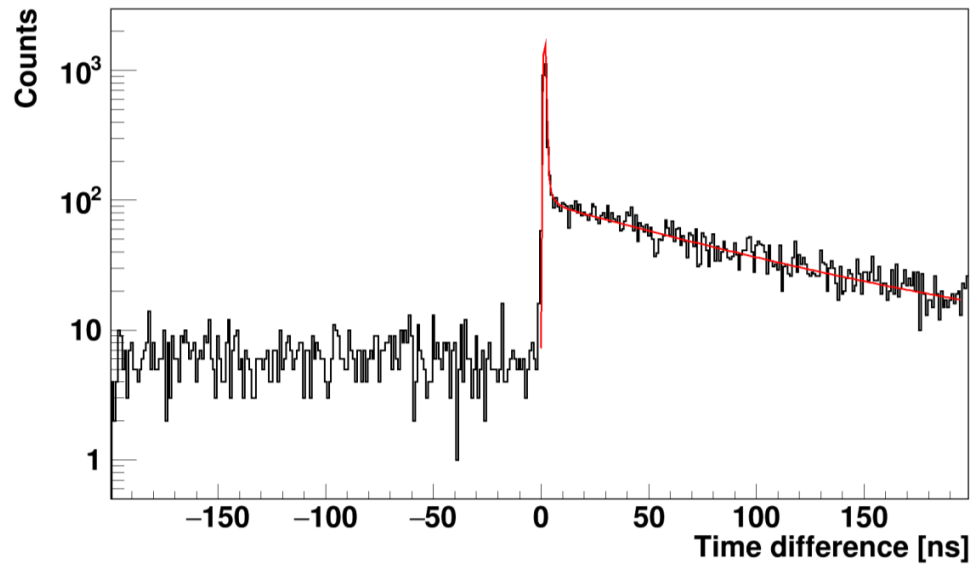
Breaking of T and CP was observed but only for processes involving quarks.

So far breaking of these symmetries was not observed for purely leptonic systems.

10^{-9} vs upper limits of $3 * 10^{-3}$ for T, CP, CPT

P.A. Vetter and S.J. Freedman, Phys. Rev. Lett. 91, 263401 (2003)

T. Yamazaki et al., Phys. Rev. Lett. 104 (2010) 083401



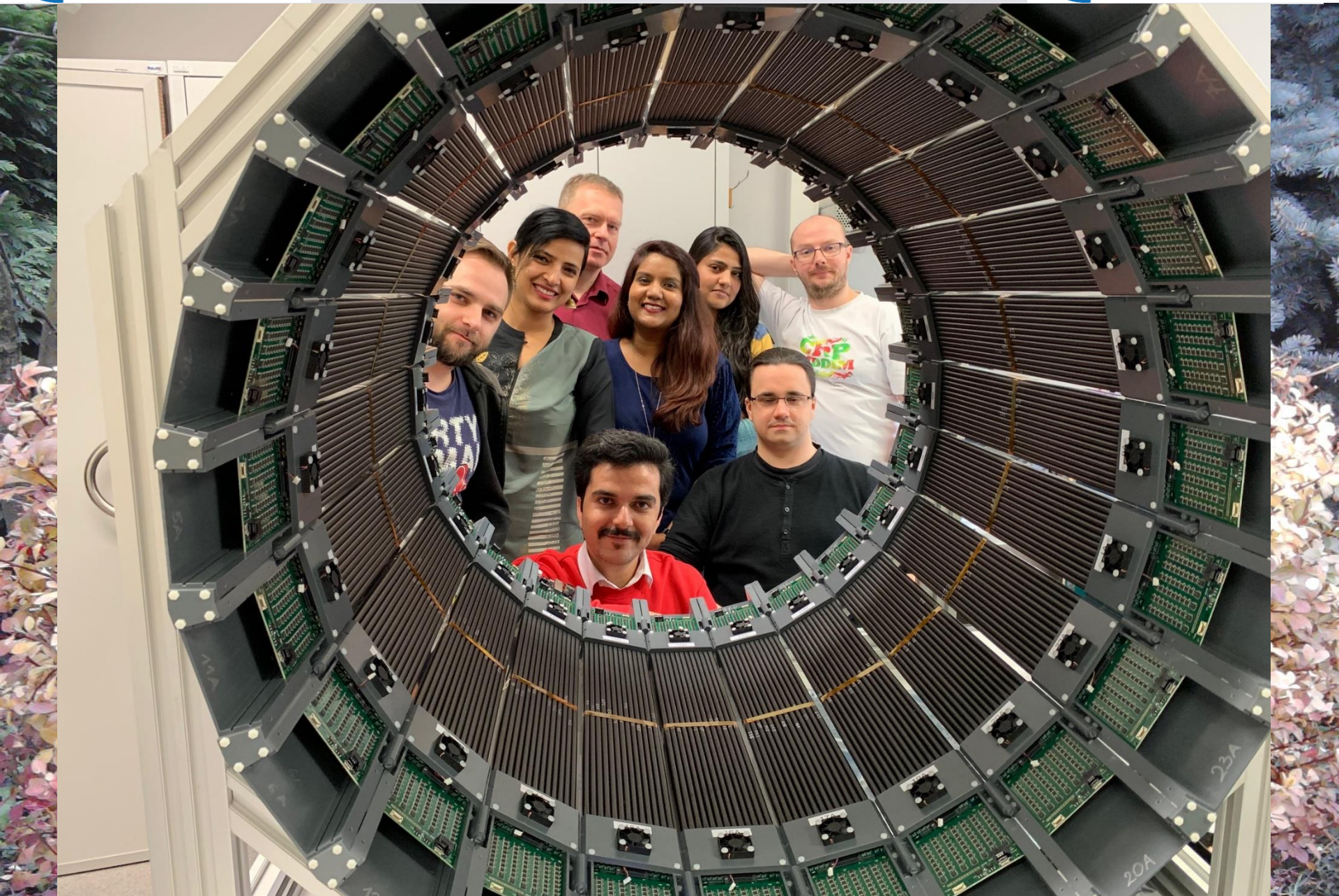


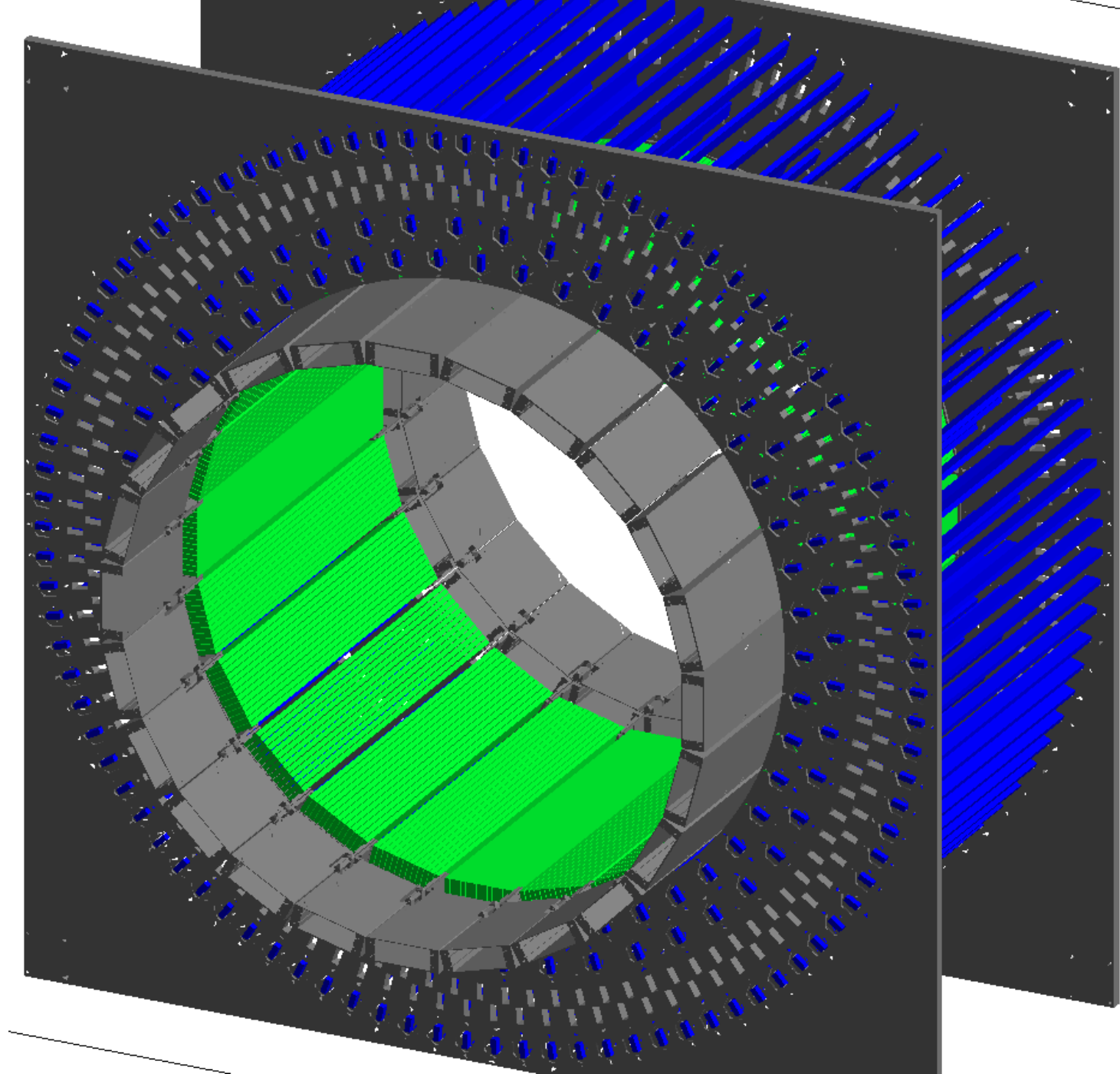
J-PET

Jagiellonian PET



J-PET

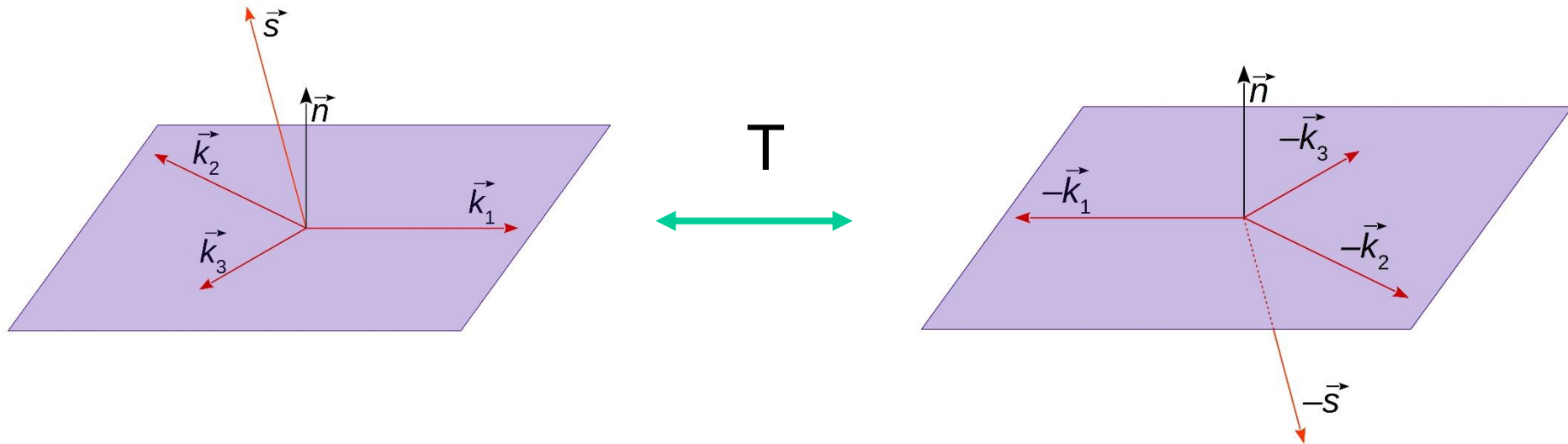




Operators for the $o\text{-Ps} \rightarrow 3\gamma$ process, and their properties with respect to the C, P, T, CP and CPT symmetries.

$$|\mathbf{k}_1| > |\mathbf{k}_2| > |\mathbf{k}_3|$$

Operator	C	P	T	CP	CPT
$\vec{S} \cdot \vec{k}_1$	+	-	+	-	-
$\vec{S} \cdot (\vec{k}_1 \times \vec{k}_2)$	+	+	-	+	-
$(\vec{S} \cdot \vec{k}_1) (\vec{S} \cdot (\vec{k}_1 \times \vec{k}_2))$	+	-	-	-	+



So far best accuracy for tests of **CP and CPT violation** was reported by

-0.0023 < CP < 0.0049 at 90% CL T. Yamazaki et al., Phys. Rev. Lett. 104 (2010) 083401

CPT = 0.0071 ± 0.0062 P.A. Vetter and S.J. Freedman, Phys. Rev. Lett. 91, 263401 (2003).



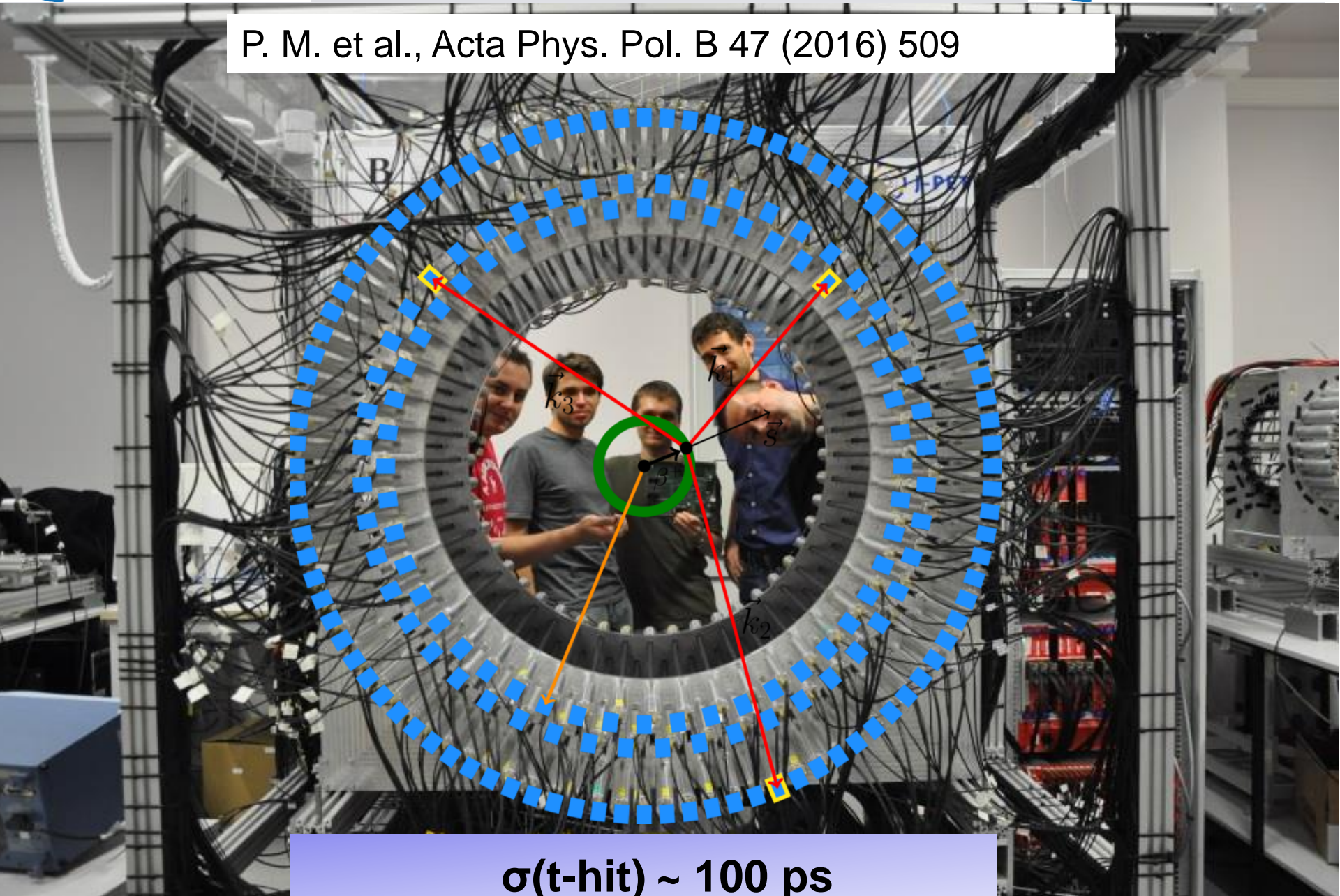
J-PET

Jagiellonian PET



J-PET

P. M. et al., Acta Phys. Pol. B 47 (2016) 509



$\sigma(t\text{-hit}) \sim 100 \text{ ps}$



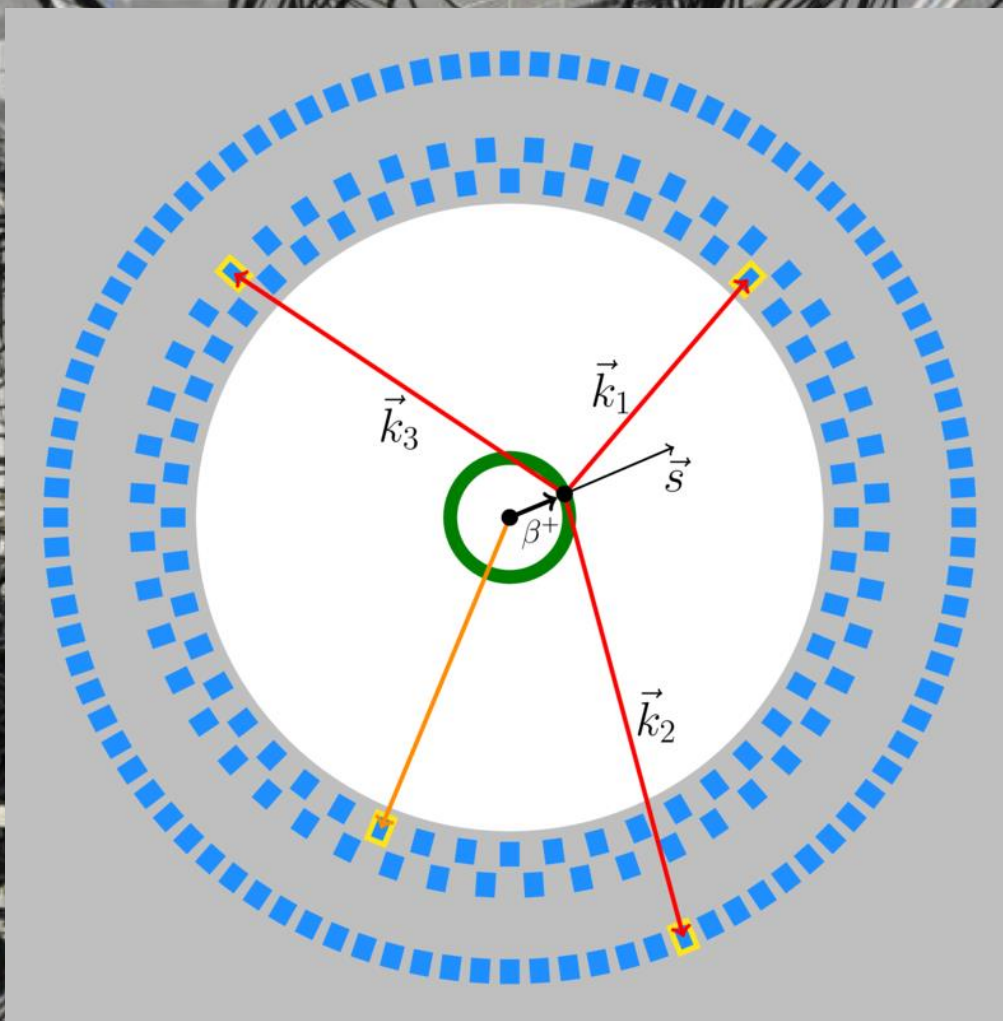
J-PET

Jagiellonian PET



J-PET

P. M. et al., Acta Phys. Pol. B 47 (2016) 509



$\sigma(\text{t-hit}) \sim 100 \text{ ps}$



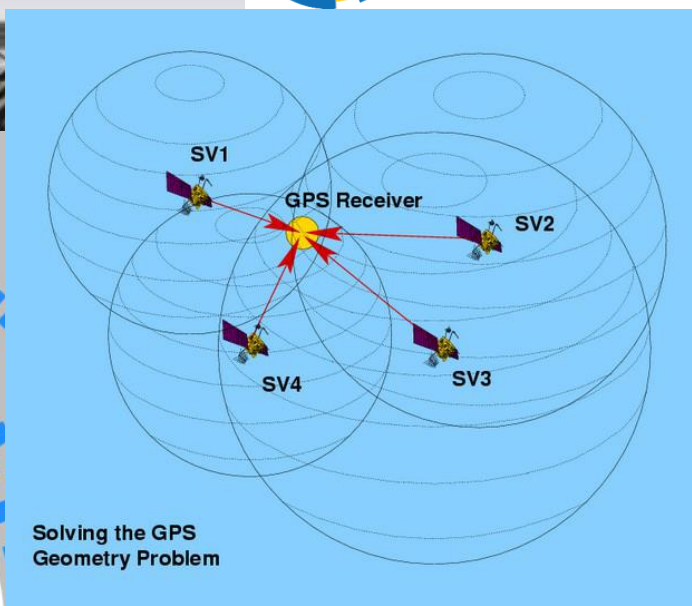
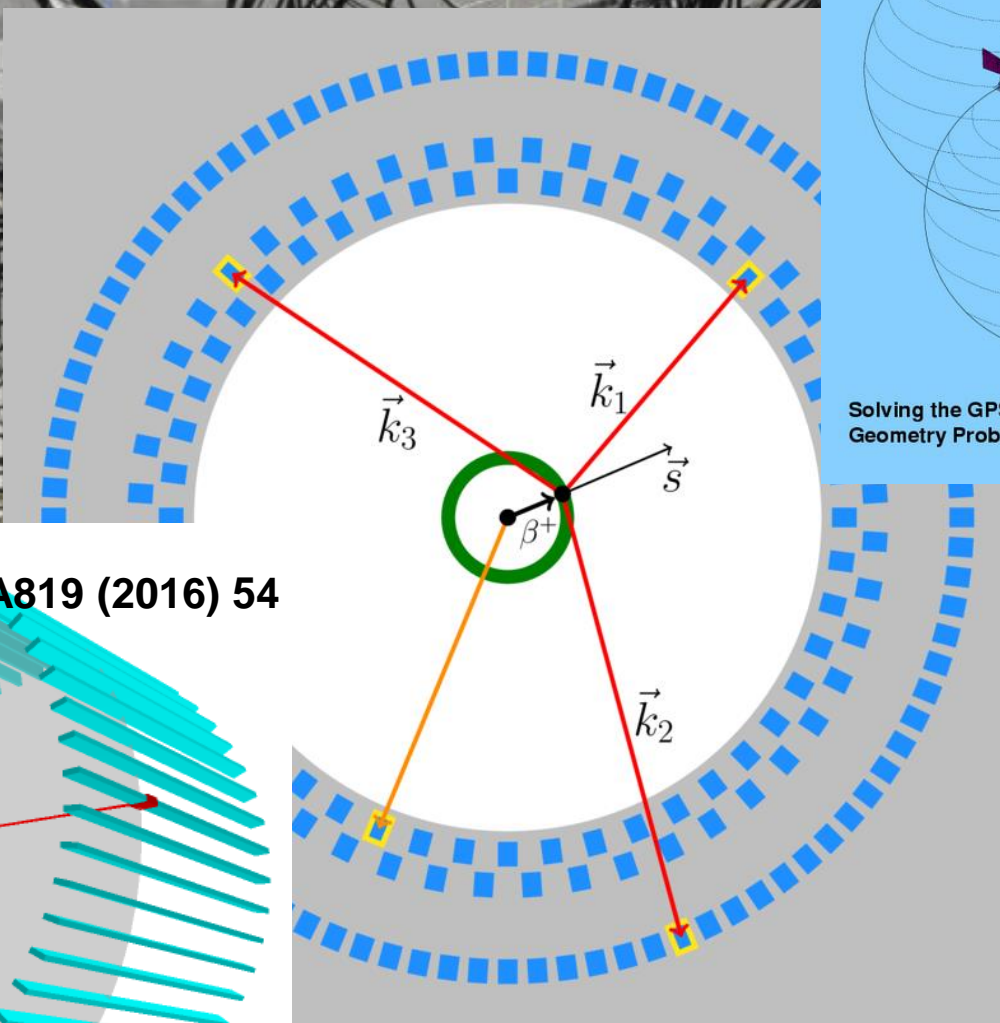
J-PET

Jagiellonian PET



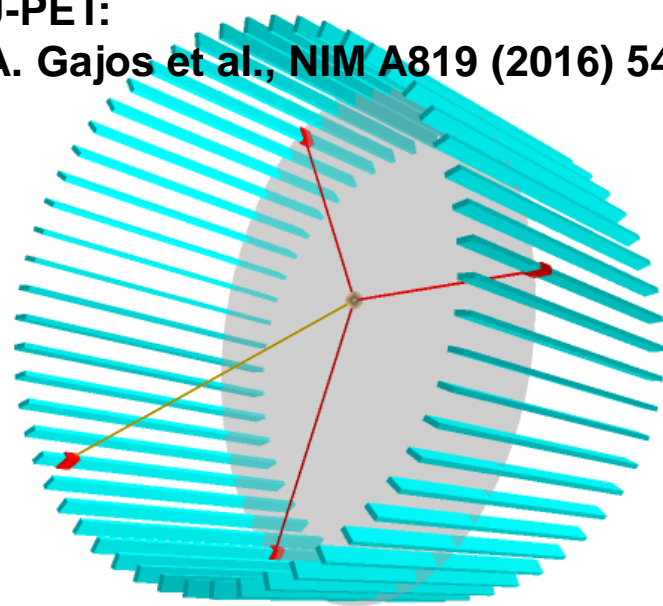
J-PET

P. M. et al., Acta Phys. Pol. B 47 (2016) 509

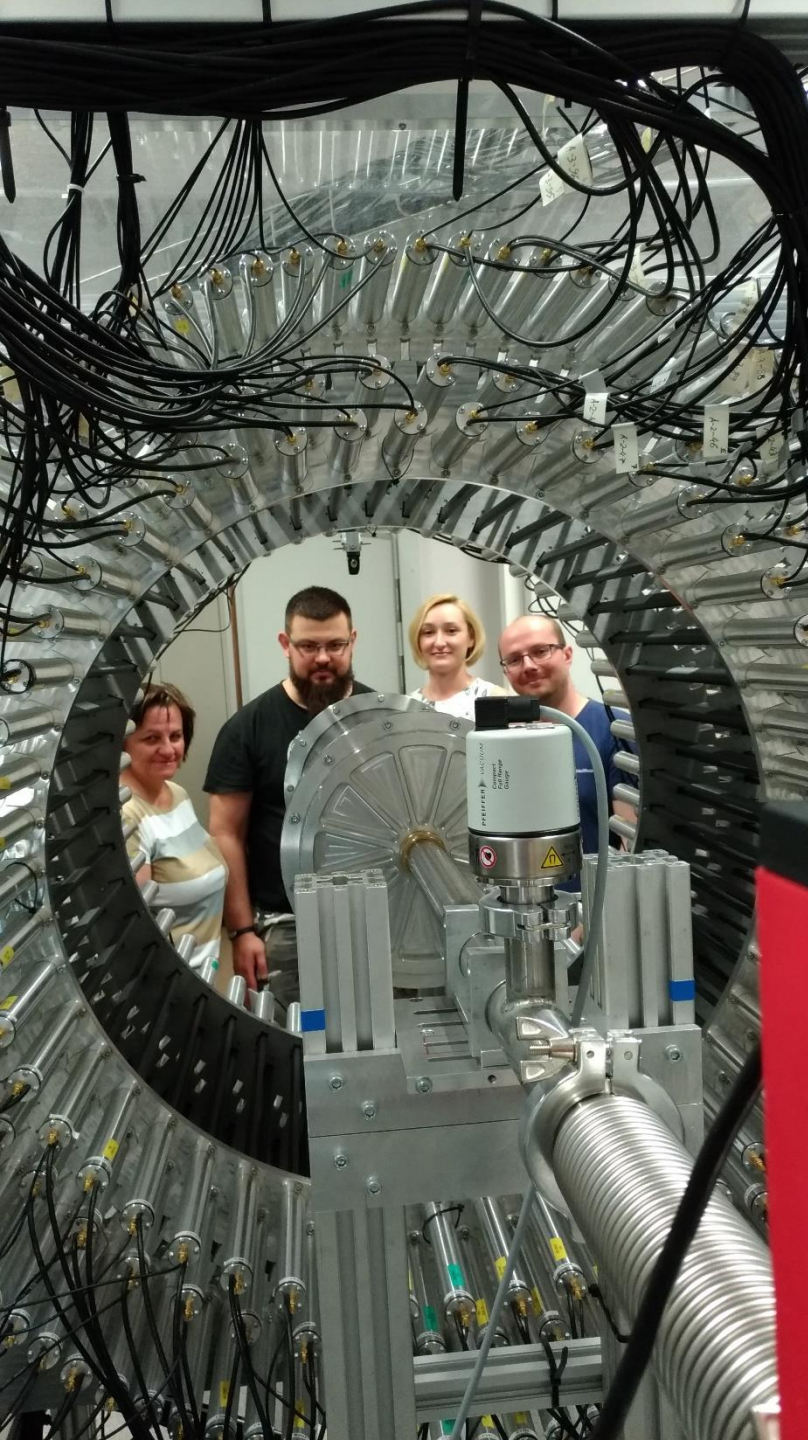


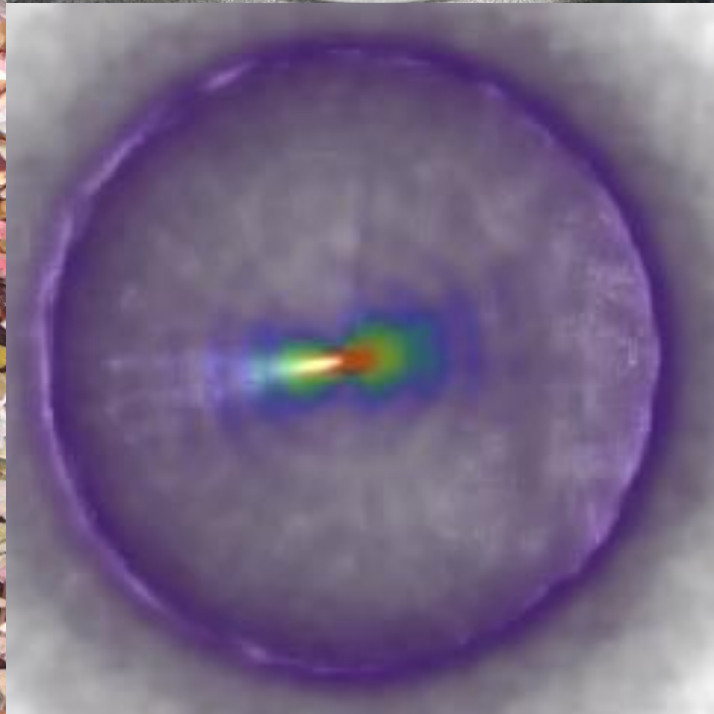
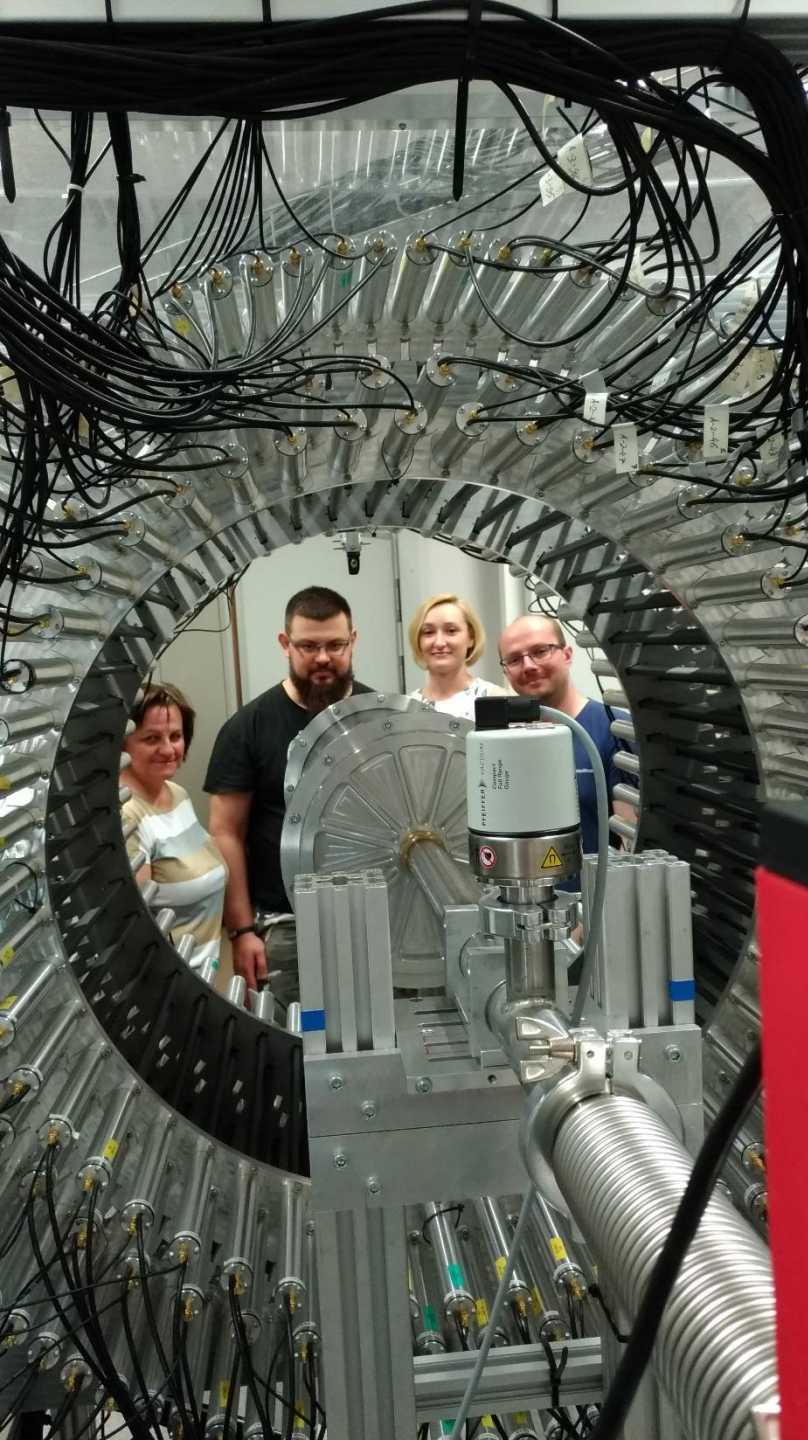
Solving the GPS Geometry Problem

J-PET:
A. Gajos et al., NIM A819 (2016) 54



$\sigma(t\text{-hit}) \sim 100 \text{ ps}$







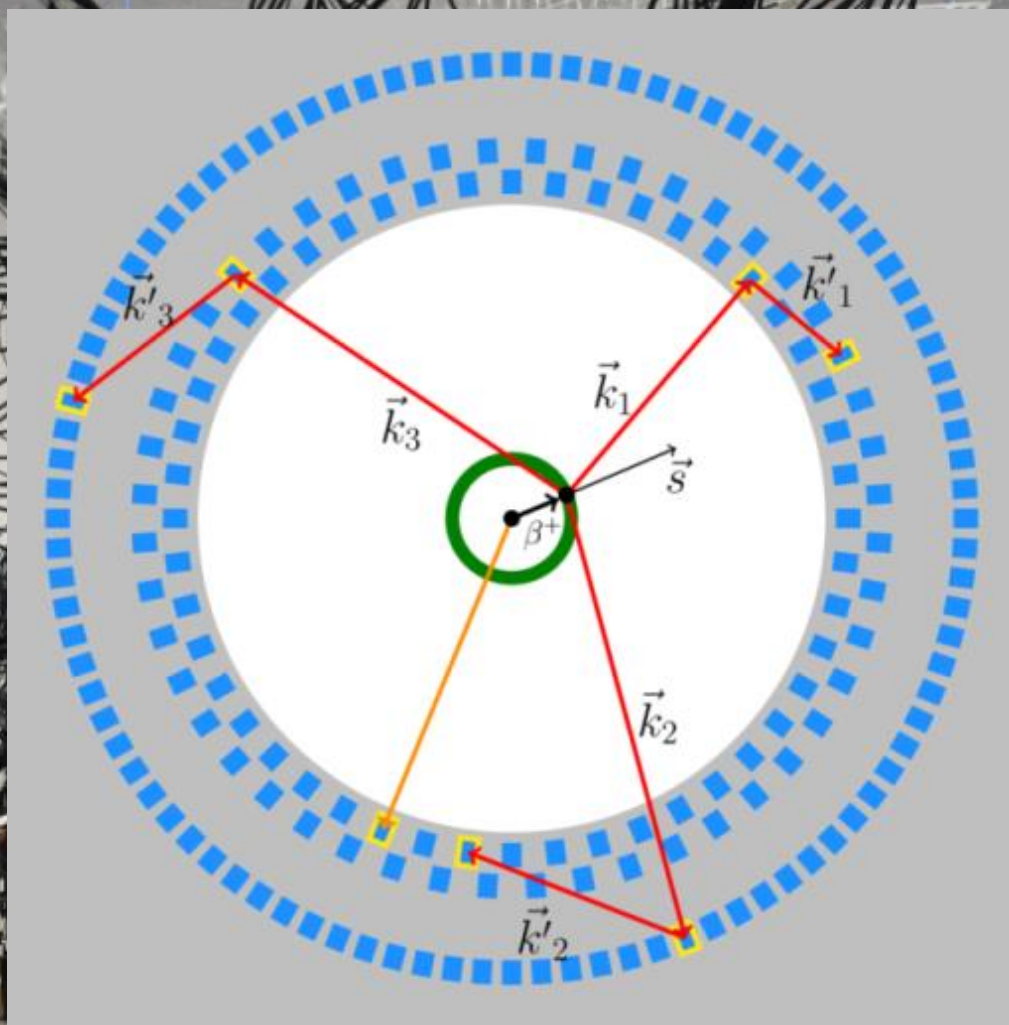
J-PET

Jagiellonian PET



J-PET

P. M. et al., Acta Phys. Pol. B 47 (2016) 509

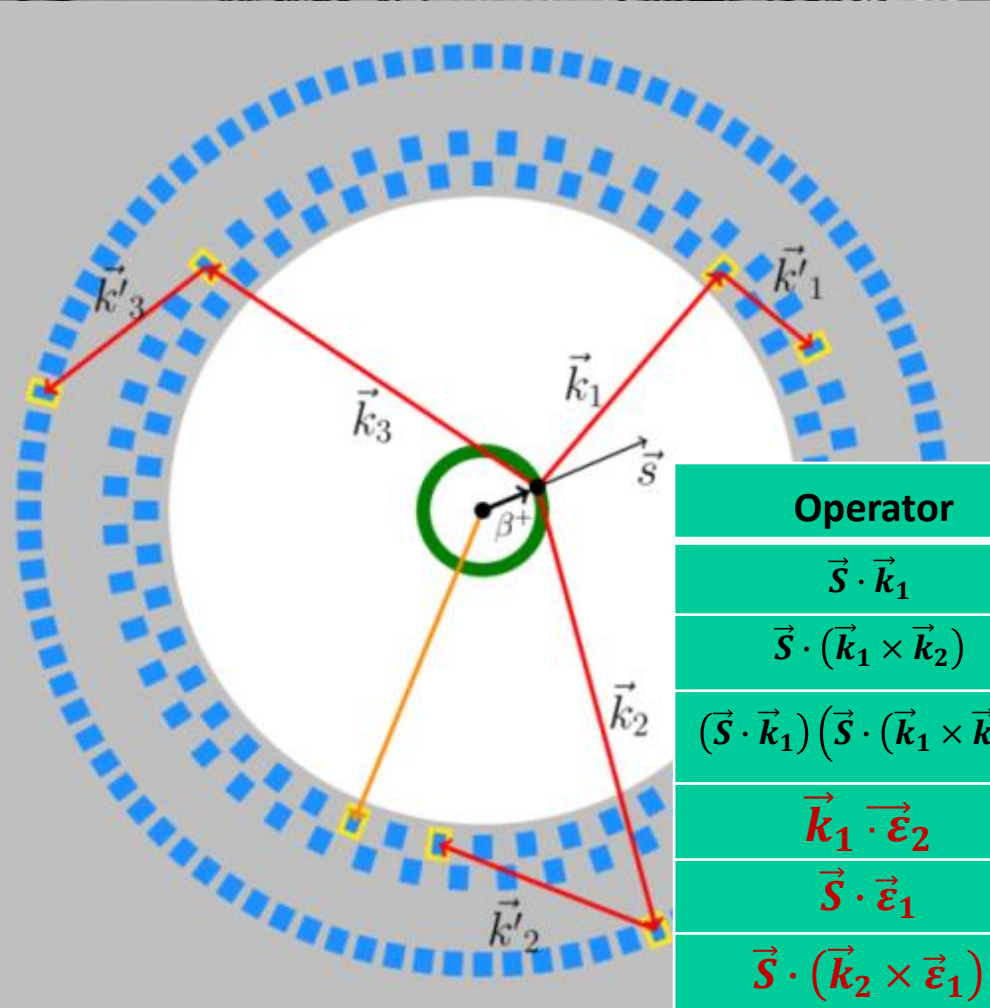


$$\vec{\varepsilon}_i = \vec{k}_i \times \vec{k}'_i$$

$\sigma(\text{t-hit}) \sim 100 \text{ ps}$



P. M. et al., Acta Phys. Pol. B 47 (2016) 509



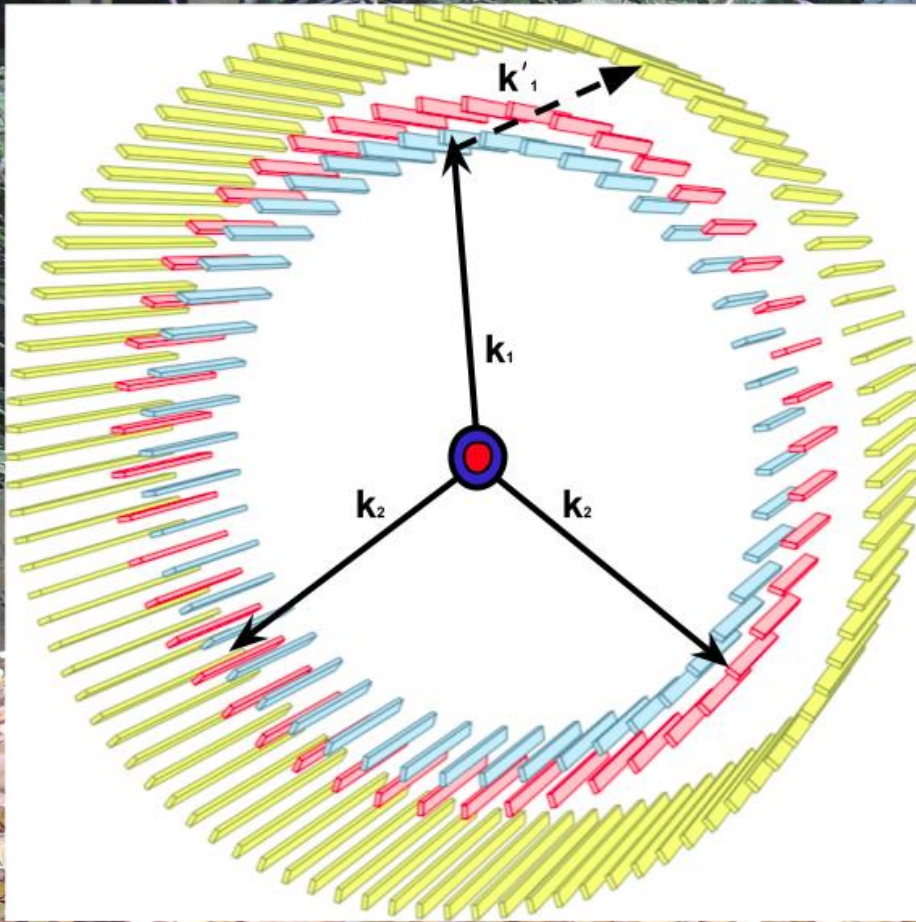
Operator	C	P	T	CP	CPT
$\vec{S} \cdot \vec{k}_1$	+	-	+	-	-
$\vec{S} \cdot (\vec{k}_1 \times \vec{k}_2)$	+	+	-	+	-
$(\vec{S} \cdot \vec{k}_1) (\vec{S} \cdot (\vec{k}_1 \times \vec{k}_2))$	+	-	-	-	+
$\vec{k}_1 \cdot \vec{\varepsilon}_2$	+	-	-	-	+
$\vec{S} \cdot \vec{\varepsilon}_1$	+	+	-	+	-
$\vec{S} \cdot (\vec{k}_2 \times \vec{\varepsilon}_1)$	+	-	+	-	-

$$\vec{\varepsilon}_i = \vec{k}_i \times \vec{k}'_i$$

$\sigma(\text{t-hit}) \sim 100 \text{ ps}$

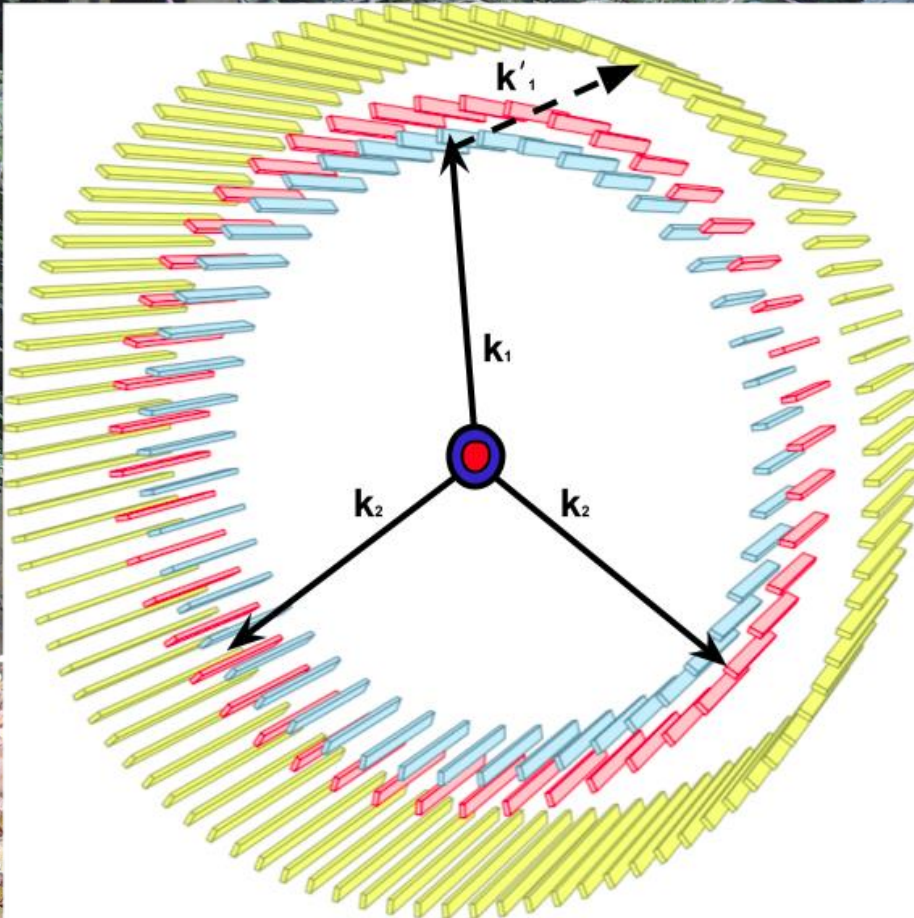
SM 10^{-9} vs upper limits of $3 \cdot 10^{-3}$ for T, CP, CPT





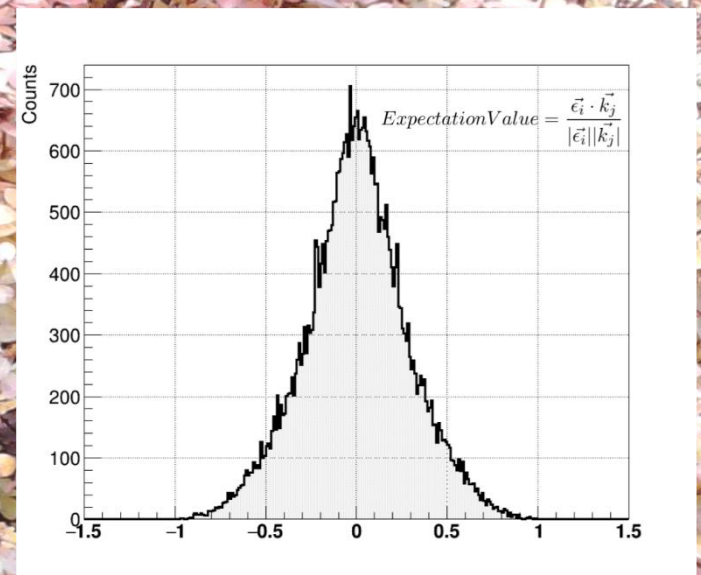
Operator	C	P	T	CP	CPT
$\vec{S} \cdot \vec{k}_1$	+	-	+	-	-
$\vec{S} \cdot (\vec{k}_1 \times \vec{k}_2)$	+	+	-	+	-
$(\vec{S} \cdot \vec{k}_1) (\vec{S} \cdot (\vec{k}_1 \times \vec{k}_2))$	+	-	-	-	+
$\vec{k}_1 \cdot \vec{\epsilon}_2$	+	-	-	-	+
$\vec{S} \cdot \vec{\epsilon}_1$	+	+	-	+	-
$\vec{S} \cdot (\vec{k}_2 \times \vec{\epsilon}_1)$	+	-	+	-	-

P. M. et al., Acta Phys. Pol. B 47 (2016) 509



Operator	C	P	T	CP	CPT
$\vec{S} \cdot \vec{k}_1$	+	-	+	-	-
$\vec{S} \cdot (\vec{k}_1 \times \vec{k}_2)$	+	+	-	+	-
$(\vec{S} \cdot \vec{k}_1) (\vec{S} \cdot (\vec{k}_1 \times \vec{k}_2))$	+	-	-	-	+
$\vec{k}_1 \cdot \vec{\epsilon}_2$	+	-	-	-	+
$\vec{S} \cdot \vec{\epsilon}_1$	+	+	-	+	-
$\vec{S} \cdot (\vec{k}_2 \times \vec{\epsilon}_1)$	+	-	+	-	-

P. M. et al., Acta Phys. Pol. B 47 (2016) 509



Best so far:
 $-0.0023 < CP < 0.0049$ at 90% CL
 T. Yamazaki et al., Phys. Rev. Lett. 104 (2010) 083401

Total No. of Entries = 39816
Expectation Value = 0.0005 +/- 0.0014
PRELIMINARY from 5% of data



J-PET

Jagiellonian PET



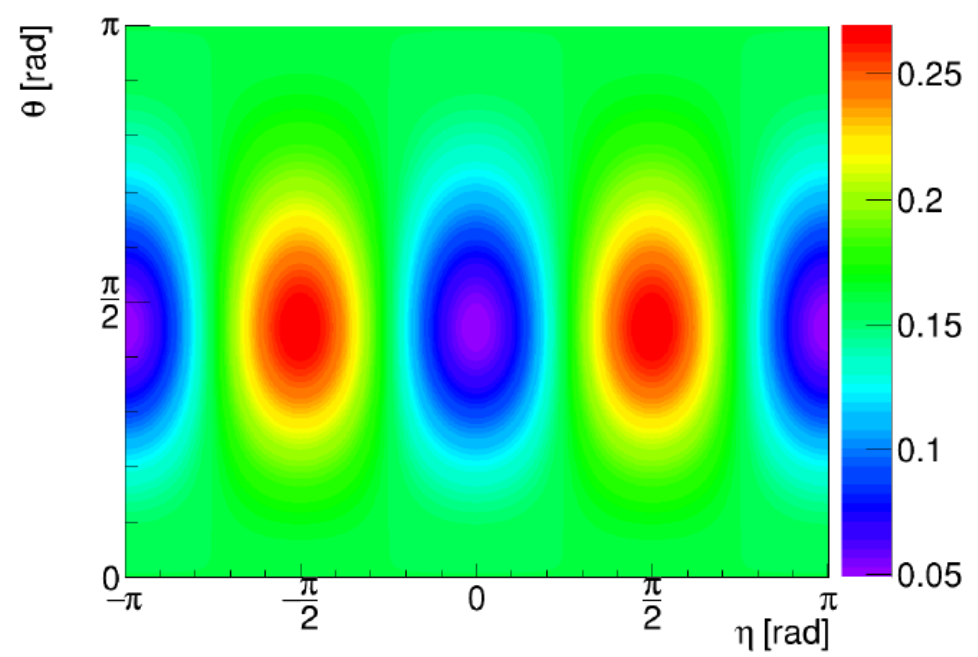
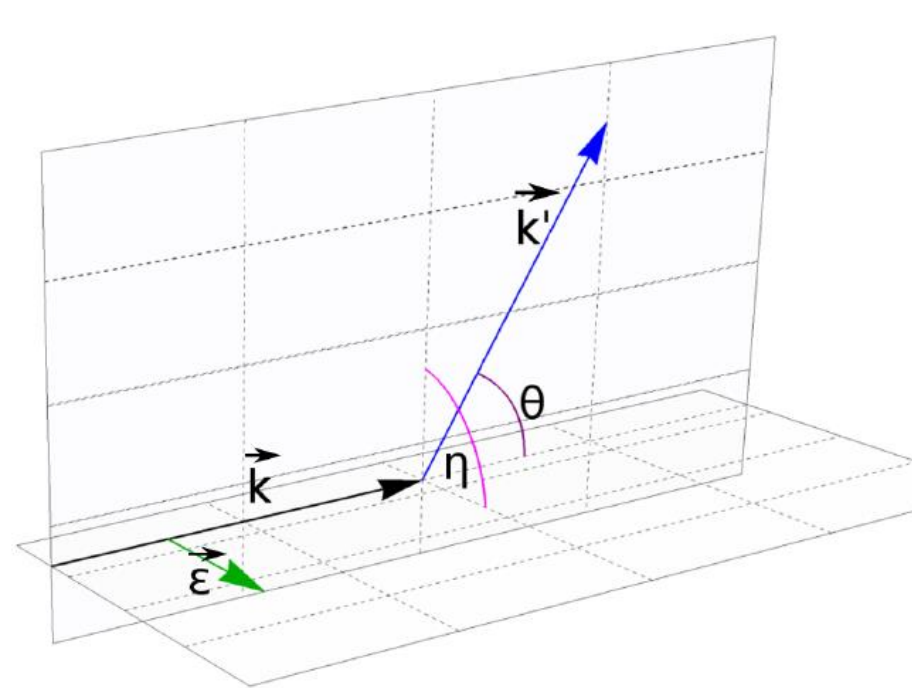
J-PET



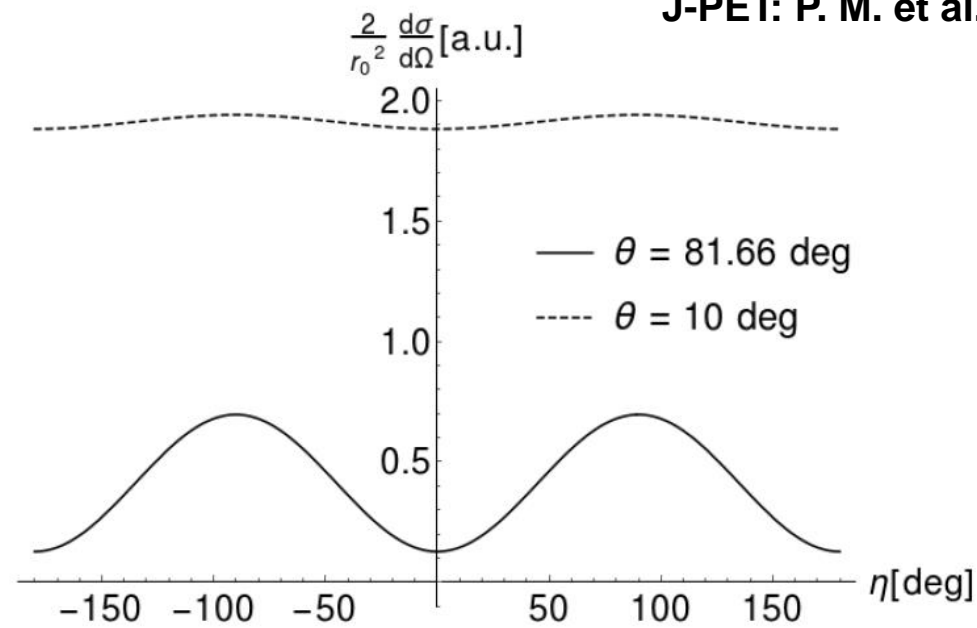
THANK YOU
FOR YOUR ATTENTION

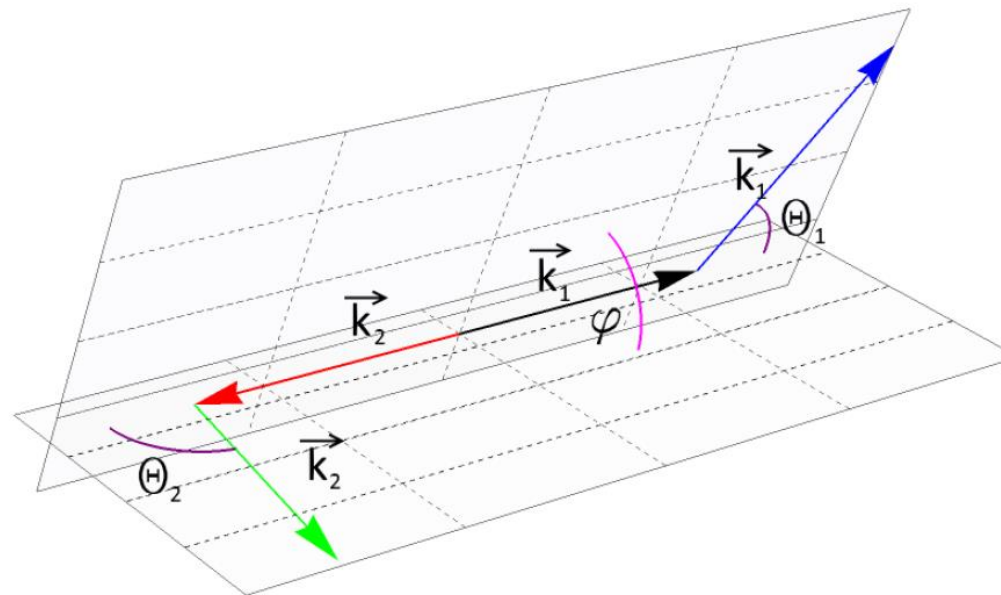
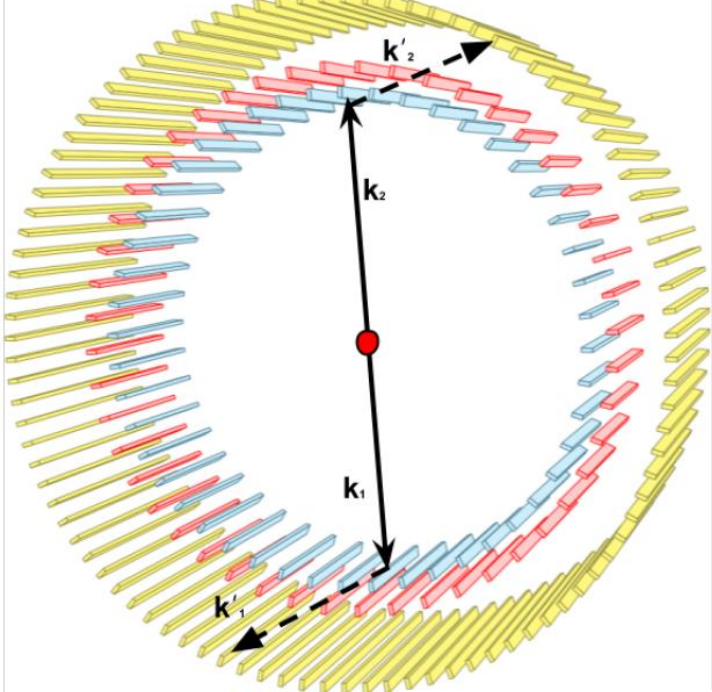


- **PET**
- **Jagiellonian-PET (J-PET)**
- **Positronium imaging (PET & PALS)**
- **Discrete symmetries**
- **Quantum Entanglement Tomograph**
- **Hadrontherapy beam monitoring**

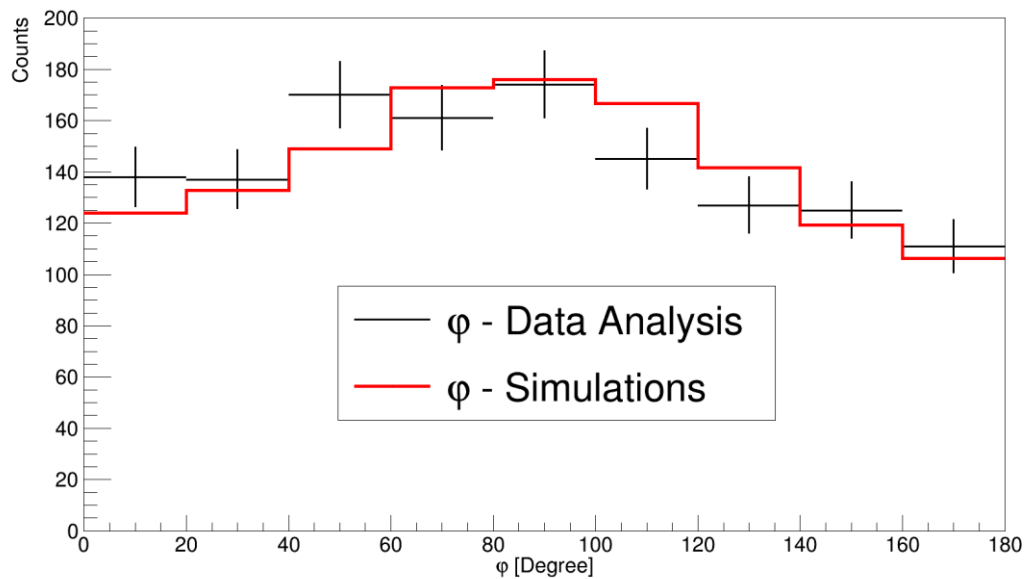


J-PET: P. M. et al., Eur. Phys. J. C 78 (2018) 970

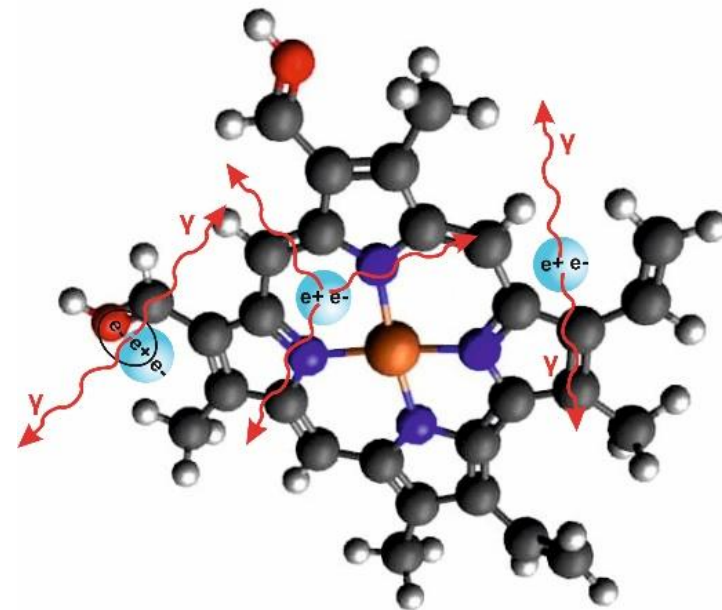
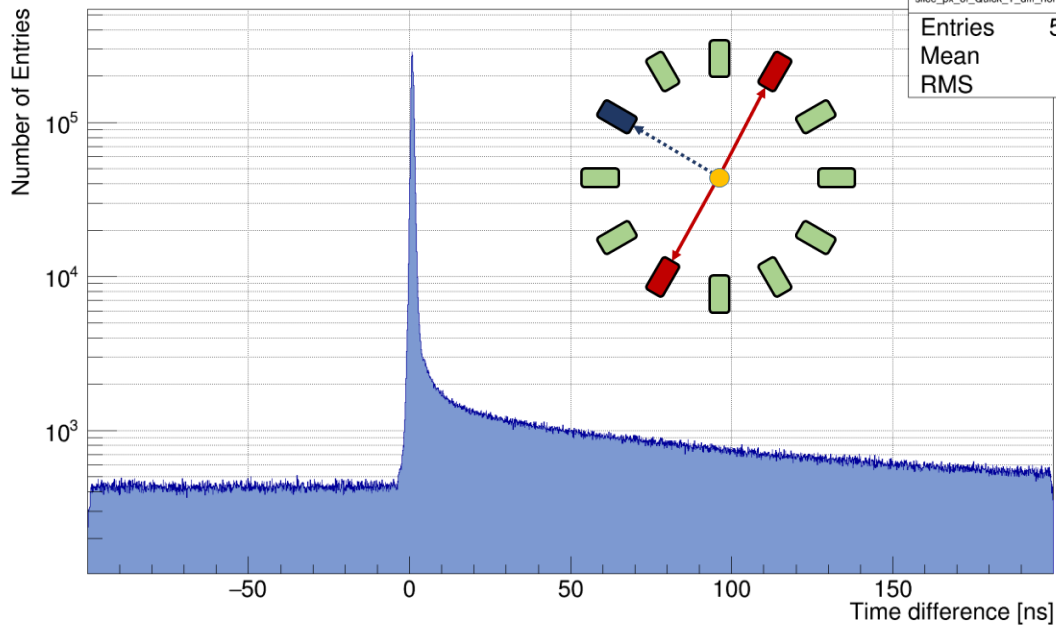




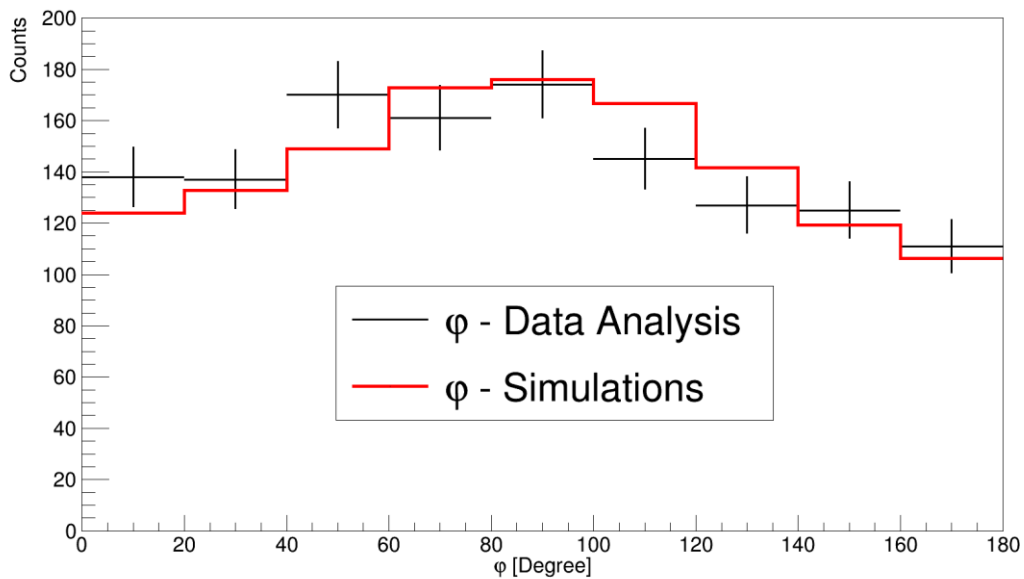
QUANTUM PALS

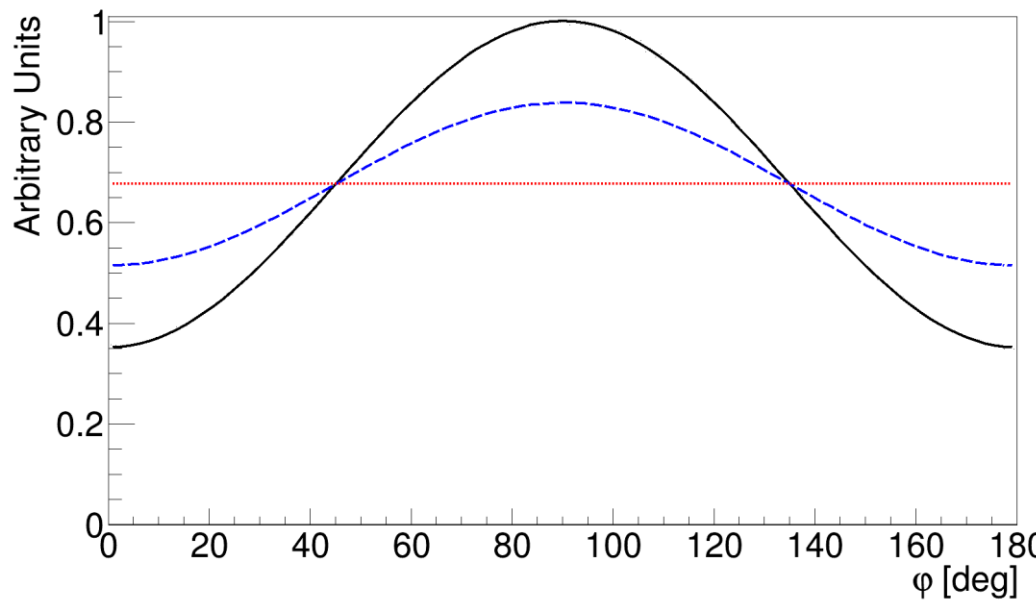
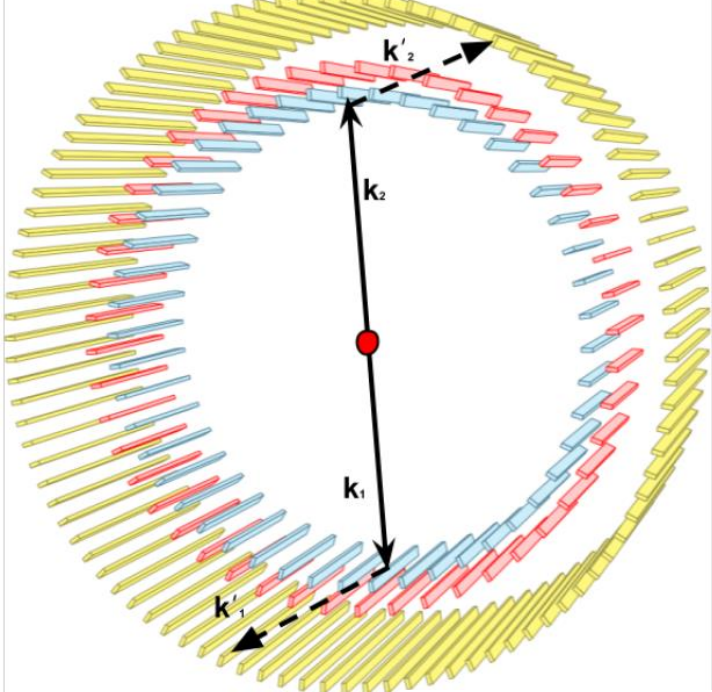


ProjectionX of biny=[1,200] [y=-0.5..199.5]

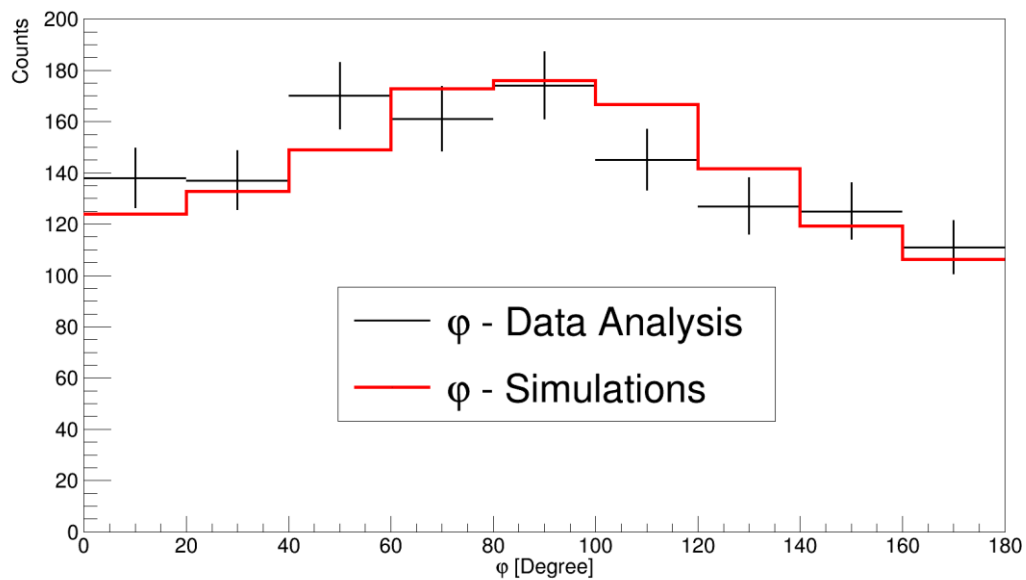


QUANTUM PALS





QUANTUM PALS



SCIENTIFIC REPORTS

OPEN

Genuine Multipartite Entanglement in the 3-Photon Decay of Positronium

Beatrix C. Hiesmayr¹ & Pawel Moskal²

Received: 23 June 2017

Accepted: 25 October 2017

Published online: 10 November 2017

The electron-positron annihilation into two photons is a standard technology in medicine to observe e.g. metabolic processes in human bodies. A new tomograph will provide the possibility to observe not only direct e^+e^- annihilations but also the 3 photons from the decay of ortho-positronium atoms formed in the body. We show in this contribution that the three-photon state with respect to polarisation degrees of freedom depends on the angles between the photons and exhibits various specific entanglement features. In particular genuine multipartite entanglement, a type of entanglement involving all degrees of freedom, is subsistent if the positronium was in a definite spin eigenstate. Remarkably, when all spin eigenstates are mixed equally, entanglement –and even stronger genuine multipartite entanglement– survives. Due to a “*symmetrization*” process, however, *Dicke*-type or *W*-type entanglement remains whereas *GHZ*-type entanglement vanishes. The survival of particular entanglement properties in the mixing scenario may make it possible to extract quantum information in the form of distinct entanglement features, e.g., from metabolic processes in human bodies.

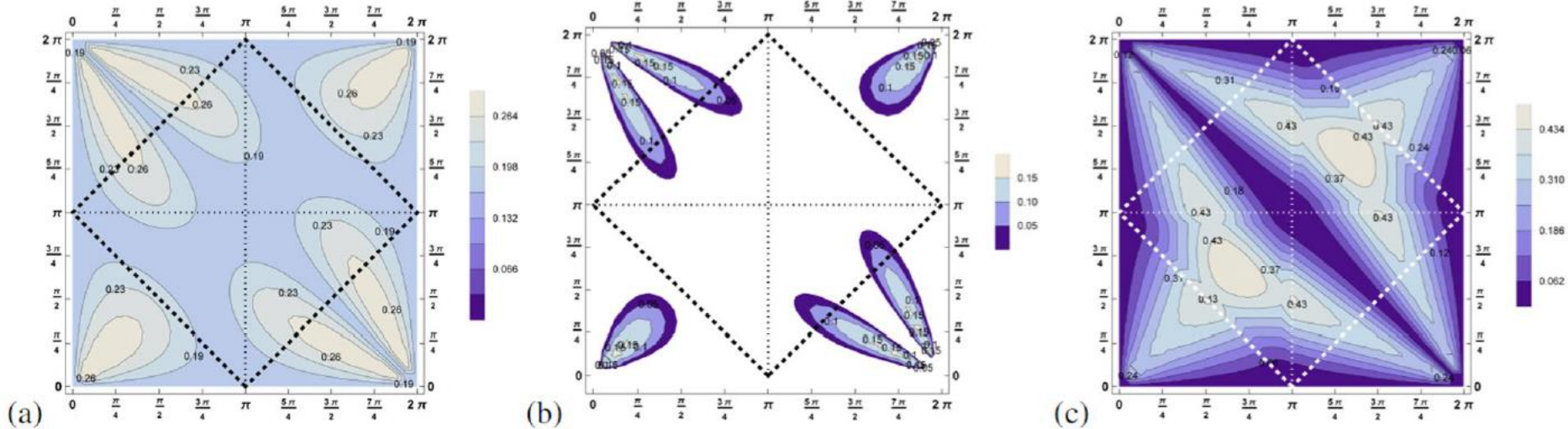
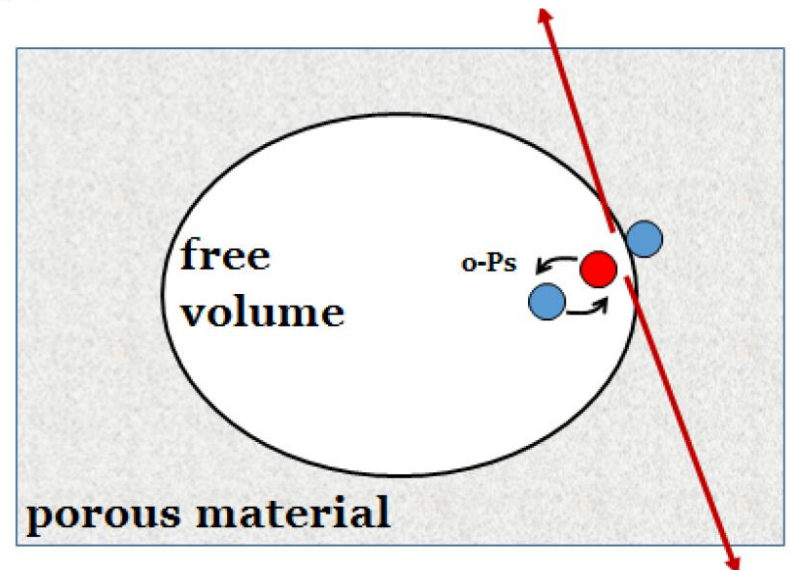
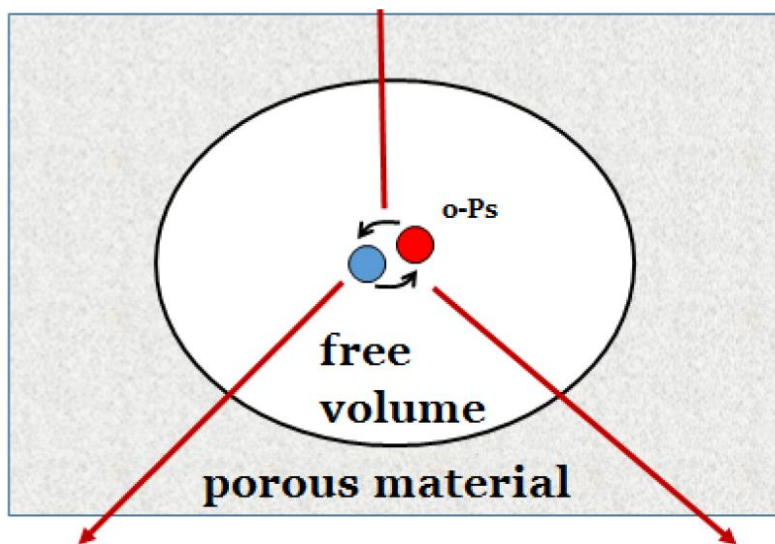
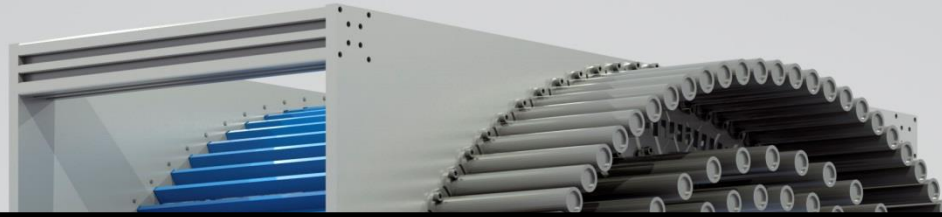


Figure 5. These three contour plots show (a) Q_{SEP} , (b) Q_{GHZ} and (c) Q_W for the state mixed equally between all three possible quantum states $s_{\hat{\alpha}} = 0, +1, -1$, equation 17. Still genuine multipartite entanglement is revealed for some scenarios ($\tilde{\Theta}_{ab}$, $\tilde{\Theta}_{bc}$). The criterion Q_W detecting W -type of genuine multipartite entanglement is by far more sensitive to reveal genuine multipartite entanglement.





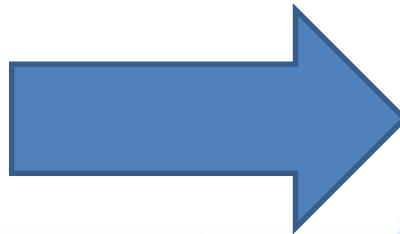
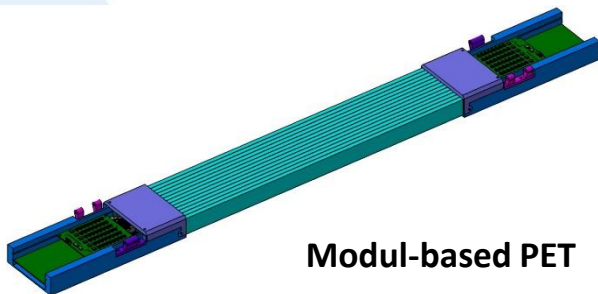
- **PET**
- **Jagiellonian-PET (J-PET)**
- **Positronium imaging (PET & PALS)**
- **Discrete symmetries**
- **Quantum Entanglement Tomograph**
- **Hadrontherapy beam monitoring**



Plastic-scintillator based PET detector: Proton beam therapy range monitoring strategies

Characterization of the detector performance and optimization of the detector acceptance for in-room PET-gamma based range monitoring strategies:

- Off-beam
- Inter-spill
- In-beam

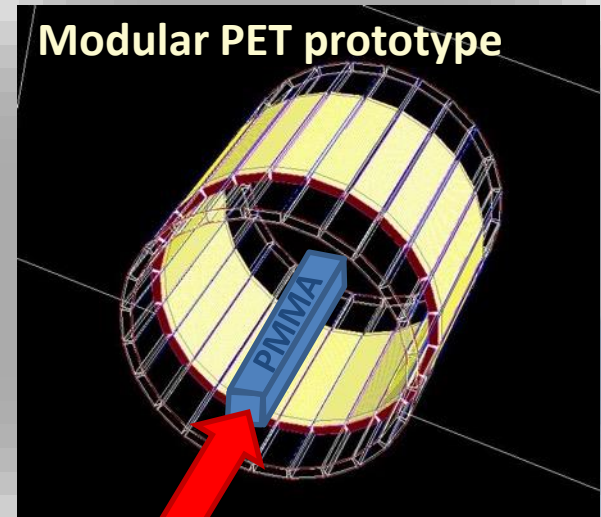




Monte Carlo simulations

GATE software toolkit is currently used to investigate the proton beam induced β^+ signal that can be detected by the plastic scintillator based diagnostic PET detector prototype.

Modular PET prototype



Proton beam



J-PET

Jagiellonian PET



J-PET



THANK YOU
FOR YOUR ATTENTION